

DOE/NASA/0327-1
NASA CR-174655
IGT Project 61067

Advanced Onboard Storage Concepts For Natural Gas-Fueled Automotive Vehicles

R. J. Remick, R. H. Elkins,
E. H. Camara, and T. Bulicz
Engineering Research Division
Institute of Gas Technology

June 1984

Prepared for
NATIONAL AERONAUTICS AND SPACE ADMINISTRATION
Lewis Research Center
Under Contract DEN 3-327

for
**U.S. DEPARTMENT OF ENERGY
Conservation and Renewable Energy
Office of Vehicle and Engine R&D**

DISCLAIMER

This report was prepared as an account of work sponsored by an agency of the United States Government. Neither the United States Government nor any agency thereof, nor any of their employees, makes any warranty, express or implied, or assumes any legal liability or responsibility for the accuracy, completeness, or usefulness of any information, apparatus, product, or process disclosed, or represents that its use would not infringe privately owned rights. Reference herein to any specific commercial product, process, or service by trade name, trademark, manufacturer, or otherwise, does not necessarily constitute or imply its endorsement, recommendation, or favoring by the United States Government or any agency thereof. The views and opinions of authors expressed herein do not necessarily state or reflect those of the United States Government or any agency thereof.

Printed in the United States of America

Available from

National Technical Information Service
U.S. Department of Commerce
5285 Port Royal Road
Springfield, VA 22161

NTIS price codes¹

Printed copy: A07

Microfiche copy: A01

¹Codes are used for pricing all publications. The code is determined by the number of pages in the publication. Information pertaining to the pricing codes can be found in the current issues of the following publications, which are generally available in most libraries: *Energy Research Abstracts (ERA)*; *Government Reports Announcements and Index (GRA and I)*; *Scientific and Technical Abstract Reports (STAR)*; and publication, NTIS-PR-360 available from NTIS at the above address.

DOE/NASA/0327-1
NASA CR-174655
IGT Project 61067

Advanced Onboard Storage Concepts for Natural Gas-Fueled Automotive Vehicles

R. J. Remic, R. H. Elkins,
E. H. Camara and T. Bulicz
Engineering Research Division
Institute of Gas Technology
Chicago, Illinois 60616

June 1984

Prepared for
National Aeronautics and Space Administration
Lewis Research Center
Cleveland, Ohio 44135
Under Contract DEN 3-327

for
U.S. DEPARTMENT OF ENERGY
Conservation and Renewable Energy
Office of Vehicle and Energy R&D
Washington, D.C. 20545
Under Interagency Agreement DE-AI01-81CS50006

TABLE OF CONTENTS

	<u>Page</u>
INTRODUCTION	2
TASK 1. ADSORPTION STUDIES	4
Task 1.1. Effect of Storage Medium Characteristics on Methane Storage Capacity	4
A. Experimental Efforts - Carbons	4
1. Suppliers	4
2. Residue After Ignition	5
3. Acidity	5
4. Surface Area Determination - Theory	8
5. Surface Area Determination - Practice	9
6. Packing Density	10
7. Particle Size - Activated Carbon Pellets	12
8. Particle Size Distribution - Carbon Black Powders	12
9. Cumulative Pore Volume	17
10. Pore Size Distribution	17
11. Methane Adsorption Isotherms for Carbons	17
B. Experimental Effort - Molecular Sieves	22
1. Description of Samples	22
2. Adsorption Isotherms	26
C. Bench-Scale Storage Experiments	28
D. Discussion of Results	31
E. Conclusions	33
Task 1.2. Modeling Effort	35
A. Calculations to Determine the Weight of a Storage Tank	35
B. Model Automobile	36
C. Fuel Consumption for Dual-Fuel Mode	37
D. Dedicated Engine Mode	38
E. Energy Density of Pressurized Storage	38
F. On-Board Storage	39
G. Additional Weight of Gas Storage Hardware	40
H. Vehicle Range and Fuel Efficiency	41
I. Discussion of Results	41
TASK 2. LITERATURE SURVEY AND ADVANCED STORAGE MEDIUM EVALUATION	45
A. Clathration of Methane	45
B. Dissolution of Methane	48
Conclusions	50

TABLE OF CONTENTS, Cont.

	<u>Page</u>
TASK 3. FUTURE RESEARCH AND DEVELOPMENT RECOMMENDATIONS	51
References	52
APPENDIX A. PORE SIZE DISTRIBUTION FOR CARBON SAMPLES	A-1
APPENDIX B. METHANE ADSORPTION ISOTHERMS FOR CARBON AND ZEOLITE SAMPLES	B-1
APPENDIX C. SUPPORTING CALCULATIONS FOR TASK 1.2 WORK	C-1
APPENDIX D. EVALUATION OF CLATHRATION COMPOUNDS AS A MEANS OF STORING NATURAL GAS	D-1
APPENDIX E. EVALUATION OF DISSOLUTION AS A MEANS OF STORING NATURAL GAS	E-1

SUMMARY

The objective of this study was the evaluation, through both experimentation and a literature review, of several advanced concepts for storing natural gas at reduced pressure. The advanced concepts included in this study were adsorption on high surface area carbon, adsorption in high porosity zeolite, storage in clathration compounds, and storage by dissolution in liquid solvents. The literature review indicated that high storage capacity could be obtained with adsorption systems.

Seventeen carbon samples and seven zeolite samples were then secured and evaluated experimentally in a pressurized microbalance apparatus to determine their methane adsorption isotherm. The methane storage capacity of each sample was also determined using a bench-scale storage system. Results indicated that high surface area carbons with high packing density were the best low pressure storage mediums.

A simple mathematical model was used to compare adsorption storage on a state-of-the-art carbon with compression storage. The model indicated that a vehicle using adsorption storage of natural gas at 3.6 MPa (500 psig) will have 36% of the range, on the EPA city cycle, of a vehicle operating on a compression storage system having the same physical size and a peak storage pressure of 21 MPa (3000 psig). However, preliminary experiments and current literature suggest that the storage capacity of state-of-the-art carbons could be improved by as much as 50%, and that adsorption systems having a capacity equal to compression storage at 14 MPa are possible.

INTRODUCTION

Recently there has been increased interest in the use of natural gas (methane) as fuel for vehicles in the United States. The primary reason for this interest is that natural gas is currently lower priced than either gasoline or diesel fuel, but other factors are also important. For example, methane-fueled vehicles would decrease both oil imports and vehicular contribution to photochemical smog. At the present time, there are nearly 30,000 natural gas fueled vehicles (NGV) in regular operation in the United States; most of these are part of commercial fleet operations. However, this number pales in significance when compared to the approximately 140,000,000 licensed vehicles in the U.S. To achieve a more wide spread acceptance of NGVs and a deeper market penetration, more economical methods must be developed for refueling and for on-board storage of natural gas.

Two alternative storage approaches are available to provide compressed natural gas (CNG)-fueled vehicles with driving ranges comparable to those of liquid-fueled vehicles. These are high storage pressure at pressures up to 21 MPa (3000 psi) and low-pressure adsorption storage at pressures below 3.6 MPa. Most NGVs in operation today use high-pressure storage, and many studies are available to justify their use -- primarily for multi-vehicle fleets. But only a limited amount of work has been done in low-pressure adsorption storage where the biggest potential cost benefits lie. For example, a recent (October 1982) estimate of costs for converting a 70 vehicle fleet to dual fuel high pressure (21 MPa) operation broke down as follows: \$83,500 for vehicle conversion equipment and \$140,000 for a quick fill refueling station. When an overnight fill was substituted for the quick fill, refueling station costs dropped to \$94,000, still more than half the cost of conversion. These costs average \$3,200 per vehicle for the quick fill option and \$2,500 per vehicle for an overnight fill refueling station. Payback periods as short as 2 years are possible for this fleet if the fleet averages 45,000 miles per vehicle per year and the combined average fuel economy is under 20 miles per gallon. Clearly, the high cost of compressor equipment is a major stumbling block to deeper market penetration.

The high costs of refueling stations has also helped to bring about a "chicken or the egg" syndrome in this fledgling industry. The private sector

will not commit the large capital expenditures required to build public refueling stations until a substantial market exists. The individual consumer, however, will not opt for a dual fuel conversion or a dedicated NGV until there is widespread availability of fuel. However, if adequate low pressure, on-board storage capacity can be achieved, substantial reductions in the cost of a refueling station would result. In fact, a limited number of sites would be available, at the outskirts of major metropolitan areas, where vehicles could be refueled directly from high pressure (3.6 MPa and above) gas transmission lines, thus entirely eliminating the need for compressors. Clearly, low pressure storage warrants a closer look.

There have been some efforts in the recent past to store methane at 1.5 to 3.6 MPa using physical adsorption on solid materials such as carbons and zeolites. The most recent work,^{1,2} conducted by Ford Motor Company, has emphasized carbon over zeolites. Ford determined that a Union Carbide carbon designated 9LXC was the best adsorbent of those investigated.

The purpose of this present effort was to conduct fundamental studies on carbons with high surface areas and zeolites with high internal porosities. These studies identified the effect on methane storage of critical sorbent characteristics such as surface area, pore size, pore size distribution, particle size, and sorbent packing density.

The work in this program was divided into three major tasks. Task 1 evaluates the effect of surface area, pore size, pore size distribution, particle size, and packing density on the methane storage capacity of carbons and zeolites. Task 2 completed a literature review that was already underway at IGT and addressed alternate low pressure storage concepts utilizing clathration compounds and solvents. Task 3 summarized the entire program and recommends future research and development.

TASK 1. ADSORPTION STUDIES

Task 1.1 Effect of Storage Medium Characteristics on Methane Storage Capacity

The objective of this task was to document the effect of surface area, pore volume, pore size distribution, particle size, and packing density on the methane storage capacity of carbons and zeolites at room temperature and at pressures up to 3.6 MPa.

A. Experimental Efforts -- Carbons

1. Suppliers

Samples of high-surface-area carbon blacks and activated carbons were obtained from various manufacturers. Table 1 is a list of suppliers and product names.

Table 1. LIST OF CARBONS BY SUPPLIER

<u>Supplier</u>	<u>Designation</u>	<u>Sample No.</u>
Gulf Oil Chemicals Co. (Shawinigan Products Div.)	Acetylene Black	
	50% Dense	C1
	100% Dense	C2
Cabot, Corp.	CSX-179-B	C3
ICI Americas, Inc.	DXL-0-8334	C4
	DARCO SG	C5
Westvaco	Nuchar WV-B	C6
	Nuchar WV-G	C7
J. T. Baker Co.	Acid-Washed Carbon	C8
CECA, Inc.	GAC 50G	C9
Witco Chemicals	JXC 4 x 6	C10
Calgon, Corp.	PCB 30 x 140	C11
	BPL 30 x 140	C12
North American Carbon	G101	C13
	G104	C14
	G210	C15
	G216	C16
Union Carbide (No longer in production)	9LXC	C17

2. Residue After Ignition

One-gram samples of each of these 17 carbons were placed in weighed, porcelain crucibles and heated overnight in air at 1000°C. Weight loss was determined, and where possible the residue present after ignition was recovered. Some of the activated carbons obtained commercially are in the form of cylindrical pellets and contain a clay binder. Others have been impregnated with inorganic materials to enhance their ability to absorb reactive gases such as hydrogen cyanide. Still others, because of their origin, contain alkali metal carbonates or alkaline earth phosphates and sulfates. It is important to know how much of each sample is carbon in order that only high purity carbons might be used to evaluate the importance of surface area and pore volume. Such information will be essential in the modeling effort to be undertaken in later stages of Task 1. Results are listed in Table 2.

3. Acidity

The key to the adsorption of gases on high-surface-area activated carbons is the nature of the carbon surface. The activation of charcoal, for example, by partial oxidation in air produces an unstable surface layer. Upon contact with air at room temperature, this unstable layer reverts to a more stable modification called oxidized charcoal. This oxidized charcoal possesses a variety of carboxyl and carbonyl groups on its surface that contribute significantly to its adsorption properties. Boem, for example, has characterized the surface groups on oxidized charcoal by titration with bases of different strengths and by chemical analysis.³ He proposes that oxidized charcoal has at least four types of surface structures (Figure 1). Structures II and III both possess carboxylic acid groups while Structure IV has positively charged counter ions associated with it. When mixed with water, Structures II and III can dissociate to give a distinctly acid character to the water; Structure IV can hydrolyze to yield a base. Although quantitative chemical characterization of the 17 carbon samples with respect to the nature of the surface was beyond the scope of the present program, some indication of the surface functionality was obtained by mixing the carbon with water and measuring the pH.

One-gram samples of each of the 17 carbons were placed in approximately 50 mL of degassed, deionized water and mixed in a high-speed blender for 1 minute under a nitrogen atmosphere. The resulting suspension was allowed to settle for 10 minutes, and the pH of the solution was then determined using a

Table 2. ANALYTICAL DATA FOR CARBON SAMPLES

<u>Sample No.</u>	<u>Residue after Ignition, %</u>	<u>Residue Color</u>	<u>pH of Carbon Sample</u>
C1	<0.5	---	5.3
C2	<0.5	---	5.4
C3	<0.3	--	10.1
C4	7.6	Orange	8.4
C5	14.5	Cream	8.1
C6	3.9	Colorless Glass	3.8
C7	6.6	Orange	10.0
C8	<0.3	--	6.3
C9	13.5	White	8.3
C10	<0.1	--	9.8
C11	82.0	Orange	9.6
C12	73.6	Colorless Glass	9.7
C13	11.8	Colorless Glass	6.4
C14	12.0	Colorless Glass	2.6
C15	1.5	Colorless Glass	9.9
C16	1.2	Colorless Glass	9.6
C17	1.0	Black Fibers	9.9

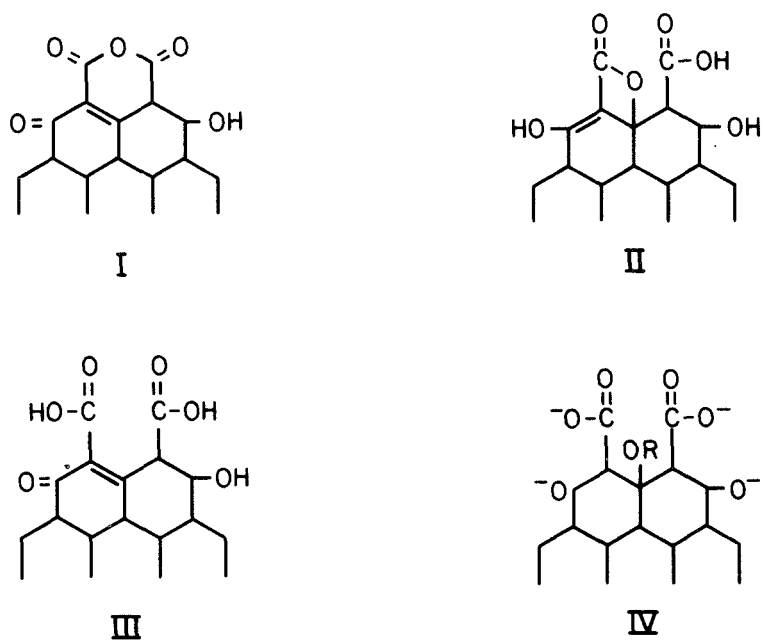


Figure 1. FOUR TYPES OF SURFACE STRUCTURES FOUND IN OXIDIZED CHARCOAL AS PROPOSED BY BOEM IN REFERENCE 3

Corning Model 476223 Semi Micro Combined Electrode and a Markson Scientific Model 90 digital pH meter. The results are listed in Table 2. It should be noted that with those carbons having a high amount of residue after ignition, a substantial contribution to pH could come from sources other than carbon.

4. Surface Area Determination — Theory

The physical adsorption of gas molecules onto the surface of a solid results from relatively weak interaction between molecules of the solid and molecules of the gas. This interaction is frequently referred to as van der Waal's forces. Physical adsorption contrasts with chemical adsorption, where chemical bonds are responsible for the interaction between solid and gas. In physical adsorption, the quantity of adsorbed gas increases with decreasing temperature. In chemical adsorption, because it depends upon chemical reaction, the quantity of adsorbed gas decreases with decreasing temperature. For this reason, adsorption measurements to determine surface area or pore distribution are made at lower temperatures where physical adsorption predominates. Brunauer, Emmett, and Teller (B.E.T.)^{4,5} have derived the following expression for relating the volume of gas adsorbed to the nature of the solid surface and the temperature and pressure of the gas:

$$V_a = \frac{V_m CP}{(P_s - P) [1 + (C - 1) P/P_s]} \quad (1)$$

where —

V_a = Volume of adsorbed gas

V_m = Volume of gas required to form a monolayer over entire surface

P = Pressure of gas

P_s = Equilibrium vapor pressure of gas and its liquid at temperature of measurement (760 torr at 77.35°K for nitrogen)

C = A constant dependent upon the nature of the solid adsorbent.

This expression describes the great majority of low-temperature adsorption data. V_m can be calculated from a series of physical measurements of the volume of gas adsorbed as a function of pressure at a fixed temperature by rearranging Equation 1 to a linear form:

$$\frac{P}{V_a(P_s - P)} = \frac{1}{V_m C} + \frac{C - 1}{V_m C} \frac{P}{P_s} \quad (2)$$

A plot of $P/V_a(P_s - P)$ versus P/P_s gives a straight line with an intercept at $1/V_m C$ and a slope of $(C - 1)/V_m C$. The value of V_m is readily determined from a series of such measurements. The linearity of the B.E.T. equation can be expected to hold only in the region of pressures where P/P_s is between 0.05 and 0.3. A more detailed discussion of B.E.T. theory can be found in References 4 and 5.

5. Surface Area Determination — Practice

The actual surface area was determined on an ORR Surface-Area Pore-Volume Analyzer. The procedure used is as follows.

A weighed carbon sample is placed in a small containment vessel and attached through a valve to a gas manifold of known volume, V_1 . The sample is warmed to over 100°C under a vacuum (<10 microns), then sealed off from the manifold and cooled to room temperature. The manifold is charged with helium to a known pressure, P_1 . The containment vessel with the sample is then opened to the manifold, where upon the manifold pressure drops to P_2 . The volume of the containment vessel with sample, V_C , can now be calculated as follows:

$$V_C = \frac{P_1 V_1}{P_2} - V_1 \quad (3)$$

This procedure assumes that no helium adsorbs on the sample at these temperatures. The containment vessel and sample are again evacuated and then cooled with liquid nitrogen. In a manner similar to that above, the manifold is pressurized again but with nitrogen at room temperature, T_R , and the pressure, P_1 , is accurately determined. The manifold is then opened to the containment vessel, allowed to come to equilibrium, and the new pressure, P_2 , is measured. Using Equation 4, the volume of gas adsorbed, V_a , at pressure P_2 can be calculated.

$$\frac{P_1 V_1}{T_R} = \frac{P_2 V_1}{T_R} + \frac{P_2 V_C}{770K} + \frac{760}{273} V_a \quad (4)$$

The process is then repeated for several incremental additions of nitrogen gas, with additional terms being added to Equation 4 to account for the fact that the initial pressure is no longer zero. In this way, several simultaneous values for V_a and P_2 can be generated from which a B.E.T. plot can be constructed using Equation 2.

The above discussion is somewhat simplified in that we have neglected several corrections to V_a that must be included because of the nonideal behavior of nitrogen and because of peculiarities of the instrument itself. But once a corrected B.E.T. plot is made using the various V_a versus P_2/P_s data points, the specific surface area of the sample may be calculated from the following formula:

$$\text{Specific Surface Area} = \frac{\text{M.A.} \times N}{\text{M.V.} (\text{Slope} + \text{Intercept})} \quad (5)$$

where —

M.A. = Molecular area in cm^2 ($16.2 \times 10^{-20} \text{ cm}^2$ for nitrogen)

N = Avogadro's number

M.V. = Molar volume in cm^3

This equation can be simplified to Equation 6 for nitrogen:

$$\text{Specific Surface Area} = \frac{4.35}{\text{Slope} + \text{Intercept}} \quad (6)$$

The results for the specific surface area determinations for the 17 carbon samples are listed in Table 3. It should be noted that with high surface area samples where V_m is large, the slope and the intercept become small, thus increasing measurement error. Although the specific surface areas are given to three significant figures in Table 3, the relative error for these measurements may be as much as $\pm 10\%$.

6. Packing Density

The packing density of the adsorbent, defined here as the mass in grams of one cubic centimeter of settled material, is one of the critical parameters associated with the use of adsorbents for CNG storage in automotive vehicles. Packing density can be conveniently measured by placing a weighed amount of material in a graduated cylinder and vibrating the cylinder a rate of 100 Hz

Table 3. SPECIFIC SURFACE AREA, APPARENT DENSITY, AND SURFACE AREA PER LITER FOR 17 CARBON SAMPLES

<u>Sample Designation</u>	<u>Specific Surface Area, m²/g</u>	<u>Packing Density, g/cm³</u>	<u>Surface Area, km²/L</u>
C1	76	0.10	0.008
C2	74	0.20	0.015
C3	1600	0.13	0.21
C4	1030	0.44	0.45
C5	700	0.45	0.32
C6	1610	0.30	0.48
C7	1260	0.45	0.57
C8	480	0.37	0.18
C9	1030	0.56	0.58
C10	1050	0.45	0.47
C11	1270	0.44	0.56
C12	1100	0.47	0.52
C13	1680	0.30	0.50
C14	1650	0.30	0.50
C15	1420	0.50	0.71
C16	1370	0.50	0.69
C17	1280	0.32	0.41

or higher for several minutes to allow the sample to settle under the influence of gravity. Packing density measured in this way can be used to calculate the quantity of material that can be placed in a storage cylinder from a free-flowing reservoir. Table 3 lists the packing density of the 17 carbon samples in grams per cubic centimeter. The specific surface area and the packing density can also be used to estimate the surface area available for storage in a 1-liter container filled with carbon. The final column of Table 3 contains such estimates for the various carbon samples.

7. Particle Size — Activated Carbon Pellets

All of the activated carbons supplied to us were in the form of pellets or granules while the carbon blacks were in the form of powders. In the case of the activated carbons, the particle sizes fell within narrow limits which is likely the result of a screening step in their manufacture. The various suppliers provided us with information on the upper and lower limits of particle size for each sample as measured in U.S. mesh. Table 4 is a particle size conversion table comparing the U.S. mesh size with the equivalent particle diameter in microns. This table is included solely for convenience. Table 5 contains a list of the 17 carbon samples and the maximum and minimum mesh sizes for the 13 activated carbons. Because better than 95% of the particles in any given sample fell within the narrow limits of size listed by the respective supplier, no further attempt was made to determine a particle size distribution for the activated carbon samples.

8. Particle Size Distribution — Carbon Black Powders

The particle size distributions for the four carbon black samples were determined on an automated Coulter counter. Table 6 lists the results for 50% dense Shawinigan Acetylene Black. These results do not agree with the particle size distribution provided by the manufacturer. When viewed under an electron microscope, Shawinigan Acetylene Black appears to consist of spherical particles clumped together in much larger agglomerates. The median particle size for these spheres as determined from a micrograph is 42.5 nm whereas the mean agglomerate size as determined by the Coulter counter is 23 μm or about 540 times larger. Since it is the agglomerate size rather than the particle size which determines handling characteristics such as packing density, the agglomerate size distribution is the more important parameter. Table 7 lists the agglomerate size distribution for 100% dense Shawinigan

Table 4. PARTICLE SIZE CONVERSION TABLE

<u>Mesh Size</u>	<u>Approximate Size in Microns*</u>
4	4760
6	3360
8	2380
12	1680
16	1190
20	840
30	590
40	420
50	297
60	250
70	210
80	177
100	149
140	105
200	74
230	62
270	53
325	44
400	37
625	20
1250	10
2500	5

* 1 mm = 1000 microns.

Table 5. PARTICLE SIZE DISTRIBUTION BY MESH SIZE

<u>Number</u>	<u>Carbon</u>	<u>Size</u>
C1	Shawinigan 50%	(see Table 6)
C2	Shawinigan 100%	(see Table 7)
C3	Cabot CSX-179-B	(see Table 8)
C4	ICI DXL-0-8334	20 x 60 mesh
C5	ICI DARCO-SG	20 x 60 mesh
C6	Nuchar WV-B	14 x 35 mesh
C7	Nuchar WV-G	12 x 14 mesh
C8	Baker Acid Washed	(see Table 9)
C9	CECA GAC-50G	20 x 50 mesh
C10	Witcarb JXC	4 x 6 mesh
C11	Calgon PCB	30 x 140 mesh
C12	Calgon BPL	30 x 140 mesh
C13	North American G101	10 x 25 mesh
C14	North American G104	14 x 35 mesh
C15	North American G210	8 x 16 mesh
C16	North American G216	14 x 35 mesh
C17	Union Carbide 9LXC	12 x 28 mesh

Table 6. PARTICLE SIZE DISTRIBUTION FOR 50% DENSE
SHAWINIGAN ACETYLENE BLACK

<u>Size Range</u>	<u>Weight Percent</u>
Less than 4 microns	0
4.0 to 5.0 microns	1.1
5.0 to 6.4 microns	2.4
6.4 to 8.0 microns	4.4
8.0 to 10.1 microns	5.9
10.1 to 12.7 microns	6.5
12.7 to 16.0 microns	7.6
16.0 to 20.2 microns	11.2
20.2 to 25.4 microns	16.0
25.4 to 32.0 microns	20.4
32.0 to 40.3 microns	13.7
40.3 to 50.8 microns	6.9
Larger than 50.8 microns	3.9

Table 7. PARTICLE SIZE DISTRIBUTION OF 100% DENSE
SHAWINIGAN ACETYLENE BLACK

<u>Size Range</u>	<u>Weight Percent</u>
Less than 4 microns	0
4.0 to 5.0 microns	5.9
5.0 to 6.4 microns	10.3
6.4 to 8.0 microns	10.3
8.0 to 10.1 microns	9.9
10.1 to 12.7 microns	9.8
12.7 to 16.0 microns	10.1
16.0 to 20.2 microns	11.2
20.2 to 25.4 microns	14.4
25.4 to 32.0 microns	10.7
32.0 to 40.3 microns	4.8
40.3 to 50.8 microns	1.6
Larger than 50.8 microns	0

Acetylene Black; Table 8, for Cabot Corporation carbon black CSX-179-B; and Table 9, the agglomerate size distribution for Baker-Acid Washed Carbon.

9. Cumulative Pore Volume

Both nitrogen adsorption and desorption isotherms were determined at 78°K for all carbon samples and the results used to estimate the cumulative pore volume of each sample and to ascertain the pore size distribution. Table 10 lists 16 carbon samples and the cumulative pore volume of all pores less than 200 Angstroms in radius. It should be noted that our cumulative numbers have a cut-off for maximum pore radius at 200 Angstroms and, therefore, pores larger than 200 Å are ignored, since the interior surfaces of pores larger than 200Å in radius would be little different from flat surfaces. However, as a consequence, our cumulative pore volume may differ somewhat from the total pore volume numbers advertised for these carbons by their various manufacturers.

It can be seen from Table 10 that Cabot's CSX-179-B has the highest cumulative pore volume of the carbon blacks, while Nuchar WV-B is highest among the activated carbons. Of particular interest are the four North American Carbon, Inc., samples. The 100 series samples have high cumulative pore volume while the 200 series have the lowest measured.

10. Pore Size Distribution

The nitrogen desorption isotherm data were used to plot pore size distributions for 16 of the carbon samples. Subsequent work indicated no identifiable relationship between pore size distribution and methane storage capacity. Individual plots of pore size distribution as pore volume versus pore radius are provided in Appendix A for carbons C1 through C16.

11. Methane Adsorption Isotherms for Carbons

Figure 2 is a schematic diagram of the apparatus used to determine the methane adsorption isotherms for selected carbon and zeolite samples. The experimental technique used was to suspend a measured quantity of adsorbent from an electronic transducer type balance in a methane atmosphere and determine the weight of the sample as the vessel is pressurized from 101.4 KPa (0 psig) to 3.6 MPa (500 psig) in 50 psi steps. Weight changes as little as 1 part in 2000 can be measured with this apparatus. However, it is necessary to make corrections on the indicated weight for the buoyancy of the sample. The following may serve as an example. In the carbon experiments, a sample of JXC

Table 8. PARTICLE SIZE DISTRIBUTION FOR
CABOT CSX-179-B

<u>Size Range</u>	<u>Weight Percent</u>
Less than 4 microns	0
4.0 to 5.0 microns	7.7
5.0 to 6.4 microns	12.5
6.4 to 8.0 microns	14.0
8.0 to 10.1 microns	15.4
10.1 to 12.7 microns	14.7
12.7 to 16.0 microns	11.8
16.0 to 20.2 microns	8.2
20.2 to 25.4 microns	4.9
25.4 to 32.0 microns	2.7
32.0 to 40.3 microns	1.5
40.3 to 50.8 microns	0.8
Larger than 50.8 microns	5.8

Table 9. PARTICLE SIZE DISTRIBUTION FOR BAKER ACID WASHED CARBON

<u>Size Range</u>	<u>Weight Percent</u>
Less than 3.2 microns	0
3.2 to 4.0 microns	1.3
4.0 to 5.0 microns	2.7
5.0 to 6.4 microns	3.4
6.4 to 8.0 microns	4.4
8.0 to 10.1 microns	4.2
10.1 to 12.7 microns	2.4
12.7 to 16.0 microns	1.3
16.0 to 20.2 microns	1.1
20.2 to 25.4 microns	0.7
25.4 to 32.0 microns	0.5
32.0 to 40.3 microns	0.2
40.3 to 75 microns	17.5
75 to 100 microns	35.3
150 to 300 microns	17.7
300 to 600 microns	6.9
Larger than 600 microns	0.4

Table 10. CUMULATIVE PORE VOLUME FOR PORES OF
RADIUS LESS THAN 200 ANGSTROMS

<u>Number</u>	<u>Carbon</u>	<u>Pore Volume</u>
C1	Shawinigan 50%	0.10 ml/g
C2	Shawinigan 100%	0.11 ml/g
C3	Cabot CSC-179-B	0.99 ml/g
C4	ICI DXL-0-8334	0.17 ml/g
C5	ICI DARCO-SG	0.53 ml/g
C6	Nuchar WV-B	0.66 ml/g
C7	Nuchar WV-G	0.14 ml/g
C8	Baker Acid Washed	0.82 ml/g
C9	CECA GAC-50G	0.09 ml/g
C10	Witcarb JXC	0.13 ml/g
C11	Calgon PCB	0.05 ml/g
C12	Calgon BPL	0.09 ml/g
C13	North American G101	0.54 ml/g
C14	North American G104	0.58 ml/g
C15	North American G210	0.024 ml/g
C16	North American G216	0.026 ml/g

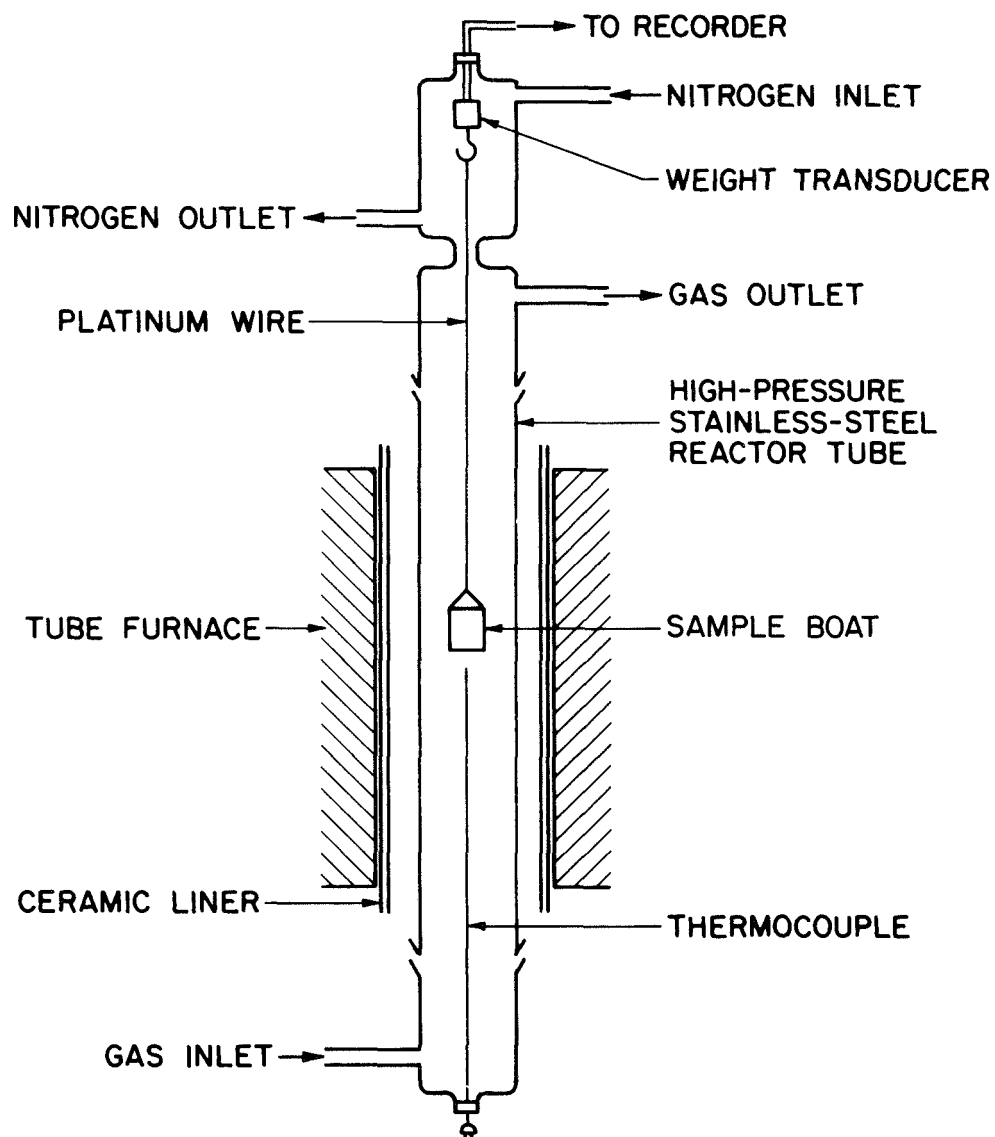


Figure 2. EXPERIMENTAL APPARATUS USED TO DETERMINE METHANE ADSORPTION ISOTHERM

carbon weighing 10.076 grams under one atmosphere pressure (101.3 KPa) of methane was pressurized to 35 atmospheres (3.6 MPa). Using the adsorption isotherm data previously obtained, we would expect this sample to gain 0.856 gram in weight due to methane adsorption. The microbalance, however, indicated a gain of only 0.746 gram. The difference, 0.11 gram, is due to buoyancy effects. The carbon in a 10.076 gram sample of JXC carbon has an actual volume of only 4.80 cc and displaces 0.110 gram of methane at 35 atmospheres. The key to calculating the buoyancy correction is the actual density of the solid material. Witco's JXC carbon (C10) has a packing density of only 450 grams/liter; however, almost 80% of a sample of JXC is accessible void space which can fill with compressed gas and does not contribute to buoyancy. In the case of most of the carbon samples, the solid material contributing to buoyancy effects can be considered to have an effective density equal to that of graphite, 2100 grams/liter.

Adsorption isotherms for each of the carbons C3 through C17 are provided in Appendix B. Table 11 summarizes the results. Since Ford Motor Co.¹ and others are working with adsorption systems operating at about 2.2 MPa (300 psig), we have reported data for methane adsorption at this pressure in Table 11. We have also included data for methane adsorption at 3.6 MPa (500 psig) which is the maximum pressure used in the present study. Because of the particulate nature of the Shawinagan Acetylene Blacks, these carbons tended to fluidize during depressurization of the microbalance and reliable adsorption measurements were not possible for Samples C1 and C2.

B. Experimental Effort -- Molecular Sieves

1. Description of Samples

Zeolites. Six samples of commercially available crystalline molecular sieves were obtained from the Linde Division of Union Carbide. Four of these samples are zeolites of the Sodalite Group, one sample is of the Chabazite Group, and one sample is of the Mordenite Group. One additional sample was prepared by ion exchange. Table 12 lists the samples by experimental designation (Z1 through Z7) and provides information on structure, critical diameter, and nonframework cation.

Table 11. ADSORPTION CHARACTERISTICS OF CARBON SAMPLES*

<u>Sample No.</u>	<u>Packing Density</u>	<u>Methane Adsorbed in grams/gram</u>	
		<u>2.2 MPa</u>	<u>3.6 MPa</u>
C3	0.15	0.099	0.110
C4	0.42	0.074	0.081
C5	0.44	0.050	0.053
C6	0.26	0.072	0.085
C7	0.49	0.085	0.091
C8	0.40	0.042	0.045
C9	0.54	0.069	0.076
C10	0.45	0.083	0.087
C11	0.44	0.090	0.095
C12	0.47	0.074	0.079
C13	0.24	0.079	0.091
C14	0.27	0.068	0.078
C15	0.49	0.092	0.099
C16	0.45	0.095	0.103
C17	0.32	0.101	0.115

* At 23°C.

Table 12. INFORMATION ON VARIOUS ZEOLITES

<u>Designation</u>	<u>Structure</u>	<u>Linde Designation</u>	<u>Critical Diameter, Å</u>	<u>Nonframework Cation</u>
Z1	Zeolite A	3A	3	Potassium
Z2	Zeolite A	4A	4	Sodium
Z3	Zeolite A	5A	5	Calcium
Z4	Zeolite X	13X	10	Sodium
Z5	Zeolite A	--	11	Lithium
Z6	Mordenite	AW-300	3 to 4	Mixed
Z7	Chabazite	AW-500	4 to 5	Mixed

The structure of the Sodalite Group, Zeolite A, is based on frameworks that are simple arrangements of truncated octahedra. These truncated octahedra share square and hexagonal faces. In the structure of Zeolite A, the octahedra are linked by adjoining cubes (Figure 3). This produces a central truncated octahedron with an internal cavity of 11Å diameter. Access to this cavity is by way of the six apertures, which are the cubes with a free diameter of 4.2Å. In Zeolite A of the formula $\text{Na}_2[(\text{AlO}_2)_{12}(\text{SiO}_2)_{12}] \cdot 27 \text{H}_2\text{O}$, there are 12 nonframework sodium ions per unit cell. Eight of these sodium ions reside in the center of the eight hexagonal faces and are referred to as Type I cations. The other four cations, Type II, occupy positions adjacent to the openings that interconnect the cavities. When completely hydrated, these four ions probably float within a coordination sphere of water molecules; but when dehydrated, they locate on the walls of the cavity and exert an influence on the critical diameter of the opening between cavities. The critical diameter is, for our purposes, the largest diameter a gas molecule can have and still pass between cavities. As is illustrated in Table 12, the large diameter of the potassium ion (2.66Å) restricts the critical diameter in Type A zeolites to 3Å. Thus, methane with a kinetic diameter of 3.8Å cannot gain access to the interior of the cavity, whereas water molecules with a kinetic diameter of 2.65Å can be admitted. Type A zeolites with smaller nonframework ions (sodium and lithium, having ionic diameters of 1.90Å and 1.36Å, respectively) increase the critical diameter to 4Å and thus permit methane to enter the cavity. Divalent calcium ions increase the critical diameter to 5Å partly because of size, 1.98Å, and partly by perturbing the framework itself. The Type X zeolites, on the other hand, have a different crystallographic morphology in which adjacent cavities share large hexagonal openings. Type X

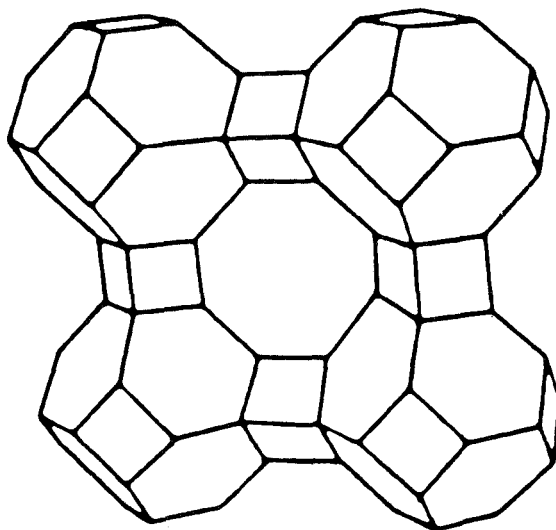


Figure 3. CUBIC ARRAY OF TRUNCATED OCTAHEDRA
IN TYPE A ZEOLITE

zeolites have a critical diameter of 10\AA . In dehydrated chabazite, the cavities share ellipsoidal apertures with dimensions of 4.4\AA by 3.1\AA . The zeolite mordenite possesses a predominance of 5-member rings that align to form circular channels with a free diameter of 6.6\AA . This structure is sensitive to stacking faults, however, which can reduce the large-channel diameter from 6.6 to 4\AA . A more detailed discussion of crystalline molecular sieves can be found in Reference 6. Of importance here is that the nonframework cations in both Type A and Type X zeolites can easily be exchanged. Thus, lithium-containing Type A zeolite can be prepared from sodium-containing material (Linde 4A).

The phenomenon of ion exchange was used to prepare Sample Z5. The following procedure was used.

One hundred grams of Linde 4A molecular sieves were placed in a 1-liter flask fitted with a reflux condenser, and 500 mL of a 0.1M lithium chloride solution was added. The mixture was heated to 80°C and maintained at this temperature for 24 hours with occasional gentle agitation. After 24 hours, the LiCl solution was drained and replaced with 500 mL of fresh LiCl solution and reheated. This process was repeated through four consecutive 24-hour treatments. The zeolite was then recovered and washed 10 times with 500 mL each of deionized water, drained, and allowed to air dry for 24 hours at room temperature. The lithium-containing zeolite was then dried at 200°C in air for 1 week, at 360°C in air for 24 hours, and at 360°C for 24 hours under vacuum (<10 microns). The vacuum flask was finally cooled and pressurized with dry argon to 1 atm. The lithium-containing zeolite was then loaded into an airtight container under an argon atmosphere and stored for later use.

2. Adsorption Isotherms

All zeolite samples were dried prior to determining their adsorption isotherm. The drying process used was that of heating the sample to 360°C for 24 hours under a continually increasing vacuum which was below 10 microns pressure at the end of the 24 hour period. The samples were cooled under vacuum and then pressurized to 1 atmosphere with dry argon. The sample was transported to the microbalance under argon and quickly transferred to the sample pan in a manner designed to limit its exposure to moisture laden air (ambient laboratory conditions) to a few minutes.

A problem was encountered when attempts were made to calculate a correction factor for buoyancy.

In the case of the zeolites, calculations are not easy. For example, when a sample of activated 13X zeolite pellets is packed into a graduated cylinder and weighed, it exhibits a packing density of 0.66 g/cc. When a single pellet is weighed and its geometrical volume is determined, an apparent density of 1.29 g/cc is calculated. However, Linde claims that 13X pellets contain an internal void space of 0.36 cc/g. Thus, while a single pellet of 13X has an apparent density of 1.29 g/cc and one gram would occupy 0.77 cc, 0.36 cc of this volume is void space and only 0.41 cc is solid material. Thus, for purposes of calculating buoyancy effects, the effective density of 13X zeolite is 2.44 cc/g. However, the aperture size for 3A zeolite is not accessible to methane and cannot fill with compressed gas. Consequently, this void volume will contribute to buoyancy effects. In 5A zeolite, the aperture size is larger than the kinetic diameter of methane and the 0.30 cc/g void volume in 5A zeolite can fill with compressed gas and so does not contribute to buoyancy. The effective density of 3A zeolites would, therefore, be 1.35 g/cc while the effective density, for purposes of calculating buoyancy, for 5A zeolites would be 2.2 g/cc.

To summarize, while the apparent densities of pellets of 3A, 5A, and 13X zeolites are 1.33 g/cc, 1.33 g/cc, and 1.29 g/cc, respectively, the effective density, on theoretical grounds, for use in calculating buoyancy should be 1.33 g/cc, 2.2 g/cc, and 2.44 g/cc, respectively. Unfortunately, attempts to use these theoretical densities to interpret actual experimental data produce less than satisfactory results.

An empirical solution to this problem was arrived at by careful examination of the adsorption data for 13X and 5A zeolite samples. These zeolites have large critical diameters which are completely accessible to methane. Therefore, a straightforward calculation of buoyancy is possible. The adsorption isotherm for 13X zeolite exhibits very little change over the incremental pressure change between 3.2 MPa (450 psig) and 3.6 MPa (500 psig). The raw microbalance data, however, does show an appreciable change in weight due to changes in buoyancy. If we assume that the other zeolite samples behave in the same manner, that is, that the weight change observed between 450 psig and 500 psig is due almost entirely to changes in buoyancy, we can then use the

raw microbalance data as a direct measurement of the buoyancy and eliminate the need for a calculated value.

The relative errors introduced by this assumption are cumulative. In other words, a 1% relative error in estimating the buoyancy between 450 psig and 500 psig becomes a 10% relative error over the entire range of pressures measured (0 to 500 psig). As a consequence, we cannot have a high degree of confidence in the adsorption isotherms for 3A, 4A, AW-300, and AW-400. However, since the performance of these materials falls far short of the performance of the 5A zeolites, they are effectively eliminated from consideration as an advanced concept for methane storage anyway and no harm is done.

Individual adsorption isotherms for the seven zeolite samples are provided in Appendix. B. Table 13 is a summary of their performance.

Table 13. ADSORPTION CHARACTERISTICS OF ZEOLITE SAMPLES

<u>Sample No.</u>	<u>Packing Density g/cc</u>	<u>Methane Adsorbed in grams/gram</u>	
		<u>2.2 MPa</u>	<u>3.6 MPa</u>
Z1	0.77	0.024	0.025
Z2	0.76	0.037	0.039
Z3	0.74	0.047	0.049
Z4	0.66	0.048	0.050
Z5	0.72	0.048	0.051
Z6	0.95	0.038	0.039
Z7	0.79	0.030	0.031

C. Bench-Scale Storage Experiments

Methane adsorption is only one of several important parameters contributing to the performance of an adsorption storage system. Packing density and internal pore volume are others. To assess the performance of adsorbents under realistic conditions, samples of adsorbent were packed into a stainless steel cylinder having an internal volume of 75 cm³ and the cylinder evacuated with a vacuum pump. The evacuated cylinder and sample were weighed on a top loading balance accurate to ±0.01 gram. The cylinder was then pressurized to 3.6 MPa (500 psig) with dry methane. The heat of adsorption was dissipated by

blowing air at 25°C over the cylinder for two hours while maintaining a constant pressure with a high pressure regulator. The cylinder was then reweighed. This provided a direct measure of the total mass of methane stored at 3.6 MPa and includes both that portion stored by adsorption and that portion stored by compression in the void spaces. The mass (g) of methane stored per unit volume (L) is here defined as methane storage capacity. The dependence of methane storage capacity upon packing density and specific adsorption is illustrated for selected samples in Figure 4. The solid lines represent a locus of points determined by the theoretical relationship between packing density and methane storage for carbons having specific adsorptions of 0.165, 0.115, 0.100, and 0.085 g/g at 3.6 MPa (35 atm or 500 psig) at 25°C. Actual experimentally determined values for carbon C6, C10, C15, C15C, and C17 are also plotted in Figure 4. In Reference 7, Amos Golovoy reports success in increasing the packing density of 9LXC by crushing the pellets. The storage capacity at 3.6 MPa and packing density reported by Golovoy are plotted in Figure 7 as Point R1. The same procedure was applied by IGT to increase the apparent density of Sample C15. A 50 gram sample of this carbon was placed in a hydraulic press and crushed at a pressure of 1000 psi (7.3 MPa). The broken pellets were then placed in a mortar and fragmented further with a pestle using a rocking motion rather than a grinding motion. This produced a large number of fine particles with a minimum amount of powder. This carbon was then dried at 140°C in a vacuum oven and the methane adsorption isotherm was determined. Although the crushed carbon sample now exhibited a packing density of 0.58 g/cc, the adsorption isotherm for this carbon was identical to that of the original indicating that the adsorption characteristics were not changed by the crushing process. This carbon sample was designated as C15C and is also plotted in Figure 4.

Barton et al.⁸ have determined the methane adsorption isotherm at 25°C for a carbon which was not included in this study, Amoco GX-32. This carbon has the highest surface area of any known carbon, 2500 m²/g (Nitrogen BET) and the highest specific adsorption for methane of any carbon reported in the literature, 0.165 g/g at 3.6 MPa and 25°C. Point R2 in Figure 4 represents the storage capacity of Amoco GX-32 and was placed on the basis of information provided by Barton. It is possible that the packing density of this material also might be increased by crushing.

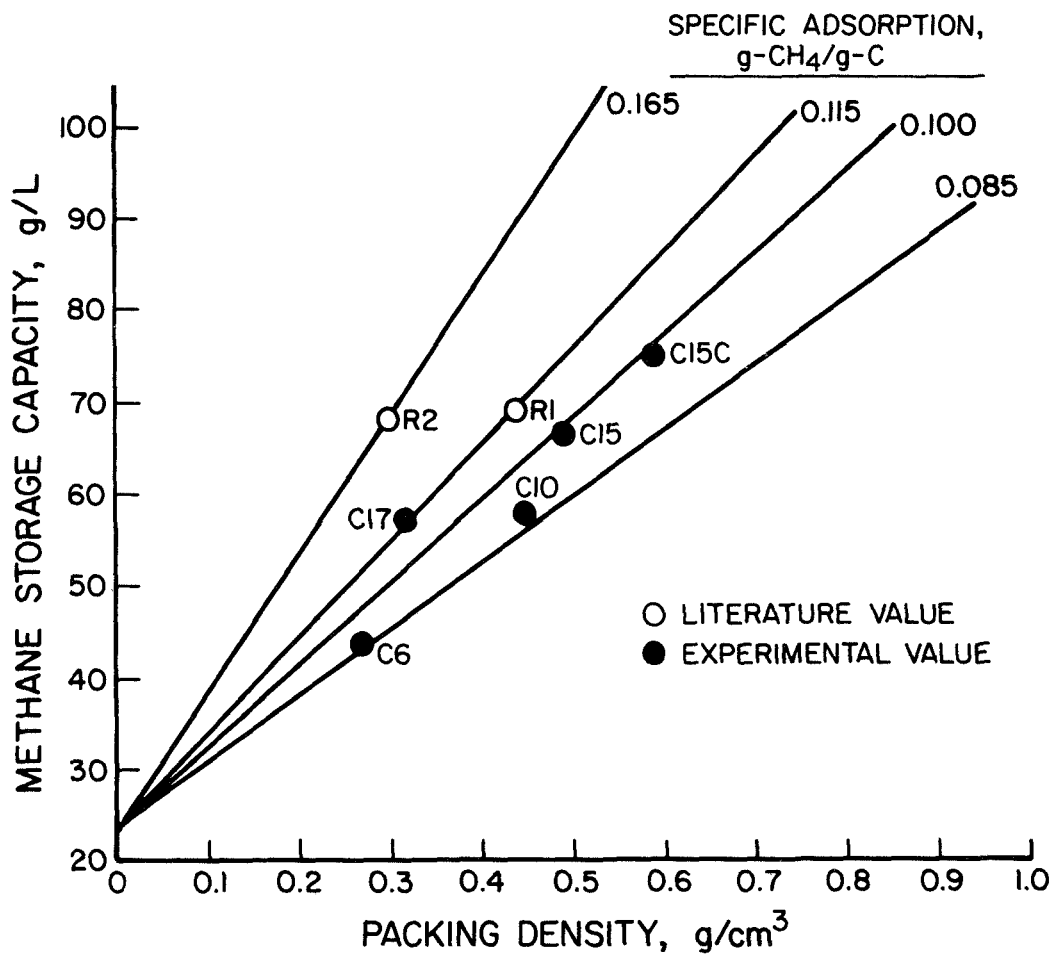


Figure 4. RELATIONSHIP OF SPECIFIC ADSORPTION AND PACKING DENSITY OF CARBON TO METHANE STORAGE CAPACITY AT 3.6 MPa PRESSURE

The amount of methane stored by compression alone in an empty cylinder at 14 MPa (2000 psig) would be about 108 grams/liter.

As can be seen from Figure 4, the storage capacity of Sample C15C is superior to any thus far reported in the literature and is 70% that of compression storage at 14 MPa. If, by some chemical means, the specific adsorption of C15C could be enhanced from 0.100 to 0.120 g/cc, at 3.6 MPa the storage capacity would also increase by 20%. Such a goal is not unreasonable but no method of attaining it has been identified as yet.

Caution should be used, however, when comparing an adsorption system with a compression storage system on the basis of methane storage capacity alone. The amount of natural gas stored by both systems is always greater than the amount delivered but because of the shape of the adsorption isotherm, this latter quantity is not a linear function of pressure for the adsorption system as it is for simple compression storage. The most practical method of determining the amount of methane that can be delivered by an adsorption system is to construct a bench-scale apparatus. This was accomplished by connecting the 75 cm³ stainless steel cylinder filled with the appropriate adsorbent to a gas manifold and a wet test meter. To determine a practical delivery capacity for the various adsorbents, the cylinder described above was pressurized with methane and the methane was then slowly bled through a wet test meter over a 2-hour period. The quantity of methane delivered by the system in cycling from 3.6 MPa (500 psig) to 101.4 KPa (0 psig) was determined directly. An air stream at 25°C was directed at the cylinder to maintain temperature during desorption. Table 14 lists the quantity of methane delivered in grams per liter and the percentage of the total adsorbed which this represents for 16 of the carbon samples and two of the best zeolite samples.

D. Discussion of Results

As can be seen from Table 14 in the previous section, Carbon Sample C15C exhibits the best performance, most methane delivered, of all samples tested. However, this sample does not have the highest specific adsorption for methane nor the highest micropore volume. It does have one of the highest specific surface areas and the highest packing density of all carbons tested. These two parameters then become the most desirable characteristics of a good sorbent material for an adsorption storage system.

Unfortunately, the methods by which the specific surface area of an activated carbon can be increased, by the creation of micropores through catalytic oxidation or chemical leaching, also decrease the packing density.

Table 14. METHANE DELIVERED BY ADSORBENT SYSTEMS
CYCLED FROM 3.6 MPa TO 101.4 KPa

<u>Sample Designation</u>	<u>Grams of Methane per Liter of Storage</u>	<u>Fraction of Total in Storage</u>
C3	34.8	91.6%
C4	45.2	86.8%
C5	36.5	86.1%
C6	41.4	92.8%
C7	54.8	86.8%
C8	31.8	85.1%
C9	51.4	86.7%
C10	49.2	84.1%
C11	51.8	84.9%
C12	48.4	86.9%
C13	40.1	93.3%
C14	39.4	94.3%
C15	56.3	84.0%
C15C	62.0	83.8%
C16	55.9	85.5%
C17	51.0	89.4%
Z3	44.1	84.7%
Z4	44.1	87.6%

Thus, for example, Amoco GX-32 with a high specific surface area also has a low packing density. Therefore, improvements in storage capacity of carbons like C15C by increasing surface area will likely reduce packing density.

On the other hand, none of the carbons used in this study have been optimized for methane adsorption. The chemical nature of these activated carbons, surface groups, or chemical additives, were optimized for the adsorption of active gases such as HCN or H₂S. A crude index of a carbon's ability to adsorb a chemical species can be determined by dividing its specific adsorption in g/g at a fixed pressure by the specific surface area in cm²/g and multiplying by Avogadro's number over the molecular weight of the adsorbed species. The resulting quantity is the coverage in terms of molecules adsorbed per cm² of surface area. For example, Equation 7 is a calculation for the coverage of C17 at 3.6 MPa.

$$\frac{0.115 \text{ g/g}}{1280 \times 10^4 \text{ cm}^2/\text{g}} \times \frac{6.023 \times 10^{23} \text{ molecules/mole}}{16 \text{ grams/mole}} = 3.38 \times 10^{14} \text{ molecules/cm}^2 \quad (7)$$

Table 15 lists the methane coverage for representative carbon samples. It can be seen that the coverage for C15 is about average. If the methane coverage of C15 can be increased to equal that of C17 or C8, without altering the surface area or the packing density, a 35% improvement in methane adsorption and a 25% improvement in methane storage capacity would result.

A comparison of the methane coverage for pure carbons having high internal porosity with substantial pore volume contributed by pores of less than 200 Å radius (C3, C6, and C8) with those carbons having virtually no pores smaller than 200Å radius (C10, C15, and C16) indicate no significant difference. Thus, micropore structure appears to contribute no additional benefits to methane adsorption. It should be noted that Carbons C5, C9, and C11 through C14 cannot be included in this evaluation because of their substantial inorganic content, see Table 2.

A comparison of methane coverage versus pH for the carbon samples indicates a slight positive relationship with the most basic carbons having a high methane coverage. Figure 5 plots methane coverage from Table 15 versus pH values from Table 2. However, here too, no significance can be assigned to this observation since the pH contribution of the inorganic materials present in each sample was not determined.

E. Conclusions

The following conclusions can be drawn from the Task 1.1 results.

1. Activated carbons proved superior to zeolites in this program, both on a grams/gram and grams/liter basis.
2. The best performance, defined here as methane delivered per liter of storage, was turned in by North American Carbon G210 crushed to a packing density of 0.58 g/cm³.
3. High surface area and high packing density are desirable attributes for candidate sorbent materials.
4. Results indicate that there is room for improvement in the performance of even the best carbon evaluated.

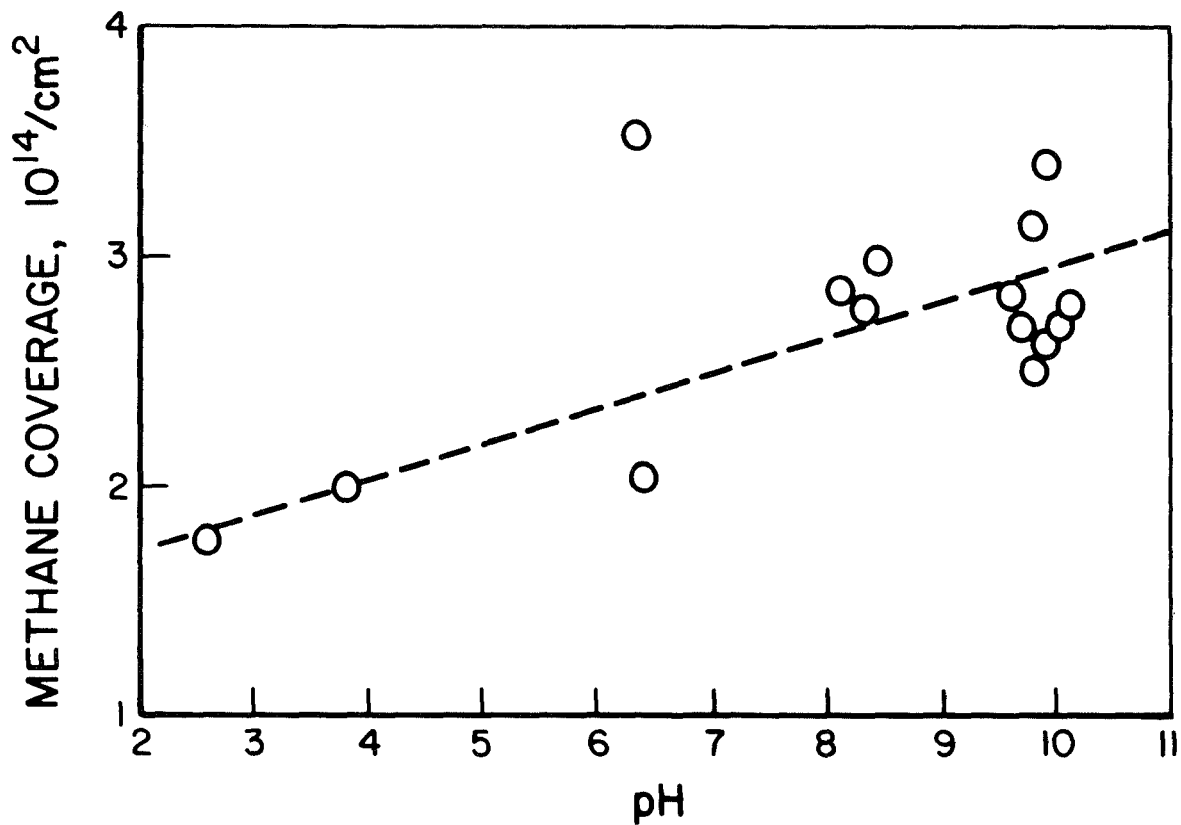


Figure 5. RELATIONSHIP BETWEEN COVERAGE AND pH

5. There is hope that an adsorption storage system operating at a maximum pressure of 3.6 MPa can be developed having a storage capacity equal to compression storage at 14 MPa (2000 psig).

Table 15. METHANE COVERAGE FOR CARBON SAMPLES AT
3.6 MPa OF METHANE

<u>Sample Designation</u>	<u>Coverage in Molecules/cm² x 10¹⁴</u>
C3	2.59
C4	2.96
C5	2.85
C6	1.99
C7	2.72
C8	3.53
C9	2.78
C10	3.12
C11	2.82
C12	2.70
C13	2.03
C14	1.78
C15	2.62
C16	2.83
C17	3.38

Task 1.2 Modeling Effort

The purpose of this modeling effort is to develop a simplified model suitable for predicting weight, capacity, and vehicle range as well as estimate the change in each parameter required to obtain a methane storage capability for adsorption systems consistent with the range, weight, and fuel tank capacity of conventional (gasoline fueled) and high-pressure CNG vehicles. Although a rigorous analytical model was beyond the scope of this work, the following results are sufficient to provide a semi-quantitative comparison of compression storage and adsorption storage.

A. Calculations to Determine the Weight of a Storage Tank

Considerable developmental work has been performed to reduce the weight of D.O.T. approved high-pressure gas cylinders for vehicular applications. Aluminum-fiberglass composite cylinders having an internal volume of 38ℓ, an operating pressure of 21 MPa (3000 psig), a burst pressure of 52 MPa, and a mass of only 28 Kg (62 lbs) are currently available from commercial suppliers. However, in order to accurately assess the performance of a low pressure

adsorption storage system, it would be necessary to determine the weight of a storage tank optimized for operation at a maximum pressure of 3.6 MPa (500 psig). Unfortunately, at the present time, there is little interest in weight reduction programs for cylinders operating in this pressure range. As a consequence, the 28 Kg cylinder was used as a storage container for both the high pressure model and the adsorption model systems.

B. Model Automobile

A state-of-the-art compact class automobile was chosen having the specifications listed in Table 16. These are the specifications for a gasoline powered Ford Tempo GL 5-speed. This size automobile was chosen for a model since its performance characteristics are expected to be more sensitive to changes in weight and fuel composition than heavier vehicles.

Table 16. MODEL AUTOMOBILE

Inertial Weight	2750 lbs (1250 Kg)
Frontal Area	20.6 ft ² (1.91 M ²)
Drag Coefficient	0.36
Road Horsepower at 50 mph	11.5 hp
Aerodynamic Drag at 50 mph	6.0 hp
Engine Displacement	140 cu. in. (2301 cc)
Compression Ratio	9.0:1
Power (SAE Net)	89 bhp at 4700 rpm
Trunk Space	13 ft ³ (0.37 M ³)
EPA Highway	41 mpg
EPA City	27 mpg

Road horsepower requirements and miles per gallon on gasoline were calculated for a constant speed of 50 mph (80 km/hr) as a function of vehicle weight using the following assumptions:

1. The EPA highway mpg approximates the fuel economy at a constant 50 mph (80 km/hr)
2. Aerodynamic drag is unchanged by changes in vehicle weight
3. Fuel consumption is related to road horsepower and engine efficiency requirements.

The power required to maintain a constant velocity (P_w) is the sum of the power required to overcome rolling resistance (P_{RO}) including drive train

losses and accessory requirements plus the power required to overcome aerodynamic drag (P_L).

$$P_w = P_{RO} + P_L \quad (8)$$

P_{RO} , in turn, is proportional to the product of the velocity (V), the coefficient of rolling resistance (C_R), and the vehicle weight (W).

$$P_{RO} = C_R \cdot W \cdot V \quad (9)$$

Reference 9 supplies all of the necessary information required to calculate changes in road horsepower requirements as a function of changes in weight for our model automobile. Table 17 lists the results of these calculations.

Table 17. ROAD HORSEPOWER REQUIREMENTS AND MPG AS A FUNCTION OF VEHICLE WEIGHT AT A CONSTANT 50 MPH

<u>Vehicle Weight, lbs</u>	<u>Road HP</u>	<u>MPG</u>
2000	10.4	47
2500	11.5	41
3000	12.6	37
3500	13.7	34

The expected EPA city mpg was also calculated as a function of vehicle weight. The approach taken here is similar to that used by Kukkonen in Reference 10. Table 18 lists the results.

Table 18. EPA CITY MPG AS A FUNCTION OF VEHICLE WEIGHT

<u>Vehicle Weight, lbs</u>	<u>MPG</u>
2000	33.7
2500	27
3000	22.5
3500	19.3

C. Fuel Consumption for Dual-Fuel Mode

Before the operational range of our model vehicle can be calculated, it is necessary to determine the fuel consumption expected during natural gas

operation. Since a gasoline fueled spark ignition (SI) engine can be made to run on natural gas with only minor modifications, it has become standard practice in the U.S.A. and elsewhere to perform dual-fuel conversions. Such conversions allow the driver to select the fuel desired and to change from one fuel to the other at will. Such conversions do not take advantage of all of the positive attributes of natural gas as an SI engine fuel but, since such conversions are common, the decision was made to include a dual-fuel mode in our model.

Work carried out by the University of British Columbia allows some quantification of the fuel consumption for gasoline engines converted to natural gas fuels.¹¹ This work indicates that the overall operating efficiency of a vehicle equipped with a natural gas-fueled converted gasoline engine is, at best, 12% better on natural gas than the same engine on gasoline, provided modifications are made to the timing curve to advance the spark when operating on natural gas. A more detailed discussion of engine efficiency in the dual-fuel mode can be found in Part 1 of Appendix C.

D. Dedicated Engine Mode

Natural gas exhibits many excellent qualities as an internal combustion (IC) spark-ignited engine fuel. Chief among these qualities is the high octane number of 130 RON. However, to take advantage of this high octane characteristic, it is necessary to use high compression ratios which are not compatible with gasoline operation.

An engine designed to make optimum use of natural gas as a fuel is classed as a dedicated engine. Such an engine could be expected to be 25% more efficient on natural gas than the same displacement size engine running on gasoline. A more detailed discussion of the efficiency of a dedicated engine can be found in Part 2 of Appendix C.

E. Energy Density of Pressurized Storage

In addition to knowing the efficiency and, therefore, the range per unit mass of fuel, it is also necessary to know the total amount of fuel stored on board. Because the term "pipeline quality" natural gas does not carry with it a definitive gas composition, it is necessary, at this point, to define terms. For purposes of this model, natural gas will have an average molecular weight of 16.0 and a lower heating value of 11,800 Kcal/kg (21,250 Btu/lb). By

placing the average molecular weight equal to that of methane, we can apply, without further adjustment, the data gathered for methane adsorption on carbons. This leads, however, to underestimating vehicle range by a factor equal to the ratio of the actual average molecular weight of a specific gas sample to that of methane.

The amounts of natural gas (methane) that can be stored per liter of volume at various pressures is summarized in Table 19.

Table 19. RELATIONSHIP BETWEEN PRESSURE AND METHANE STORAGE CAPACITY AT 23°C FOR AN EMPTY CYLINDER

	<u>Pressure</u>		<u>Energy Density,</u>
	<u>psig</u>	<u>atmospheres</u>	<u>Grams/Liter</u>
500	35	3.6	24
1000	69	7.0	50
1500	103	10.4	79
2000	137	13.9	108
2500	171	17.3	135
3000	205	20.8	160

We can now utilize this table to determine the fuel on-board given the pressure and volume of the containment vessels. There is one additional correction that must be applied to an actual system. State-of-the-art dual-fuel systems cycle between a maximum tank pressure of 16.7 to 20.8 MPa and a minimum tank pressure of 0.3 to 0.4 MPa depending on manufacturer. Thus, of the 108 grams/liter stored at 13.9 MPa, only 106 g/l is delivered by cycling the system from 13.9 MPa to 0.3 MPa. However, for purposes of calculation, the higher value of 108 g/l will be used to offset somewhat the error induced by using 16 as the average molecular weight of natural gas.

F. On-Board Storage

The calculation of the "fuel on-board" for an adsorption system is more complex than for an empty cylinder. Gas can be stored both by adsorption on the substrate and by compression in void spaces. Furthermore, the quantity of methane adsorbed is not a linear function of pressure but follows a Langmuir-type isotherm. Rather than address these problems from a theoretical point of view, actual experimental values for the best carbon identified in Task 1.1

were used. North American Carbon G-210 crushed to a packing density of 0.58 g/cc was loaded into a cylinder and cycled between 3.6 MPa and 170 kPa (500 psig and 10 psig respectively). About 58 grams of methane were delivered per liter of carbon during the discharge cycle. It is premature to conclude that the 58 g/l of methane delivered by the best carbon represents a maximum value for absorbent systems in general.

G. Additional Weight of Gas Storage Hardware

In order to determine the performance and range on natural gas of a vehicle operating in the dual-fuel mode, it is necessary to know the additional weight added to the vehicle by the gas storage system. Table 20 summarizes the additional weight of one, two, and three tank storage systems based on 38-liter, internal volume, aluminum-fiberglass composite cylinders. The 28-Kg high pressure cylinder previously described is used to calculate the weight of the various storage systems. The packing densities of the carbon adsorbents are set at 0.58 g/cc, which represents the most dense carbon evaluated in this program. A single 38l tank with manifold and bracketing hardware would occupy about one-third of the available trunk space in our model vehicle.

Table 20. APPROXIMATE MASS OF STORAGE SYSTEMS IN Kg

<u>Pressurized Storage</u>	<u>1 Tank</u>	<u>2 Tanks</u>	<u>3 Tanks</u>
	----- Kg -----		
Fuel	6	12	18
Tanks	28	56	84
Brackets	10	20	30
Conversion Kits	<u>25</u>	<u>25</u>	<u>25</u>
Total	69	113	157
<u>Adsorption Storage</u>	<u>1 Tank</u>	<u>2 Tanks</u>	<u>3 Tanks</u>
Fuel	3	5	7
Tanks	28	56	84
Brackets	15	30	45
Manifold	30	30	30
Carbon	<u>22</u>	<u>44</u>	<u>66</u>
Total	98	165	232

H. Vehicle Range and Fuel Efficiency

Having determined the weight and storage capacity of the various storage systems and the relative fuel efficiencies of the SI engine operating on gasoline and on natural gas in both dual-fuel and dedicated modes, it is now possible to combine these relationships with the relationship between total vehicle weight and vehicle fuel economy to calculate both gasoline equivalent mpg and range on natural gas for the various storage options. Table 21 compares fuel efficiency on gasoline and the estimated range on natural gas for the various storage options for a model vehicle operating in the dual-fuel mode on the EPA-city cycle. Table 22 is a similar comparison for the constant speed approach. Results in Tables 21 and 22 assume that pressurized storage system cycles between 20.8 MPa (3000 psig) and 0.3 MPa (25 psig) while adsorption storage systems cycle between 3.6 MPa (500 psig) and 0.2 MPa (10 psig). Range on natural gas is based on the results of the study discussed in Appendix C.

The projected range of the model vehicle equipped with a dedicated engine would be about 10% longer than those listed for various storage options in Tables 21 and 22.

I. Discussion of Results

Fuel Economy: The results of our model indicate that a significant penalty is paid, up to 15%, in the form of a loss in fuel economy on the EPA city cycle when a dual-fuel capability is added to the base automobile. On the other hand, there is little additional performance loss with adsorption storage over that experienced with pressurized storage. This is an important result since one of the past objections to adsorption storage has been the added weight of the sorbent bed. This has added significance since our model calls for heavier brackets and manifold hardware with adsorption storage than with pressurized storage. In other words, there is no significant difference between pressurized storage and adsorption storage in the fuel economy loss experienced in the dual-fuel mode.

Range: The range of a vehicle is directly related to the fuel stored on-board and it is generally accepted in alternatively fueled vehicle circles that for an alternatively fueled vehicle, regardless of the propulsion system,

Table 21. ESTIMATED FUEL ECONOMY AND RANGE ON THE EPA CITY CYCLE
FOR VEHICLE OPERATING IN A DUAL-FUEL MODE

<u>Storage System</u>	<u>Gasoline Fuel Economy*</u>		<u>Range on Natural Gas Only**</u>	
Gasoline Only	11.5	(27)		
Pressurized Storage (20.8 MPa)				
1 Tank	10.9	(25.4)	95	(59)
2 Tanks	10.5	(24.6)	182	(113)
3 Tanks	10.1	(23.7)	262	(163)
Adsorption Storage (3.6 MPa)				
1 Tank	10.7	(25.1)	32	(20)
2 Tanks	10.2	(23.9)	63	(39)
3 Tanks	9.7	(22.8)	93	(58)

* Kilometers per liter (miles per gallon).

** Kilometers (miles).

Table 22. ESTIMATED FUEL ECONOMY AND RANGE AT A CONSTANT SPEED OF 80 Km/hr IN THE DUAL FUEL MODE

<u>Storage System</u>	<u>Gasoline Fuel Economy*</u>		<u>Range on Natural Gas**</u>	
Gasoline Only	18	(41)	--	--
Pressurized Storage (20.8 MPa)				
1 Tank	17	(40)	148	(92)
2 Tanks	17	(39)	290	(181)
3 Tanks	16	(38)	428	(266)
Adsorption Storage (3.6 MPa)				
1 Tank	17	(39)	51	(32)
2 Tanks	16	(38)	101	(63)
3 Tanks	16	(37)	150	(93)

* Kilometers per liter (miles per gallon).

** Kilometers (miles).

to make significant market penetration it must have a range of at least 100 miles between refuelings on the EPA city cycle. Although this is less critical for a dual-fuel vehicle, it is absolutely necessary for a dedicated vehicle.

As can be seen in Table 21, our model predicts that this can be achieved with a pressurized storage system operating at 20.8 MPa (3000 psig) equipped with two 38ℓ storage tanks. On the other hand, the state-of-the-art adsorption system with three 38ℓ tanks can only manage 58 miles (93 km). It is possible that future research and development can boost the storage capacity of sorbent beds based on carbon to the point where a 100 mile range on the EPA city cycle is feasible with three tanks. Also, it should be recognized that this model assumes that storage is limited to the space available in the automobile trunk and assumes cylindrical shaped containers, the maximum possible being three 38ℓ tanks. If, however, storage volumes in excess of 180ℓ (about five 38ℓ tanks) can be made available either by locating tanks in other unused spaces, by redesigning the automobile, or by using more efficient geometrical shapes, a state-of-the-art adsorption system could achieve a range in excess of 100 miles on the EPA city cycle at the expense of an additional weight increase without further improvements in the sorbent beds. It is unlikely, however, that an adsorption storage system will ever be designed with the energy density of a pressurized storage system charged to 20.8 MPa.

TASK 2. LITERATURE SURVEY AND ADVANCED STORAGE MEDIUM EVALUATION

The objective of this task was to survey the available literature and identify materials and concepts with the potential to store methane at low pressures. The survey concentrated on the concepts of clathration, encapsulation, and dissolution. A 33-page evaluation of clathrate storage concepts, complete with its own bibliography, is included as Appendix D. A 27-page discussion of methane storage by dissolution is included as Appendix E. A summary of the findings is provided below.

A. Clathration of Methane

The term clathrate was originally defined as a compound " in which two or more molecular components are associated without ordinary chemical union but through complete enclosure of one set of molecules in a suitable structure formed by another.¹² Thus, the term clathrate implies guest molecules caged within spaces formed by the crystal structure of the host. The phenomenon is dependent primarily upon the relative size of the holes in the host crystal structure and size of the guest molecules.

Although there is considerable work in progress toward developing the know-how for tailoring new clathrate hosts for specific guest molecules, most of the work is oriented toward biological and catalytic applications such as enzymes and ionic species. Practically no references have been found for tailoring the clathrate host molecules for small and relatively inert molecules such as methane or the inert gases; thus, tailor-making host molecules for clathrating methane still requires a largely empirical approach in development. Nonetheless, there are a few precepts available to guide such a development:

- Clathrate formulation depends on the ability of the host molecules to form a crystal habit which has cavities large enough to accommodate the specified guest molecules.
- The crystal habit formed in the presence of the guest molecule is usually different from the normal crystal structure found in the absence of the guest.
- The primary prerequisite for the host is hydrogen-bonding or other complex forming ability while a secondary prerequisite is a molecular geometry which will crystallize in the presence of the guest to a structure with cavities sized to accommodate the guest.

Stability is of major importance since it controls not only whether the methane can be contained at reasonable pressures under ambient conditions but also the conditions under which the methane can be released. The hydrate of methane, for example, is not stable enough since it requires a pressure greater than 28 MPa to exist under ambient temperature conditions. On the other hand, the hydroquinone/methane clathrate is too stable. Thus, although it can be stored at ambient temperature and pressure, it requires an elevated temperature or the introduction of a solvent to release the methane. Obviously, a compromise is in order so that the clathrate will be stable at ambient temperature, at a reasonable pressure of 1.5 to 3.6 MPa, so that methane release can be achieved and controlled by pressure reduction.

The parameters controlling stability include:

- Hydrogen bonding power of the groups through which the crystallization occurs.
- Geometry and symmetry of the host molecule as it affects the structure of the crystal habit formed.

The capacity of a clathrate for methane, on the other hand, depends on two factors:

- How many host molecules are required to provide one guest "cage" (i.e., the unit cell)
- Molecular weight of the host molecules.

The structure of the unit cell and, therefore, the number of host molecules per guest molecule is dependent in a very complex way on various crystallographic factors and is beyond prediction at this time except perhaps for certain "hexamer" clathrates which tend to give a 3:1 host to guest ratio. Thus, molecular weight may be the factor of greatest importance in determining capacity and is suitable for preliminary evaluation.

It may be possible that some higher molecular weight molecules with complex symmetries form clathrate structures in which the host/guest ratio is significantly less than the 3:1 found for the hexamer types. Others may form structures with cavities sufficiently large to accommodate two or more methane molecules as in the case of the urea tunnel adducts. In the latter case, diffusion would be the primary barrier to decomposition and the system would function in a manner analogous to that of absorption in a zeolite. Most of

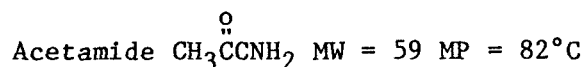
the clathration entities forming larger cavities (and there are a lot of them including Dianin's compound, the Werner complexes, deoxycholic acid, urea and thiourea cyclodextrin, etc.) have been evaluated only with larger guest molecules (usually the solvent used) at atmospheric pressure and not with permanent gases such as methane under elevated pressures. For example, urea adduction of the homologous n-paraffin series has been extended downward to include propane and butane which are stable at atmospheric pressure only at subzero temperatures. However, it is possible that adduction could be extended to include methane and ethane as well at ambient temperatures and elevated pressures.

It is apparent from the above discussion that any future work toward the development of clathrate systems for on-board storage of natural gas will be highly empirical in approach, although guided by the precepts outlined above. Two as yet unreported possibilities are a urea-methane adduct and an acetamide-methane clathrate.

1. Urea/Methane Adduct

The methane/urea adduct, if it exists, probably will show a mole ratio of about 1:3 or a weight ratio of about 16:180 = 0.089 g CH₄/g of urea. This is of the same magnitude as that for activated carbons but is not as good as the methane hydrate (0.155 g/g H₂O).

2. Acetamide/Methane Clathrate



Methane clathrates of acetamide have never been demonstrated but are good candidates because of good hydrogen-bonding ability of the amide group and low molecular weight. If a host/guest ratio of 3:1 is achieved, the weight ratio would be 0.09 g CH₄ per g acetamide. The possible methods of preparation include crystallization from a solvent or condensation from a vapor.

Conclusions:

As reported above, the highest mass ratio of guest to host is found in methane hydrates, 0.155 g/g. However, methane hydrate is not stable under ambient temperature conditions at pressures below 28 MPa. The best mass ratio that can be expected from other proposed but as yet unidentified methane clathrates is about 0.09 g/g. This is slightly less than the mass ratio already

available with state of the art carbon based adsorption systems. Also, since a clathrate-based storage system is likely to be relatively more difficult to cycle than an adsorption-based storage system, further work with clathration-based systems for on-board storage is not recommended. However, clathration-based systems may ultimately prove useful for stationary applications where weight and volume are not critical. Therefore, recommendations for future research with clathrates is presented at the conclusion of Appendix D, despite its lack of utility as an on-board storage concept.

B. Dissolution of Methane

In general, the data conforms well to the classical views of Hildebrand¹³ on regular solutions, i.e., solutions "in which orienting and chemical effects are absent and in which the distribution and orientations are random..." In other words, methane behaves in most solvents, including the rare gases, as non-polar molecules subject primarily to van der Waals dispersion forces. The primary parameters controlling solubility in regular solution theory are the molal volume and the Hildebrand solubility parameter relative to that of methane. The solubility parameter or cohesive energy density is defined as:

$$S = \left(\frac{\Delta H_T^V - RT}{V_1} \right)^{1/2} \quad (10)$$

where:

ΔH_T^V = Heat of vaporization at solution temperature

V_1 = Molal volume of Component 1.

Since the solubility parameter of methane is at the lower end of the scale ($S = <6$), the best solvents for methane are the perfluorocarbons, the silicones, and the lower aliphatic hydrocarbons such as propane. The best solvent for methane so far found is propane, in which methane is soluble to the extent of 0.15 mole fraction or 0.063 lb CH_4 /lb solvent. However, this is a lower capacity on a lb/lb basis than can be expected from adsorption on activated carbon at this pressure.

On a mole fraction basis, the solubility of methane in octamethyl cyclo-tetrasiloxane (0.32) and in perfluoro η -heptane (0.28) is greater than the propane but on a gravimetric basis the solubilities are much lower (0.025 and

0.016, respectively) due to the high molecular weights of these solvents. Nevertheless, it is possible that lower molecular weight perfluorocarbons and silicones could exhibit acceptable methane solubilities on a mass ratio basis. However, information regarding methane solubility in these solvents is not available in the literature.

In the aliphatic hydrocarbon series, the solubility of methane decreases with increasing molecular weight as the result of the solubility parameter increasing with increasing molecular weight. This trend of decreasing methane solubility with increasing molecular weight continues up to about C₆ (n-hexane). Above C₆, however, the solubility of methane on a mole fraction basis increases with increasing molecular weight to 0.32 for C₃₀ (squalane). Unfortunately, the solvent molecular weight increases more rapidly than solubility so that the solubility on a gravimetric basis continues to decrease with increasing molecular weight. These results are based primarily upon data for straight chain hydrocarbons, squalane being the exception with 6 methyl groups on a straight chain of 24 carbons. However, the solubility of methane in isobutane (2-methyl propane), 0.061 g/g, and in neo pentane (2,2-dimethyl propane), 0.057 g/g, suggest that the decrease in methane solubility on a gravimetric basis with increasing molecular weight may be less severe for highly branched paraffin hydrocarbons. Unfortunately, data on the solubility of methane in highly branched high molecular weight paraffins is not available.

The solubilities of methane in aliphatic alcohols appear to be greater, at the same solubility parameter value, than for other solvents having no hydroxyl groups. This suggests that hydrogen bonding may contribute in some as yet unidentified manner to enhancing methane solubility. This further suggests that it may be possible to enhance the adsorptive capacity of solid adsorbents by providing a multiplicity of hydroxyl groups on the surface.

The solubility data for the lower paraffin hydrocarbons (e.g., propane) actually represent the concentration of methane in the liquid phase of a mixture in equilibrium with a vapor phase containing both methane and solvent vapor. If the equilibrium concentration of methane in propane at 25°C and 3.6 MPa total pressure is corrected to 3.5 MPa partial pressure of methane, the solubility would increase from 0.063 g/g to 0.11 g/g but the total system pressure would also increase. Likewise, the solubility of methane in liquid ethane at 25°C and a methane partial pressure of 3.6 MPa is 0.35 g/g, however,

system pressures exceeding 7 MPa would be required. If we could tie down ethane or propane as ethyl or propyl groups and still maintain their solvent capacity for methane, gravimetric capacities similar to those of the best adsorbent systems might be achieved.

Conclusions

No high molecular weight solvent has been identified which can dissolve enough methane to be competitive with adsorption storage. On the other hand, no method has been identified to prevent low molecular weight highly volatile solvents such as propane, in which methane is highly soluble, from vaporizing along with the methane during system discharge. Although this is not considered a serious problem with propane, it does present a significant environmental hazard when low molecular weight fluorocarbons and silicones are considered. The possibility of tying low molecular weight solvents to polymer backbones, however, is at least within the realm of speculation, and warrants some future consideration.

TASK 3. FUTURE RESEARCH AND DEVELOPMENT RECOMMENDATIONS

Theoretical and experimental results obtained in this program clearly indicate the potential of low-pressure natural gas storage systems (based on carbons as the storage medium) for vehicular applications. As the results show, by adsorption on carbons commercially available today, it is possible to store at 500 psi approximately 70% of the volume of methane that can be stored at 2000 psi in a compressed (no adsorbent) natural gas system of the same volume, and about 45% of that stored at 3000 psi.

The cost of compressors capable of compressing natural gas to pressures greater than 2500 psi contributes a significant amount to the total cost of natural gas-fueled vehicle fleets. Consequently, lowering the compression requirements could significantly impact the total system cost and make natural gas a more attractive transportation fuel.

The potential of low-pressure storage systems has been demonstrated, although the range of vehicles operating on adsorption systems is less than for high pressure systems. Consequently, there is need for additional research, development, and optimization before these low-pressure systems can be implemented. Following is a list outlining the areas that must be resolved.

- 1) There is a need to continue research with carbons to improve their storage capacity. The likely approach to be taken is the manipulation of the surface chemistry of the carbon. As was reported in Task I, certain of the carbon samples gave a higher degree of coverage of methane than others, most notably those with high pH values on the acid-base test. An understanding of the specific surface groups which enhance methane adsorption can lead to a method of increasing methane storage capacity by increasing the population of the desirable surface group.
- 2) During the adsorption of methane on carbon, a significant amount of heat is generated. Although some work has been performed with systems using 5 liter storage cylinders, no one has addressed the problem of heat dissipation in larger cylinders.
- 3) Golovoy⁷ has observed that hydrocarbons larger than C₃ are strongly adsorbed on high surface area carbons during the charging cycle to the point that they do not desorb on discharge. It is necessary that the impact of these materials upon cycling efficiency be determined and several methods for removing them from the fuel prior to loading be evaluated.
- 4) It is expected that the use of low pressure adsorption systems in place of high pressure storage systems will reduce the capital investment required for a refueling station but may increase the cost of the vehicular

storage system. It is necessary to conduct an economic evaluation to quantify the expected savings which will be realized by reduced compressor costs so that an upper limit can be placed on the cost of the vehicular adsorption storage system.

- 5) To date, most adsorption system experiments have been conducted at about 25°C. However, real world methane storage systems may be exposed to environmental extremes of from -30° to +60°C with daily temperature swings of as much as ±20°. It is necessary to determine the impact upon both performance and safety of daily and annual temperature variations.
- 6) Vibrational settling of adsorbent may present a problem in actual vehicular systems. This problem, if it exists, needs to be identified early enough for corrective measures to be taken prior to actual full-scale demonstration tests.

The above issues need to be resolved in order that enlightened full-scale demonstration tests can be undertaken.

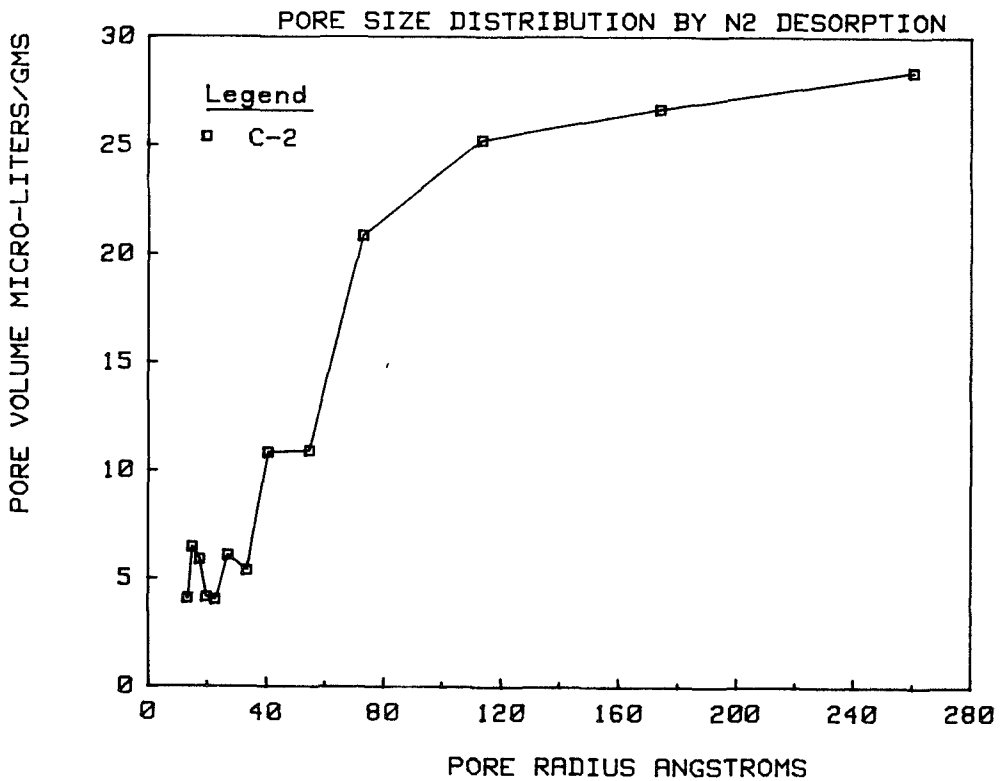
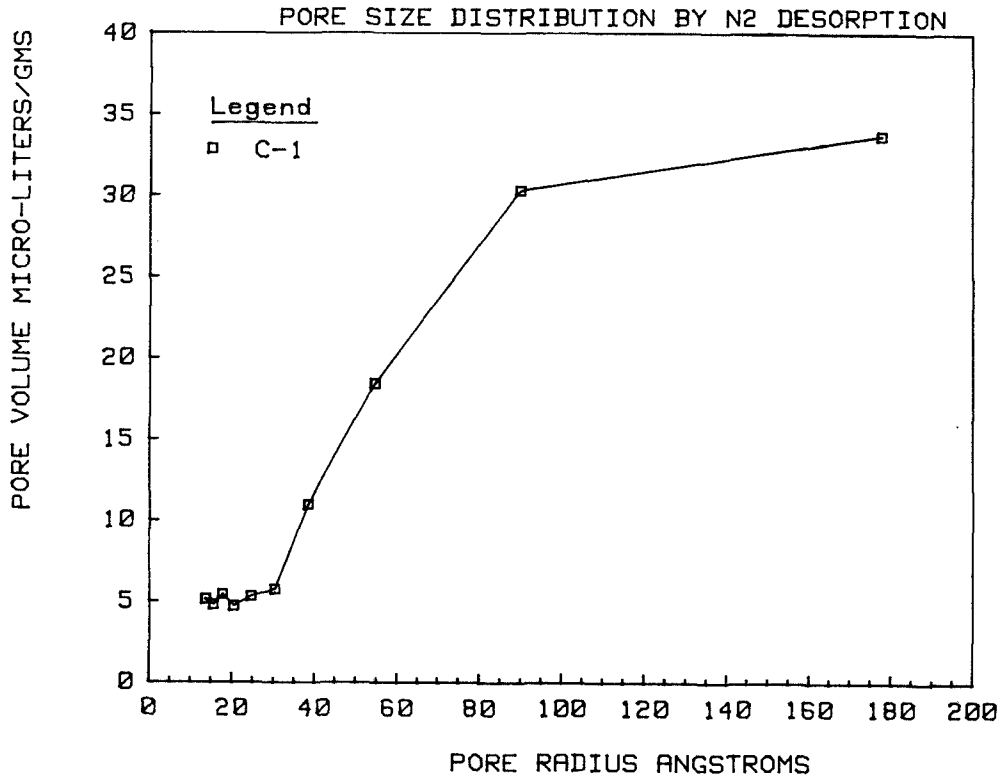
References

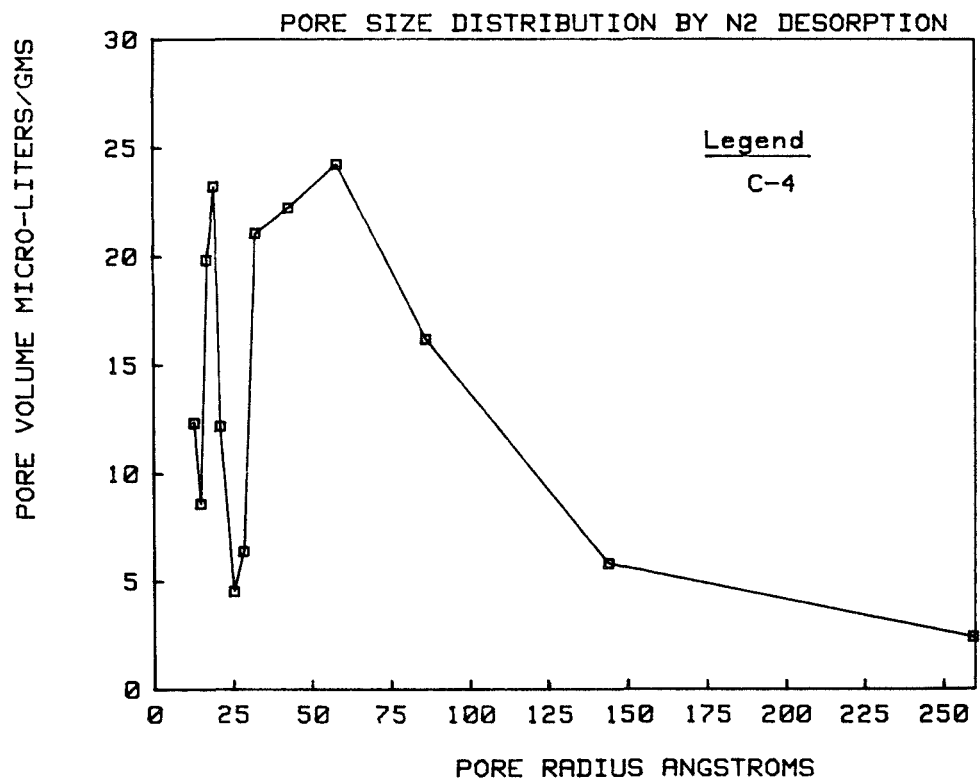
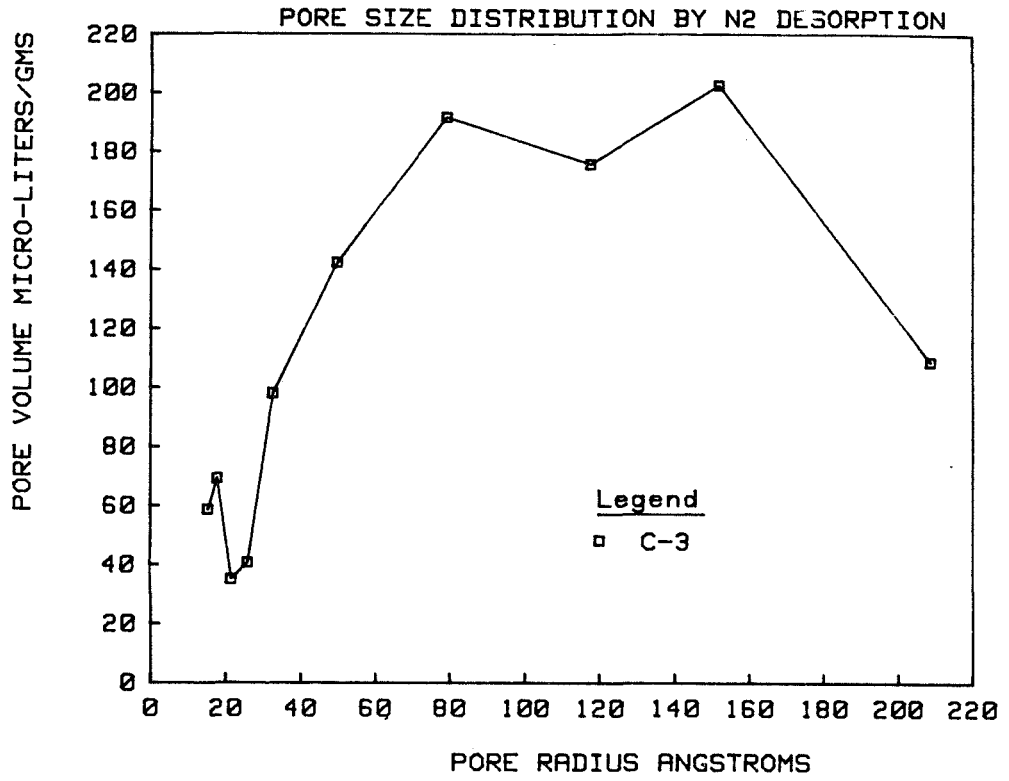
1. Braslaw, J., Nasea, Jr., J. and Golovoy, A., "Low Pressure Methane Storage System for Vehicles." Paper presented at the 4th International Conference on Alternative Energy Sources, Miami, December 1981.
2. Otto, K., "Adsorption of Methane on Active Carbons and Zeolites." Paper presented at the 4th International Conference on Alternative Energy Sources, Miami, December 1981.
3. Straszhesko, D. N., Ed., Adsorption and Adsorbents No. 1. New York: John Wiley, 1973.
4. de Boer, J. H., The Dynamical Characteris of Adsorption. London: Oxford University Press, 1968.
5. Brunauer, Stephen, The Adsorption of Gases and Vapors, Volume I. Princeton: Princeton University Press, 1943.
6. D. W. Breck, "Crystalline Molecular Sieves," Journal of Chemical Education 48m 678 (1964).
7. Amos Golovoy, "Sorbent-Containing Storage Systems for Natural Gas Powered Vehicles," SAE Conference Proceedings P-129 Page 39, June 1983. SAE Inc. Warrendale, PA 15096.
8. S. S. Barton, J. R. Dacey, and D. F. Quinn, "High Pressure adsorption of Methane on Porous Carbons," Preprint. Dept. of Chemistry and Chemical Engineering, Royal Military College of Canada, Kingston, Ontario.
9. "Car and Driver" Volume 29, Number 3, Page 81, September 1983.
10. Kukkonen, C. A., "Hydrogen as an Alternative Automotive Fuel," Society of Automotive Engineers, Paper No. 810349 (1981).

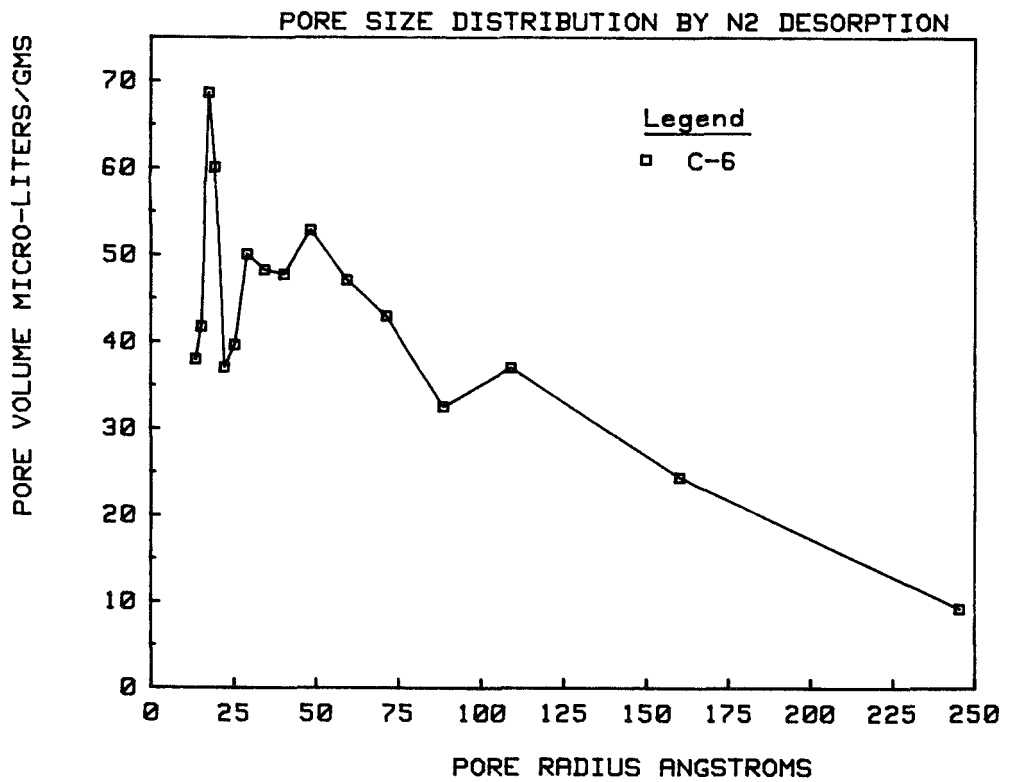
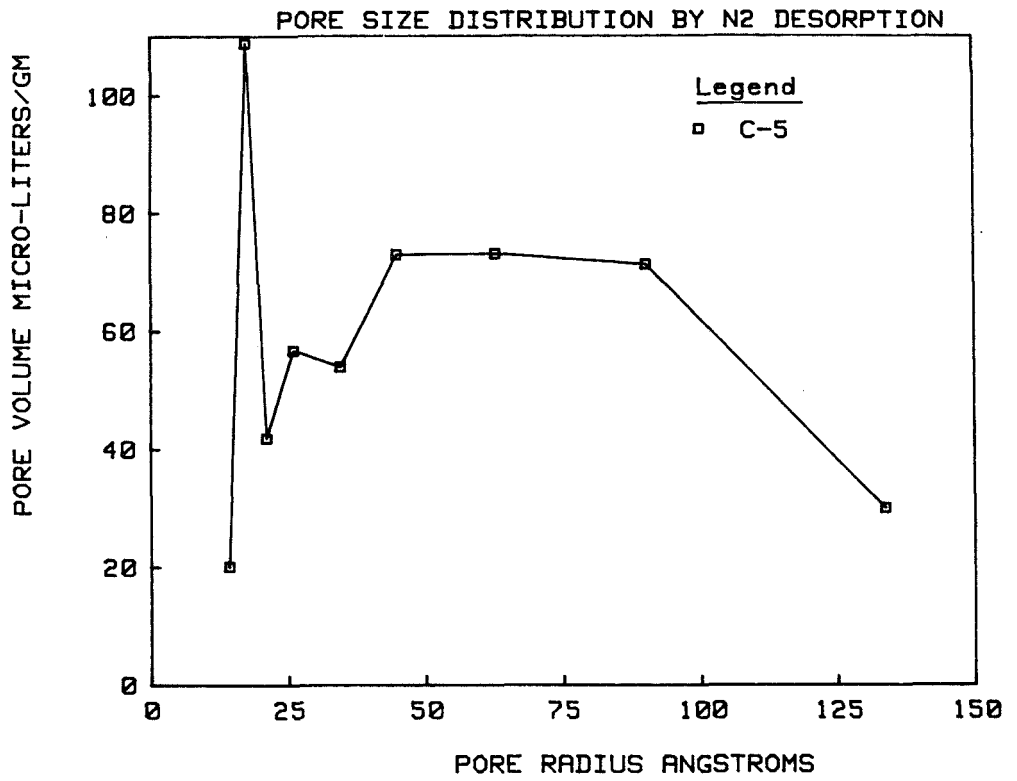
11. Sheraton, D. F., "British Columbia Methane Power Vehicle Program Test Results," Symposium papers, Nonpetroleum Vehicular Fuels III, 1982.
12. Schaeffer, W. D. and Dorsey, W. S., "Clathrates & Clathrate Separations." Advances in Petroleum Chemistry & Refining, Vol. VI, Chap. 3, pp 119-167, (1962).
13. Hildebrand, Joel H., Regular and Related Solutions; the Solubility of Gases, Liquids, and Solids. Van Nostrand Reinhold, New York, (1970).

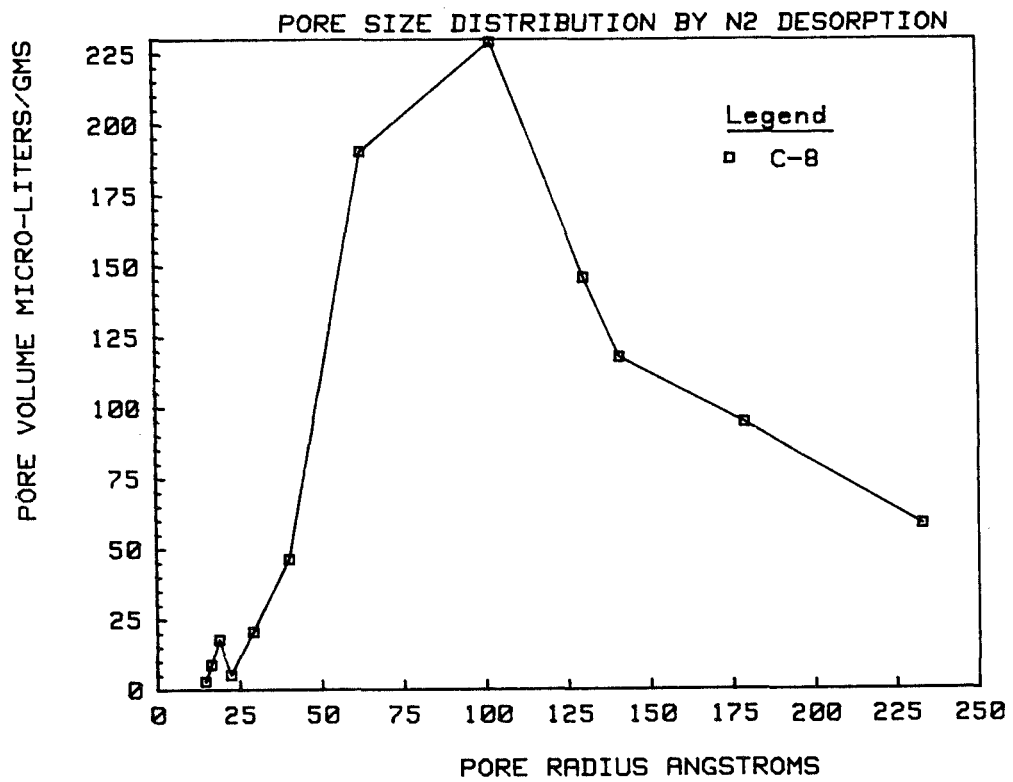
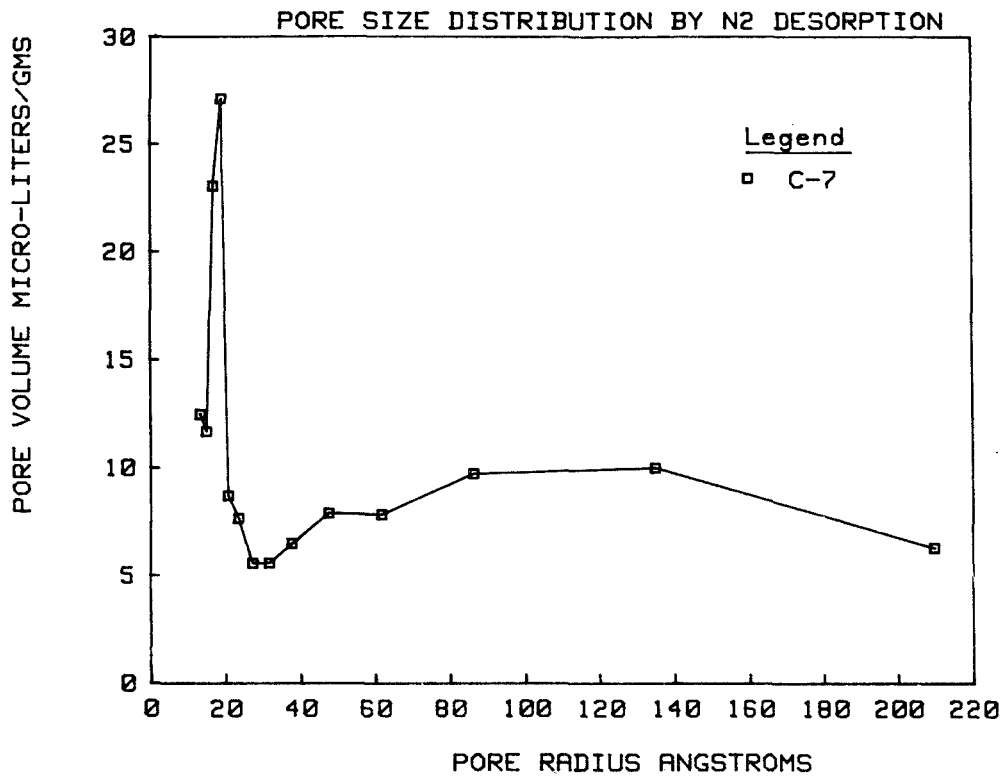
APPENDIX A.

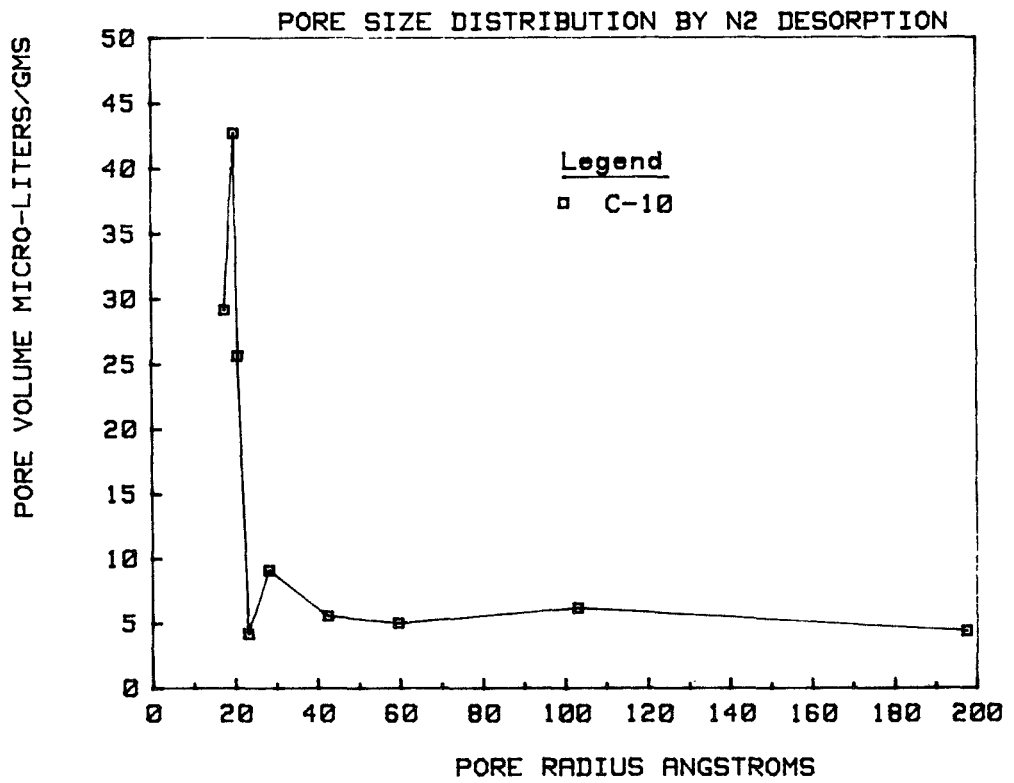
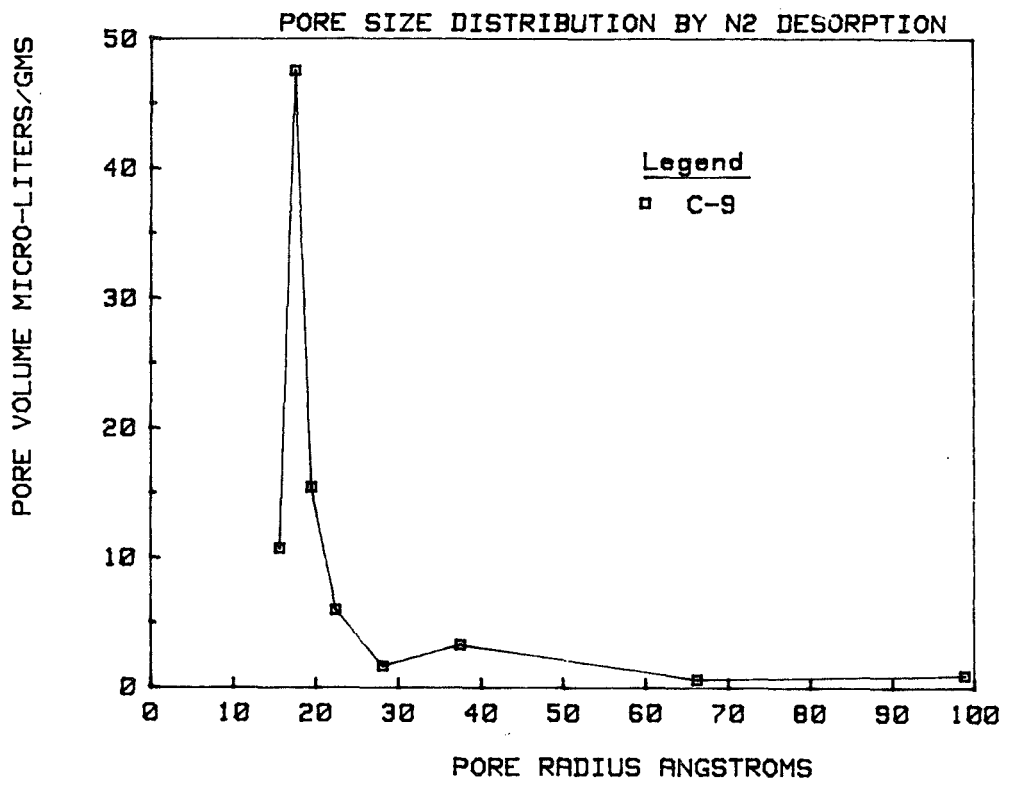
PORE SIZE DISTRIBUTION FOR CARBON SAMPLES

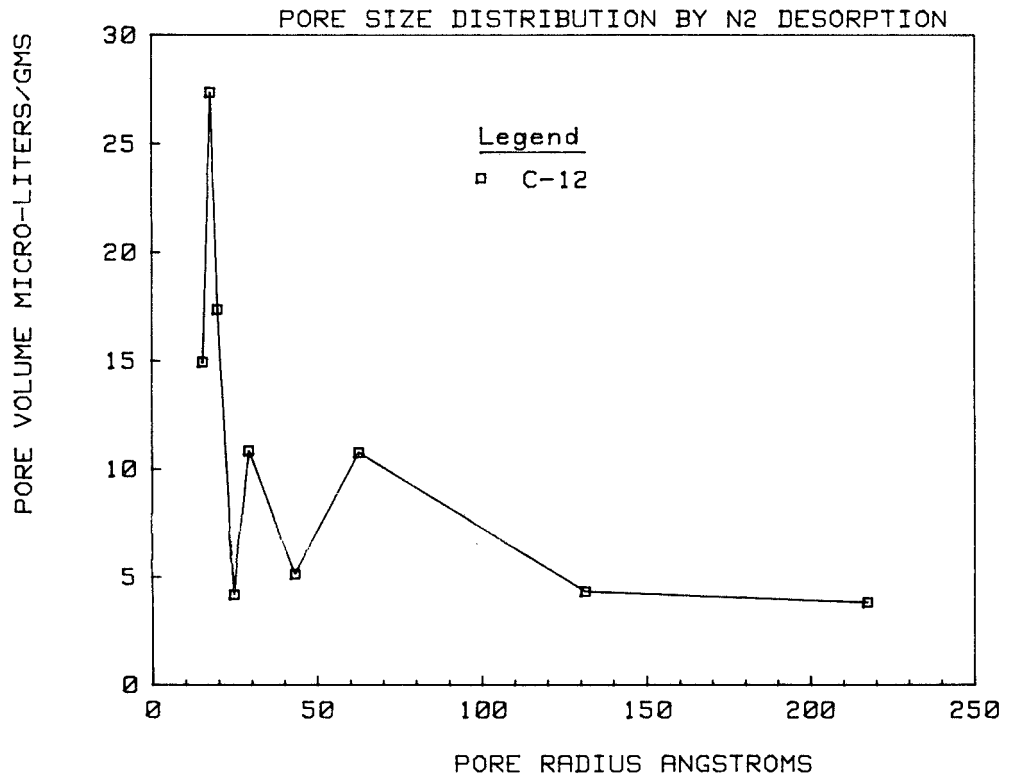
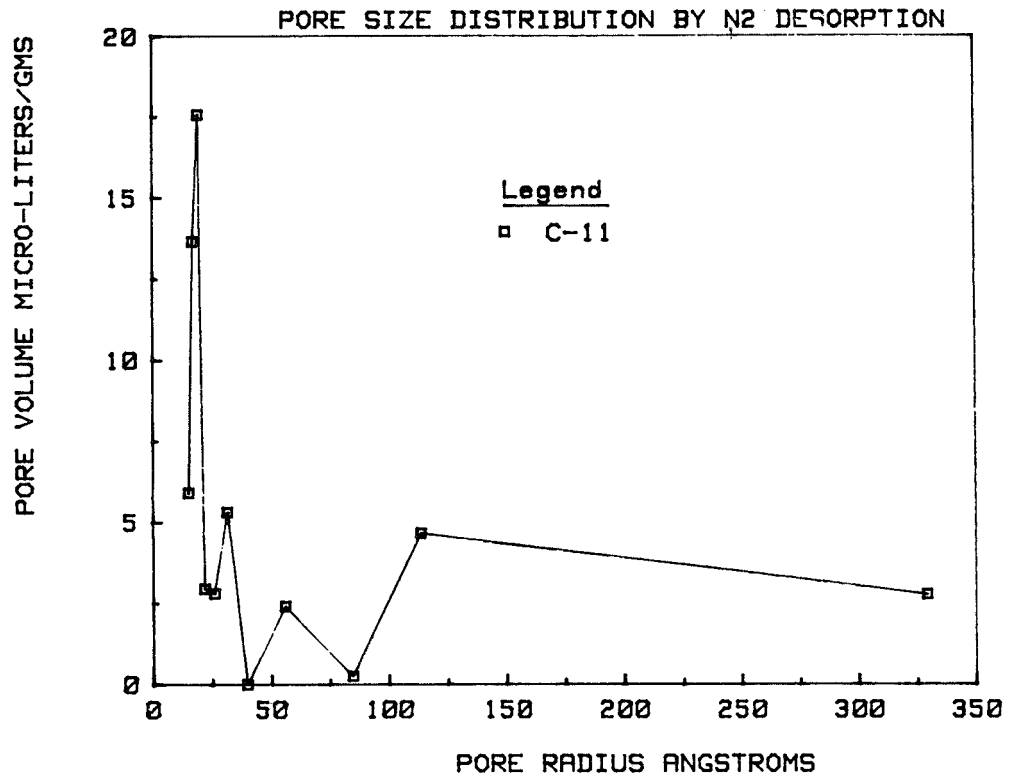


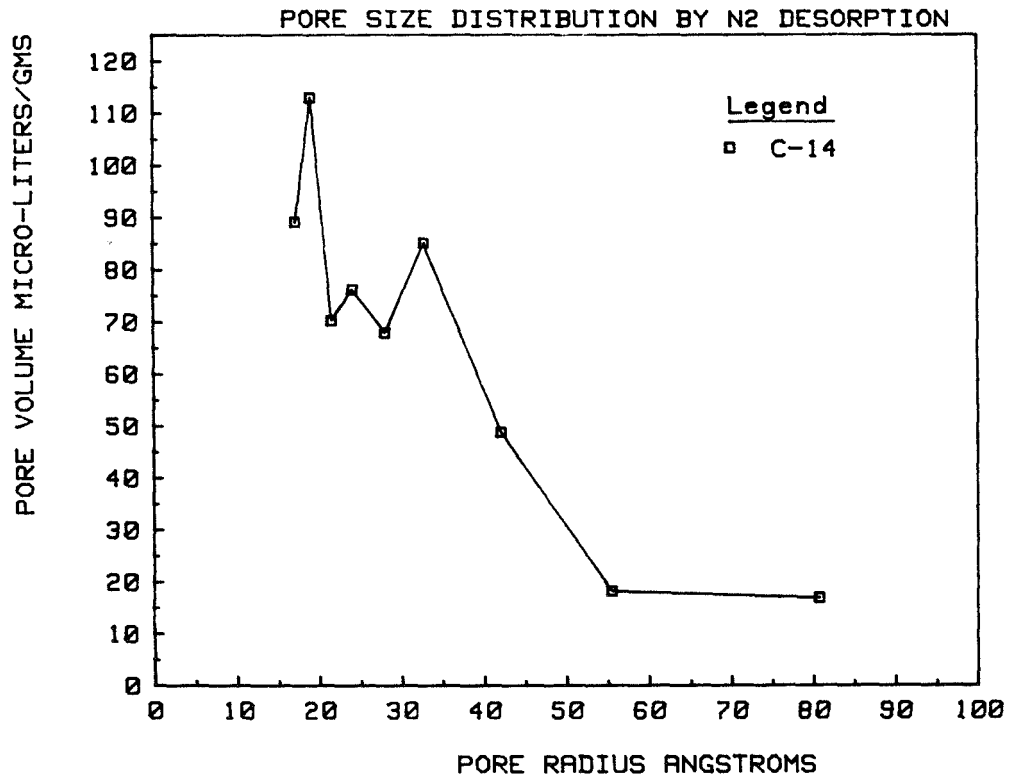
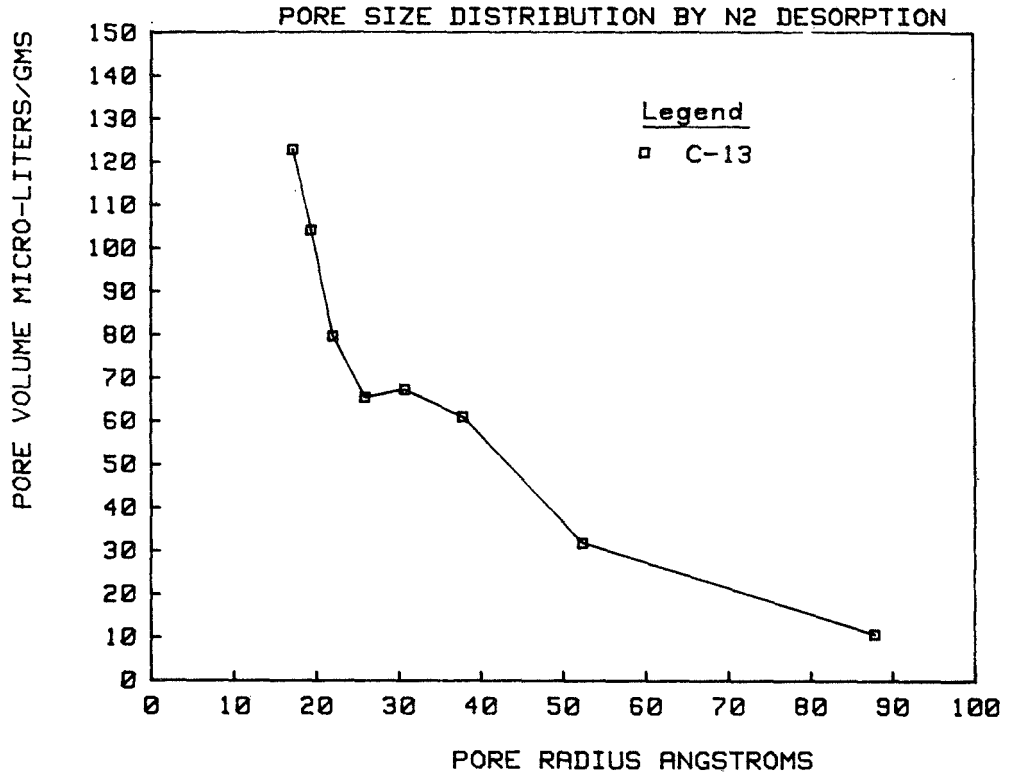


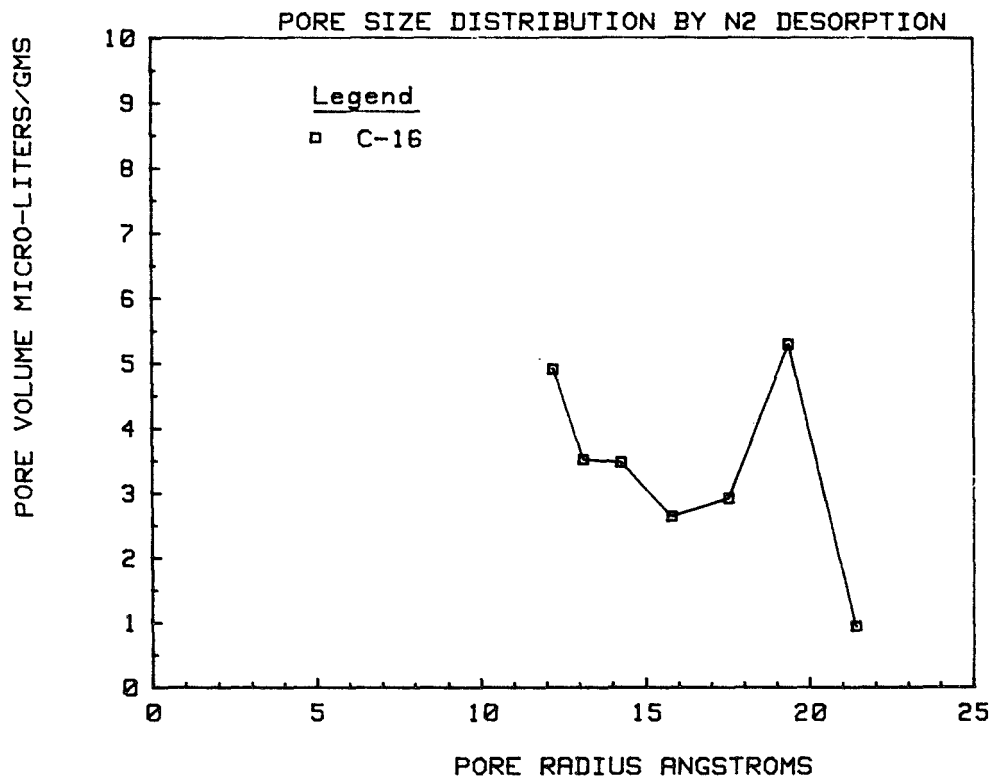
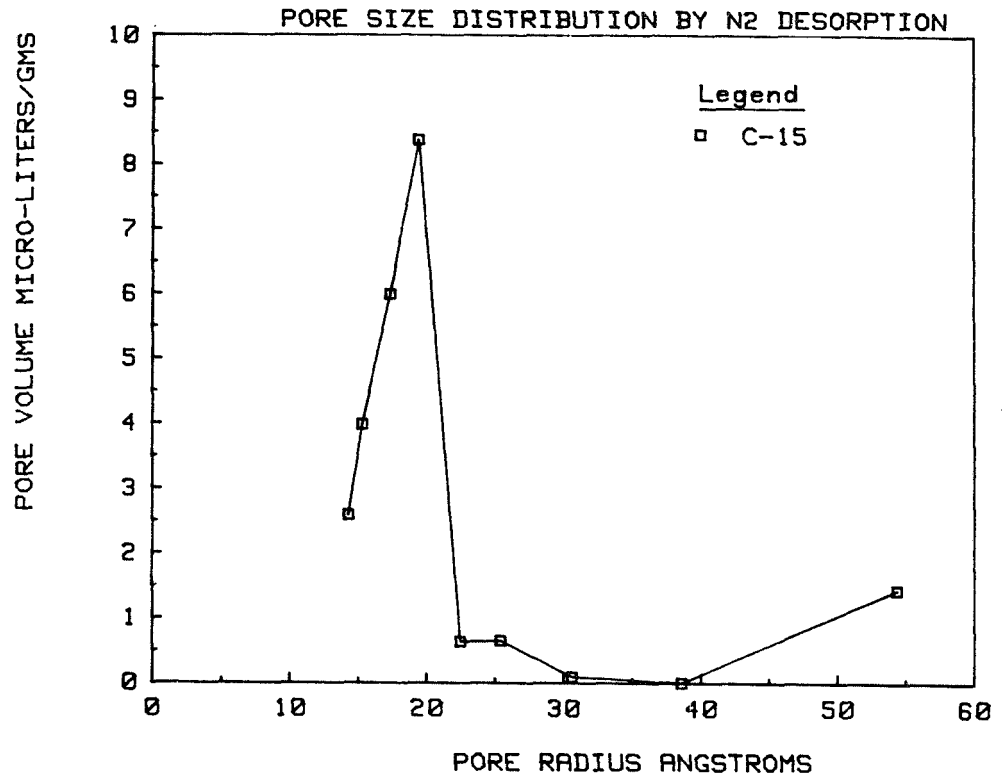






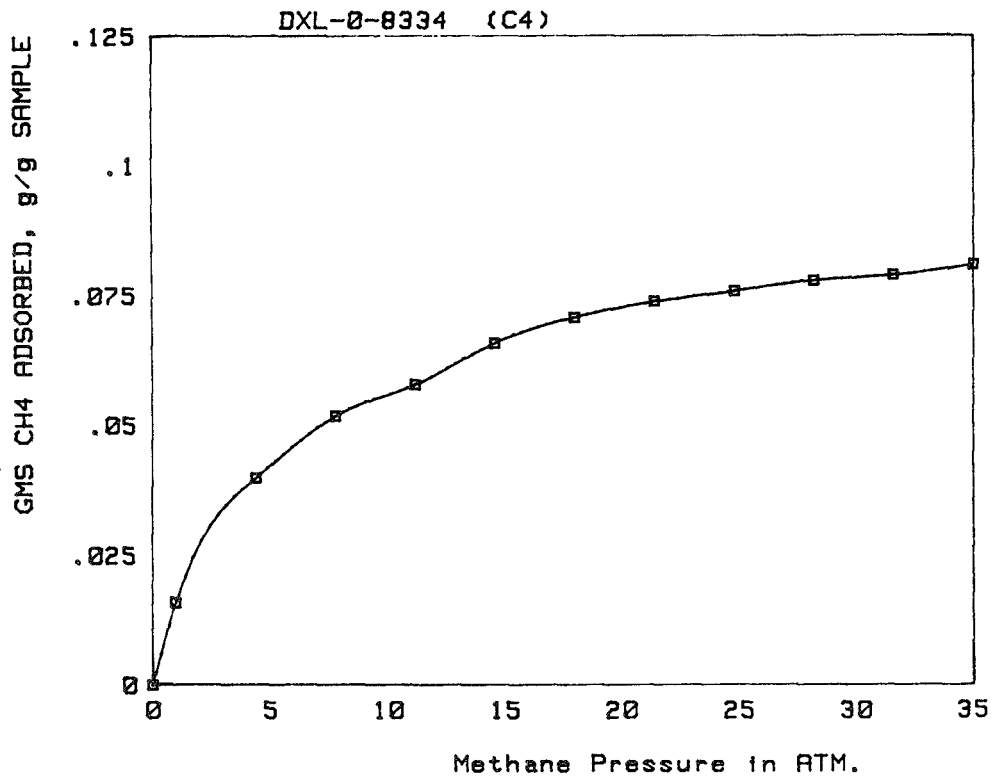
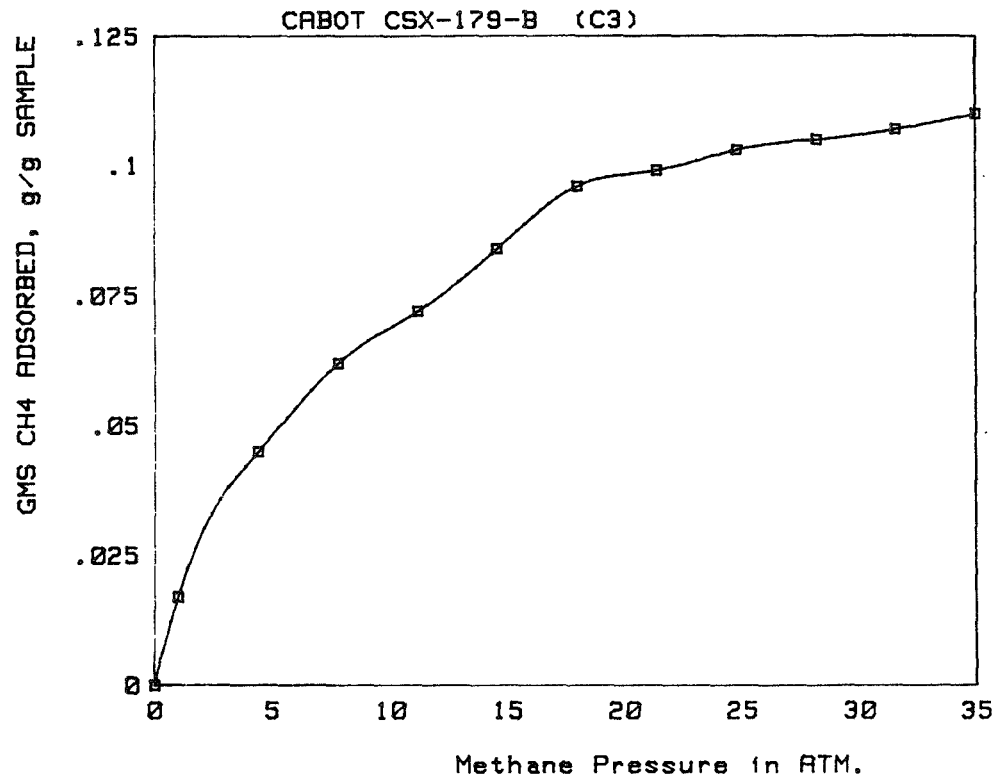


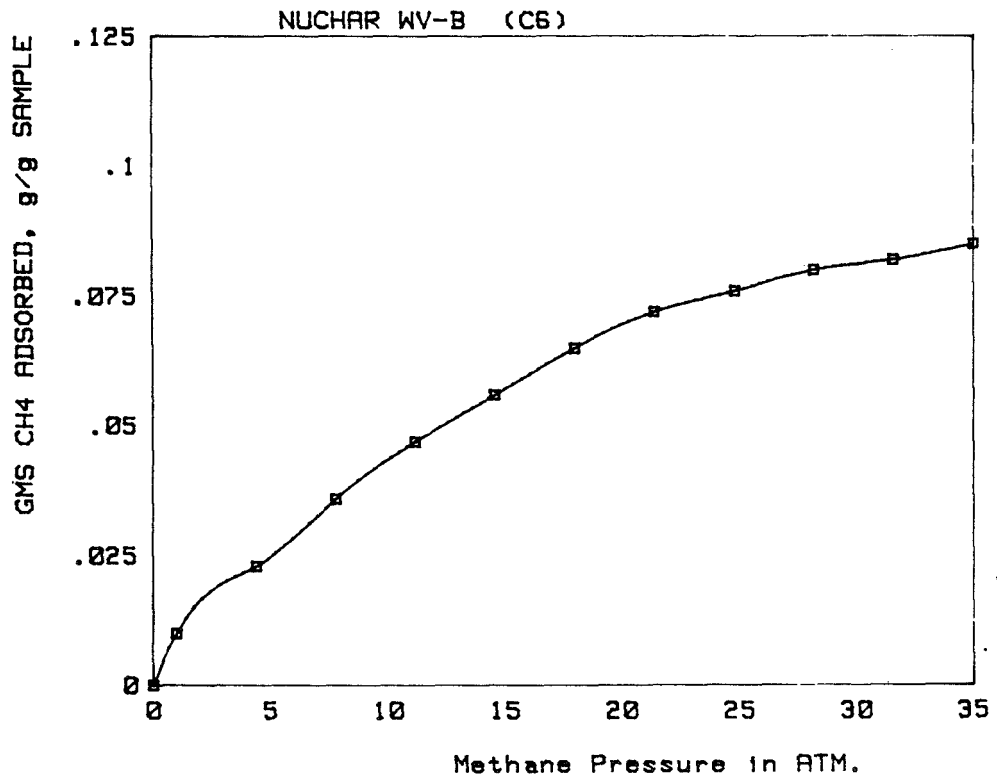
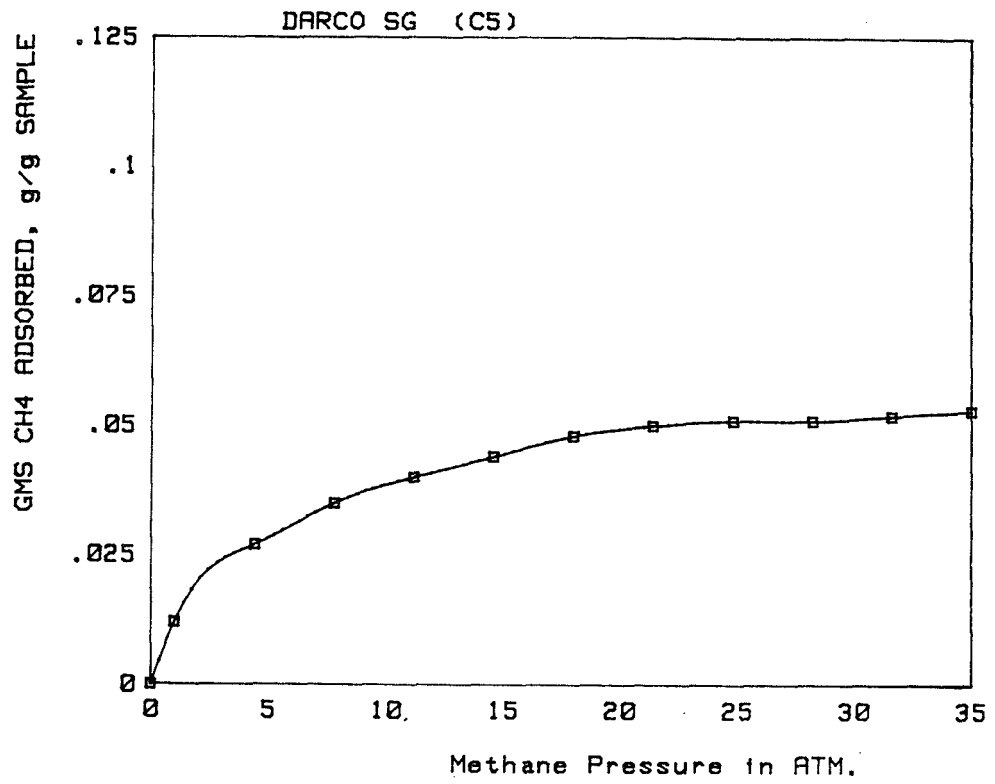


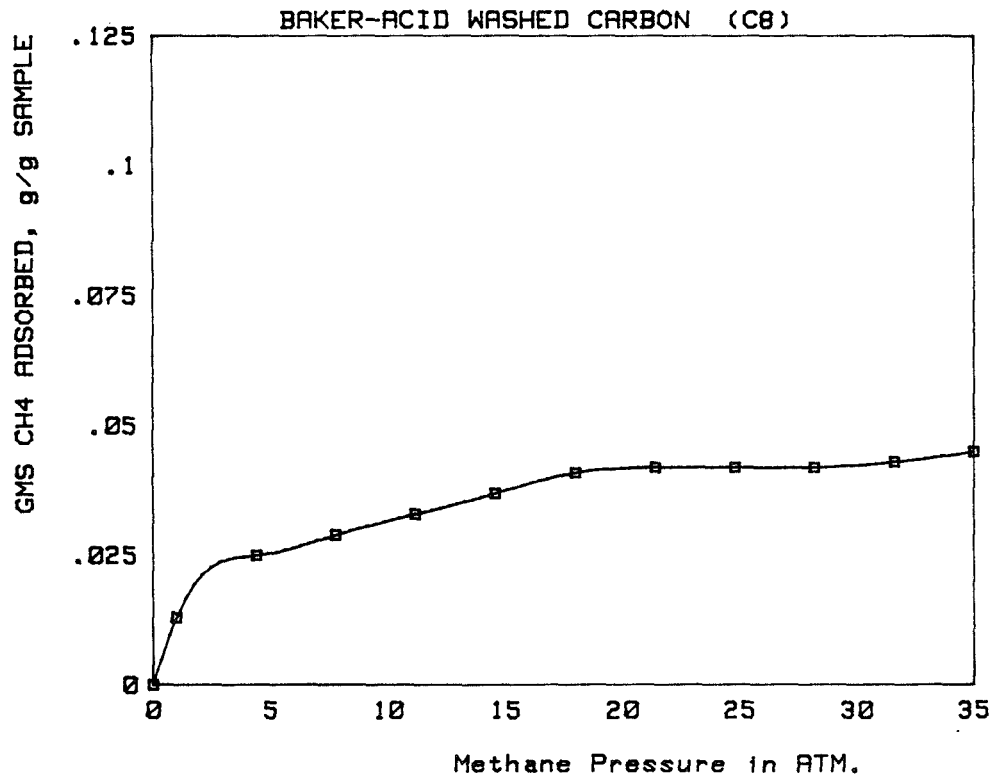
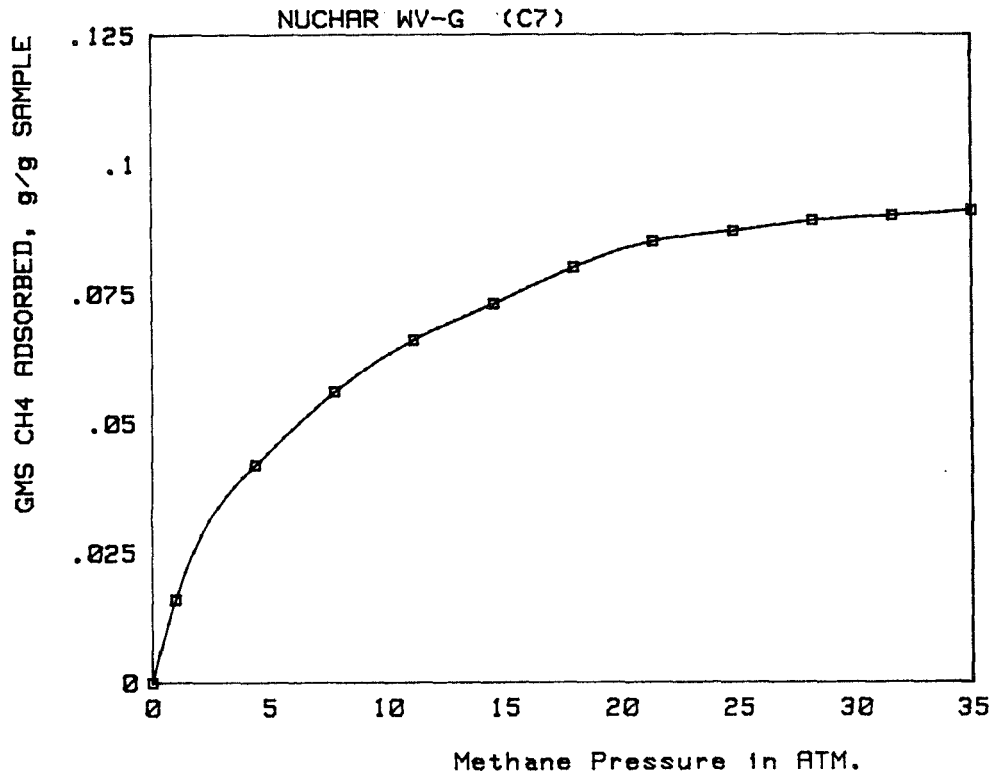


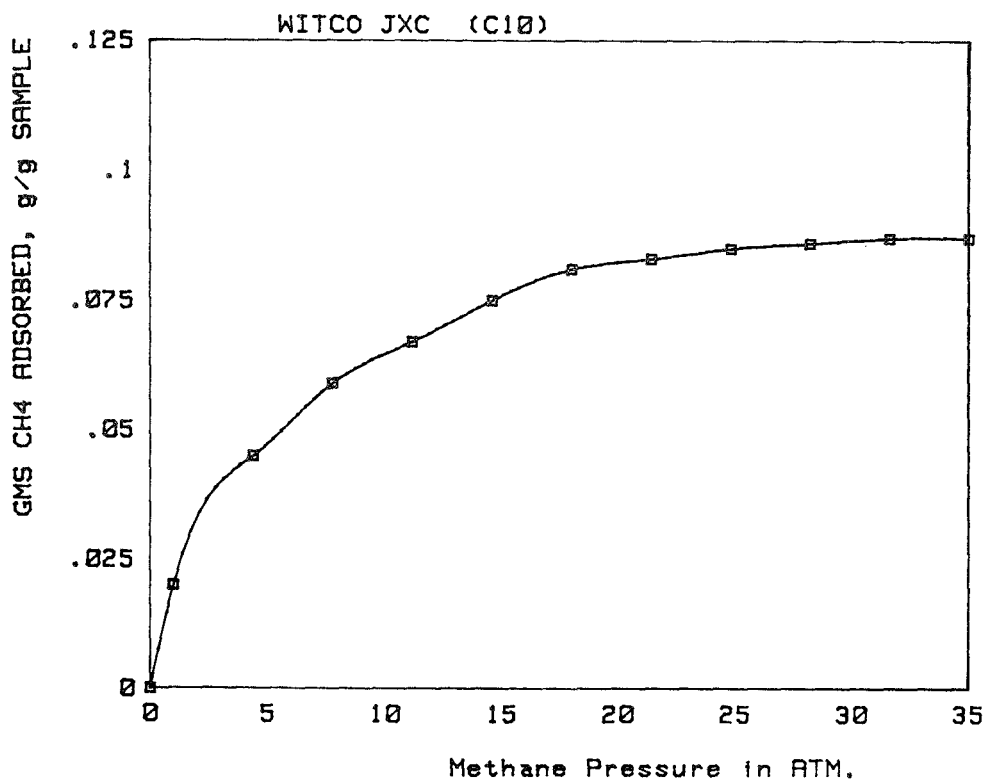
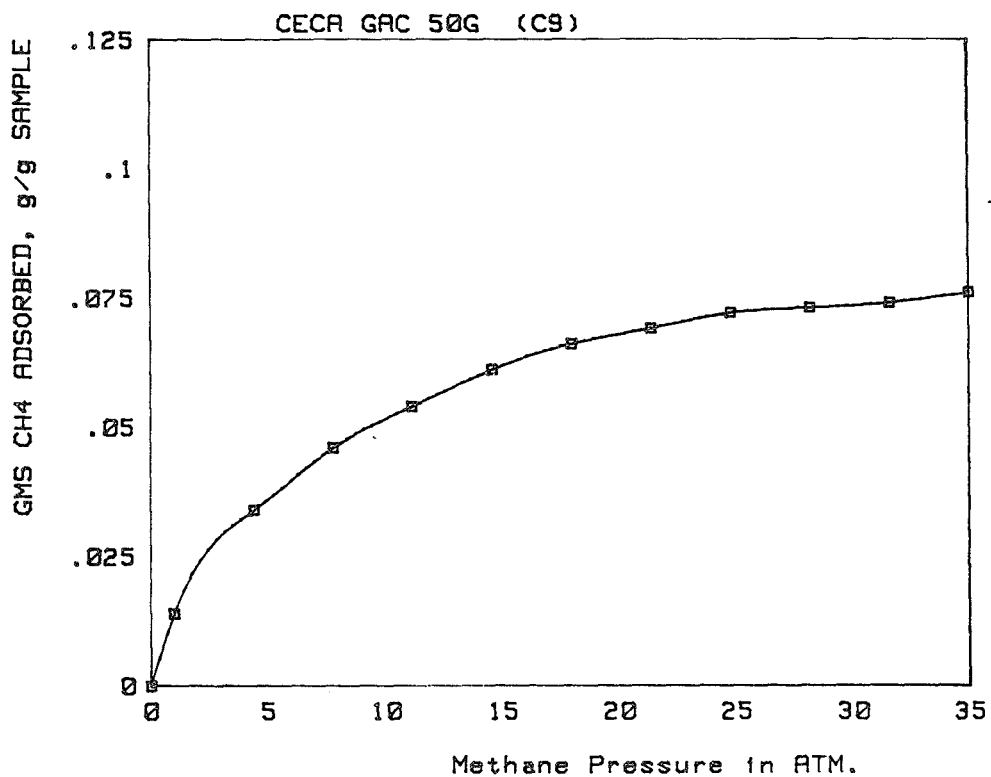
APPENDIX B.

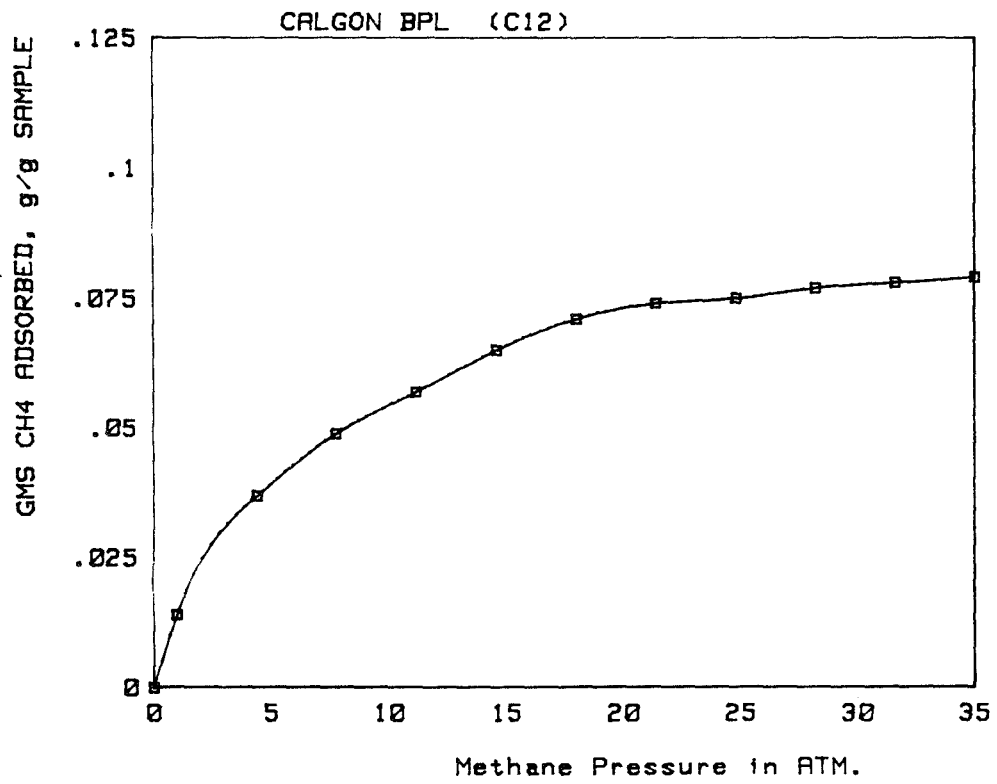
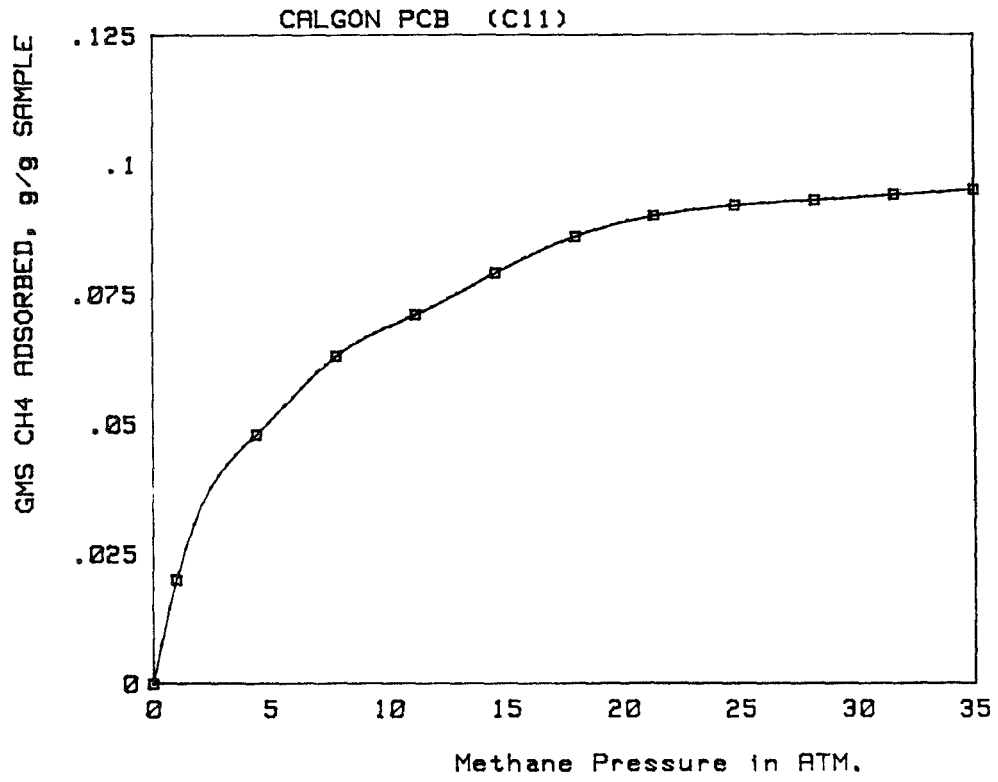
METHANE ADSORPTION ISOTHERMS FOR
CARBON AND ZEOLITE SAMPLES

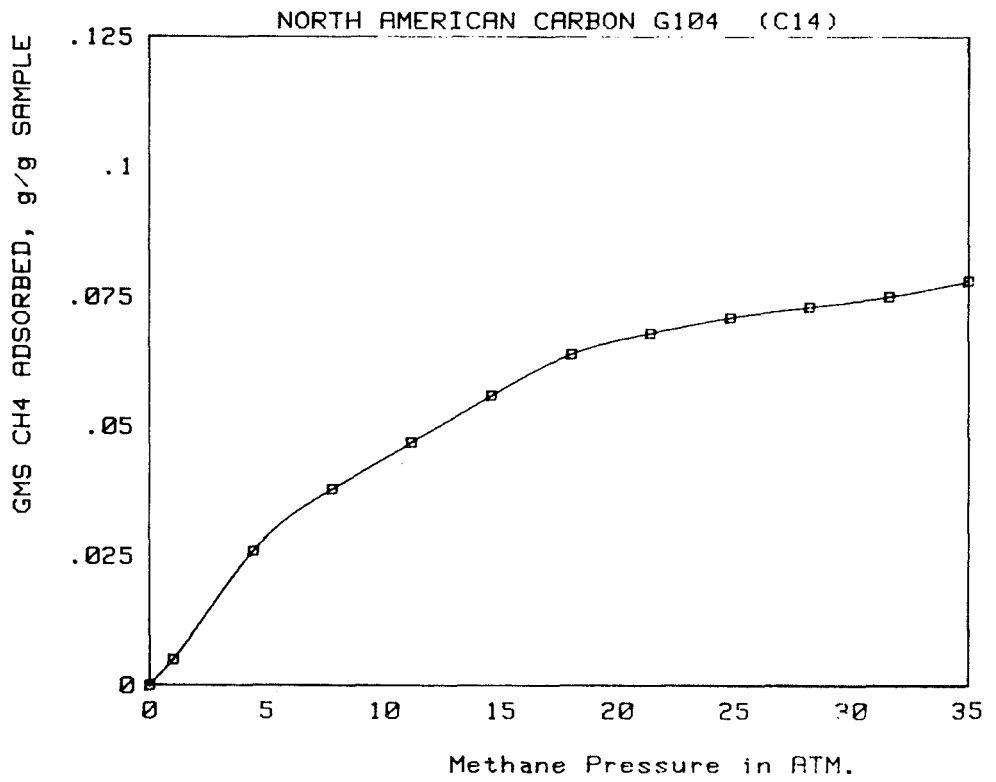
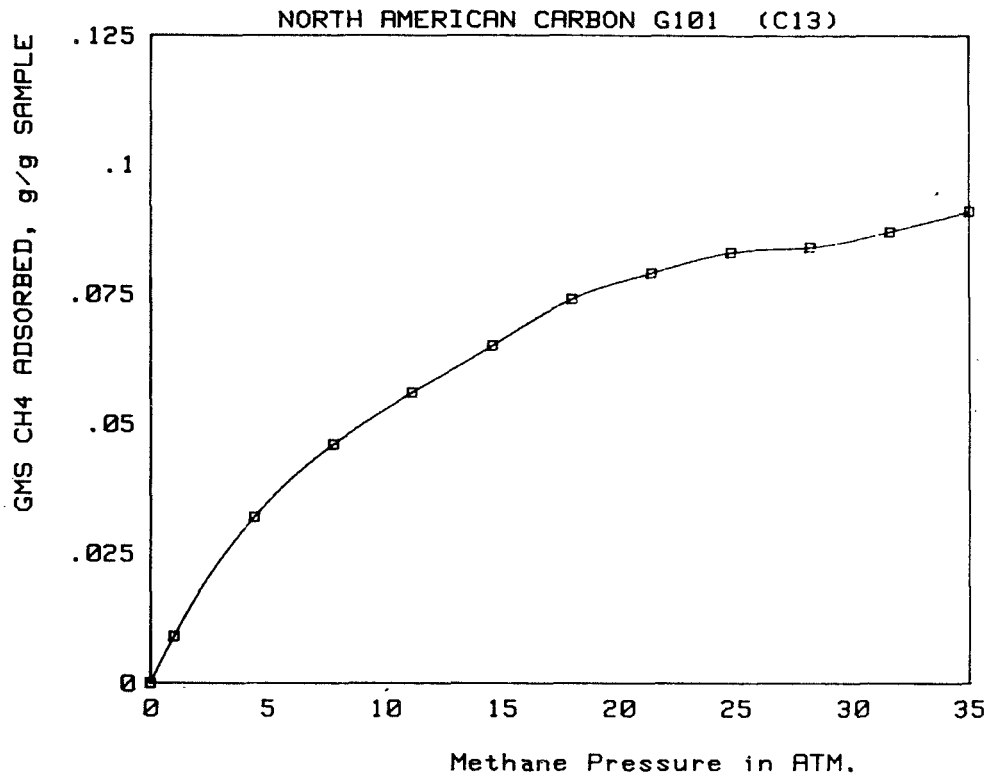


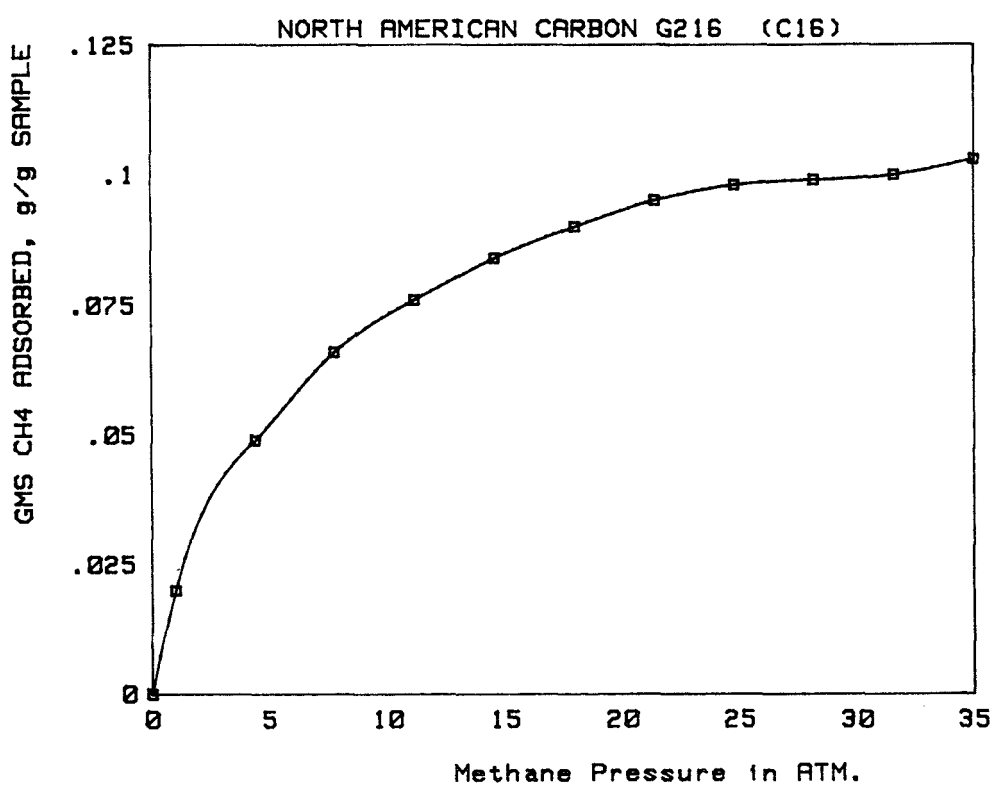
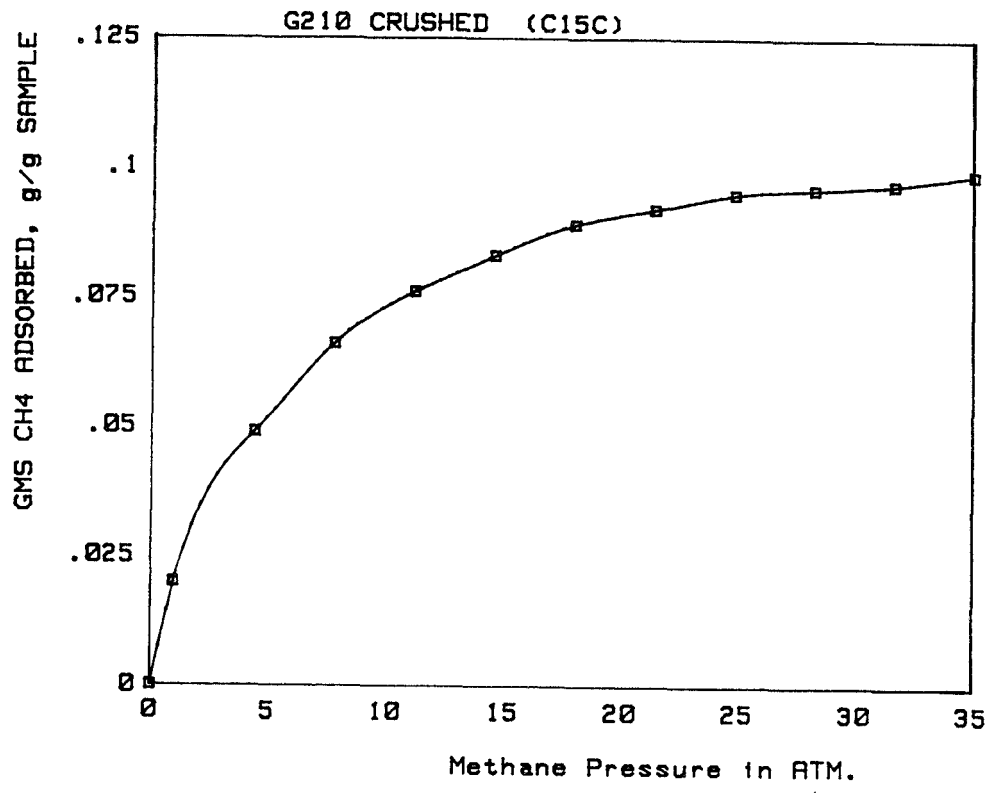


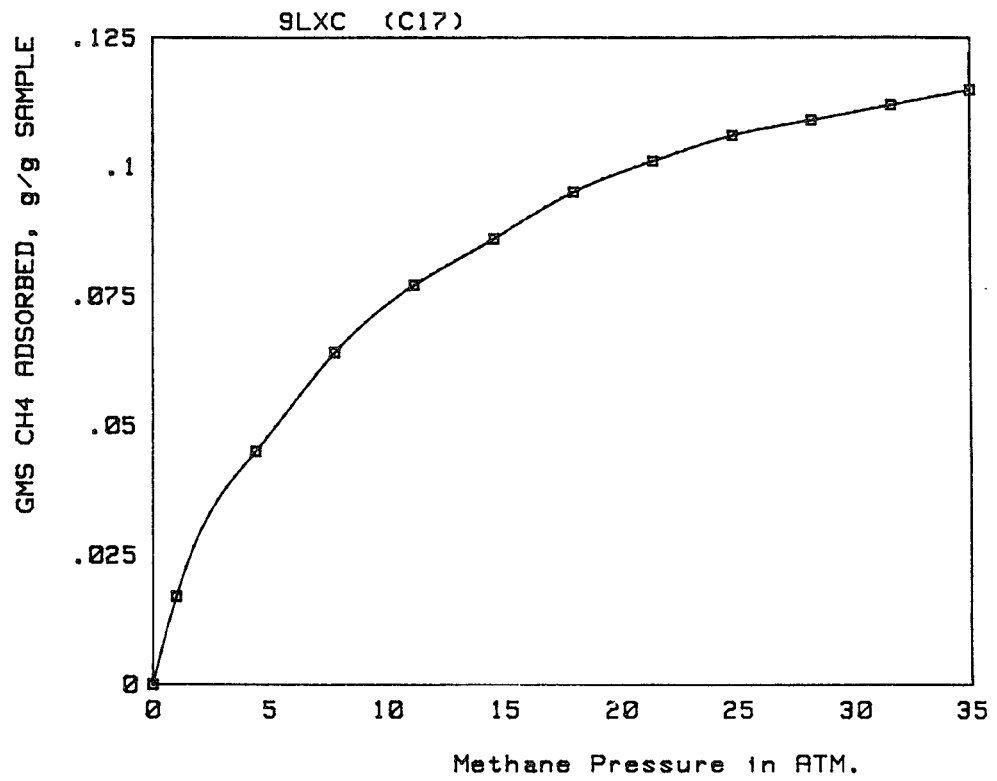


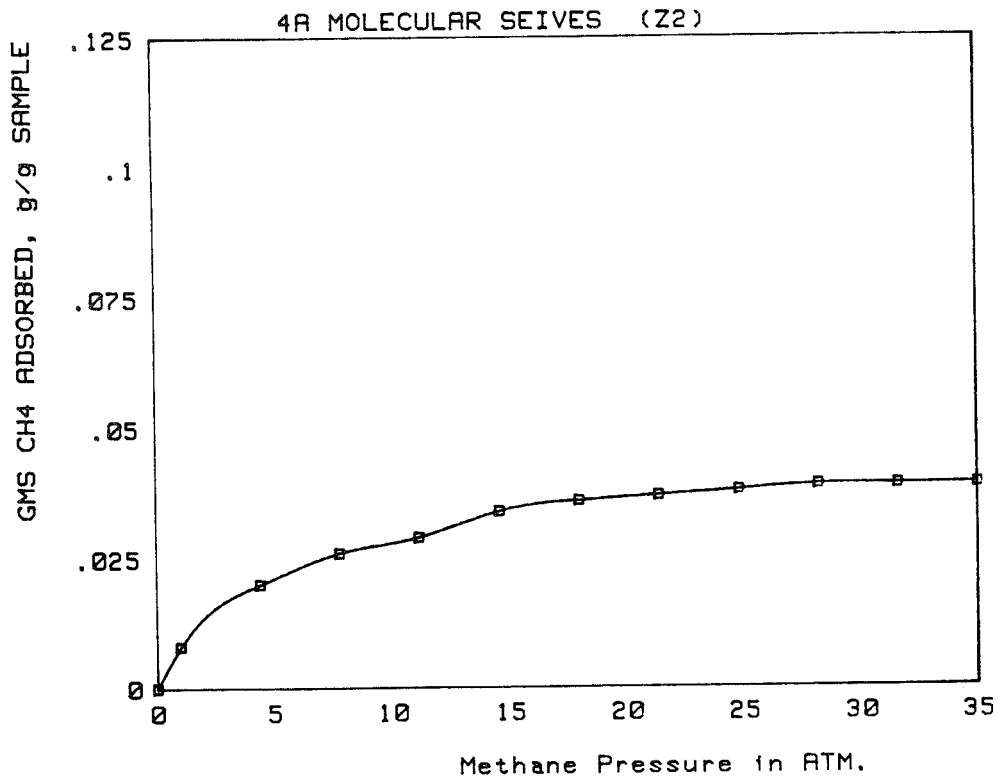
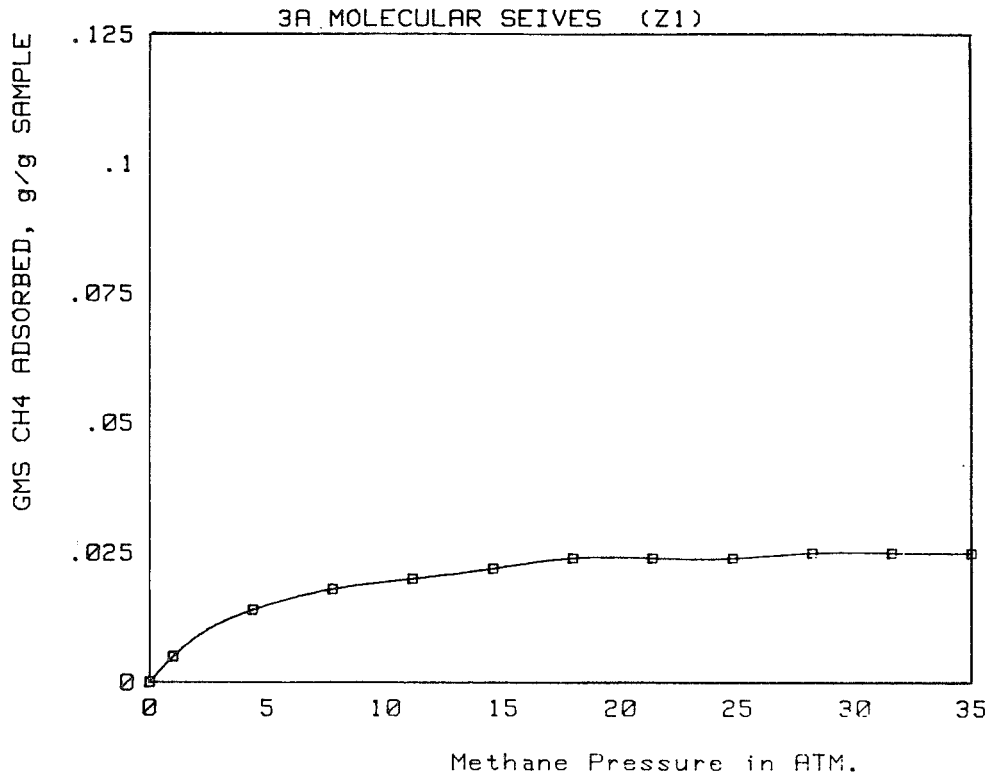


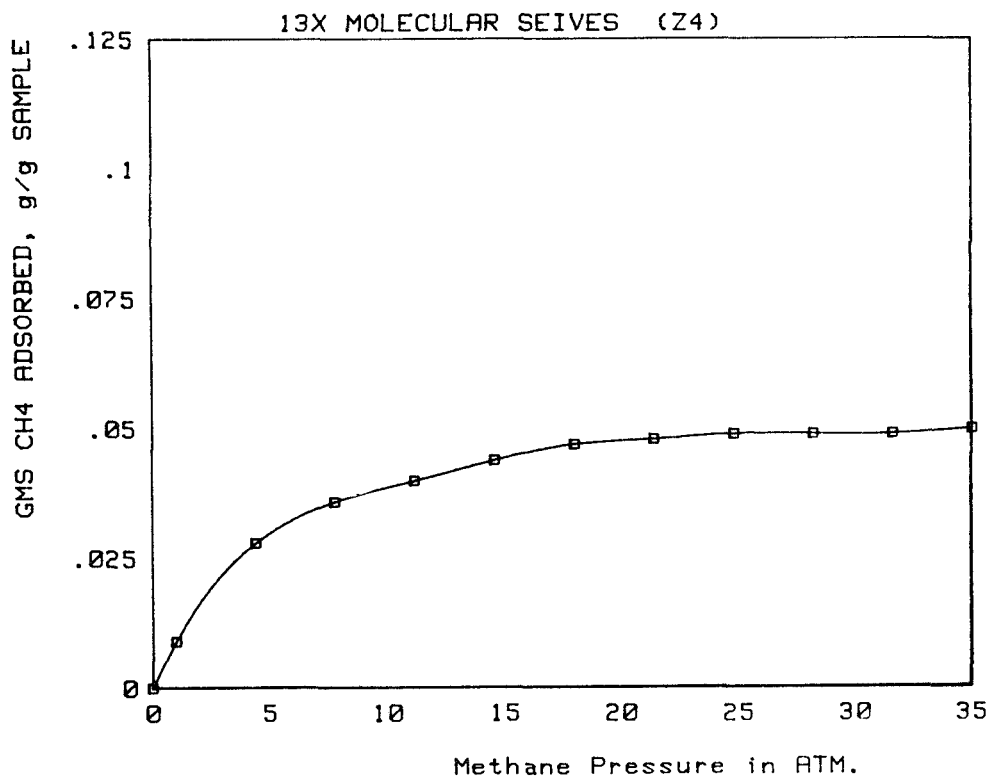
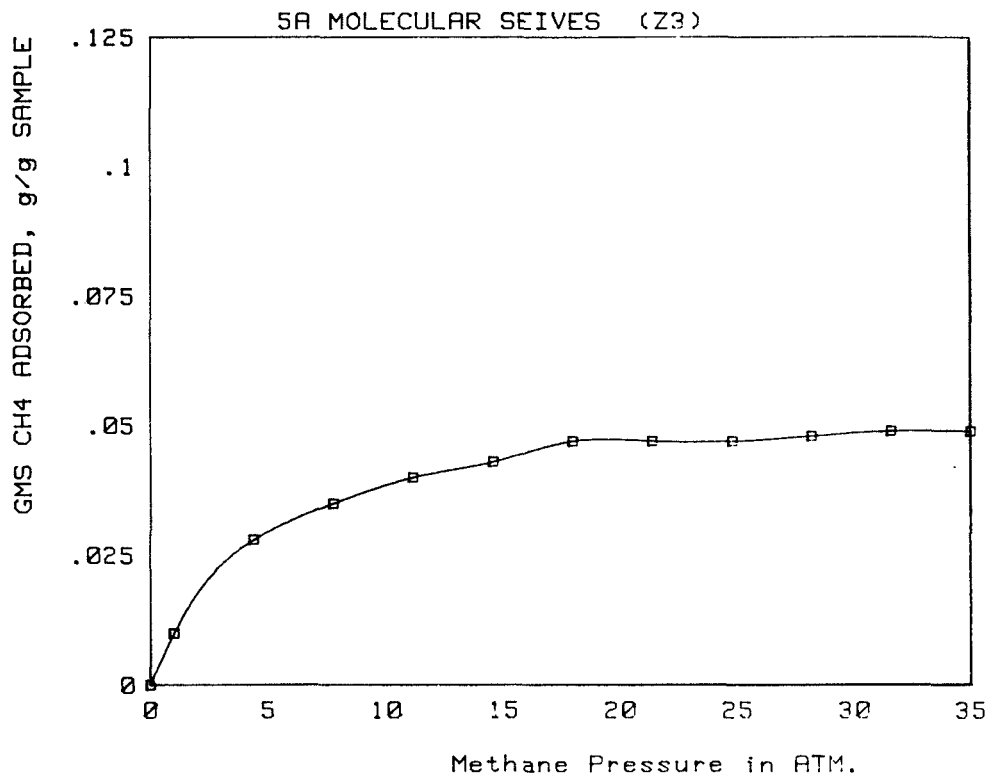


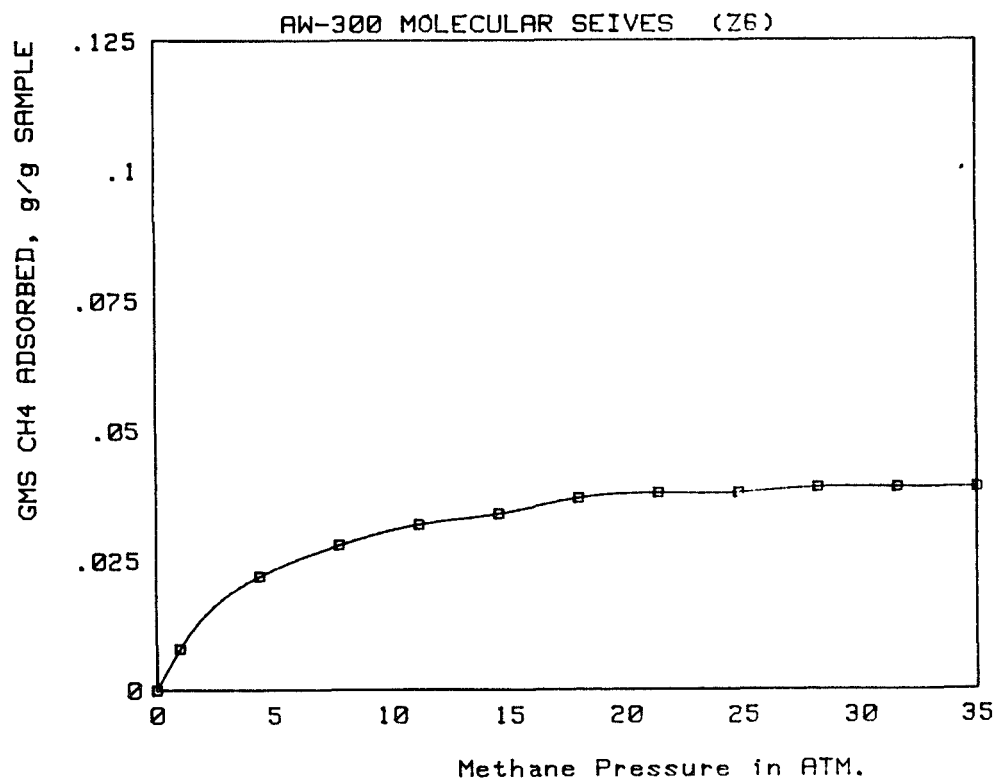
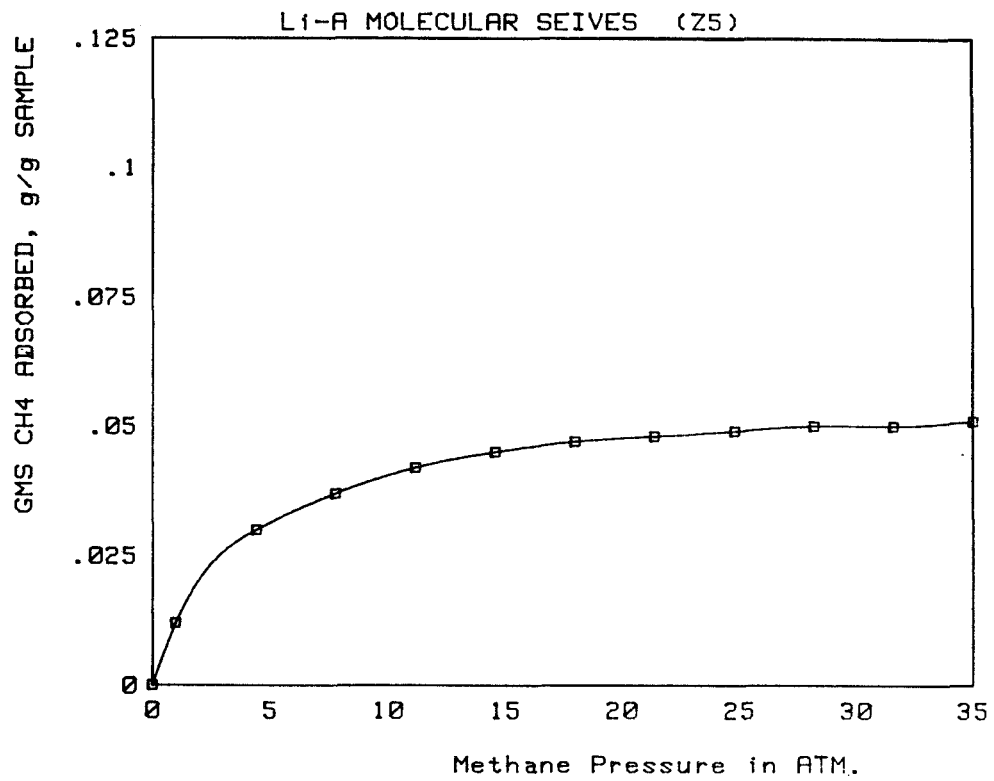


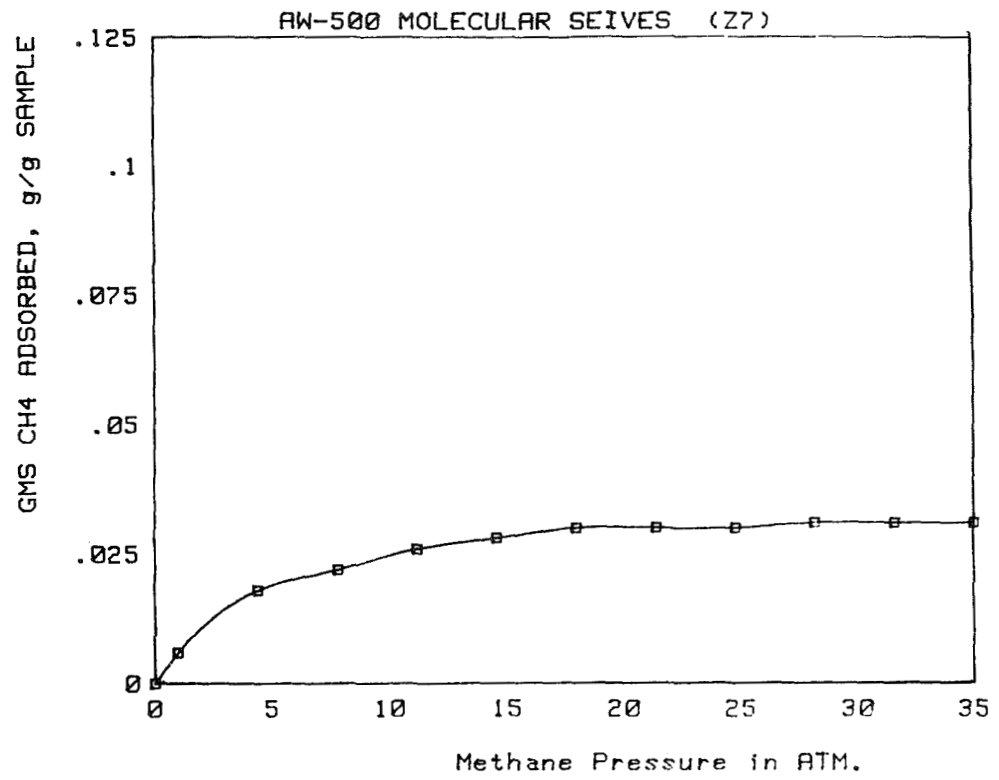












APPENDIX C.

SUPPORTING CALCULATIONS FOR TASK 1.2 WORK

I. Estimation of the Fuel Economy of a Gasoline Engine Converted to Run on Natural Gas in a Dual Fuel Mode

Assumptions

- Model vehicle achieves 17 km/l (40 mpg) or 22.9 km/kg (6.54 miles/lb) on gasoline
- Lower heating value of gasoline is 10.5 kcal/gram (18,900 Btu/lb)¹
- Lower heating value of natural gas is 11.56 kcal/gram (20,800 Btu/lb)¹

Work carried out by the University of British Columbia (UBC) has provided some quantification of the fuel economies for vehicles operating in a dual fuel mode on gasoline or natural gas.² The UBC study documented an average 12.5% increase in operating efficiencies for vehicles operating on natural gas over the same vehicle operating on gasoline on the basis of BTU input. This translates into a 23% increase in fuel economy on a mass to mass basis. In other words, the UBC results suggest that our model vehicle which achieves 22.9 km per Kg of gasoline will travel 28 km per Kg of natural gas.

The proposed explanations for such an improvement in fuel economy were a higher thermal efficiency for the engine operating cycle due to more complete combustion of the natural gas-air mixture and a leaner stoichiometric ratio in the natural gas mode. However, the performance of the older carbureted engines used in the UBC study are not representative of the high efficiency, electronic fuel injected engine used in the model vehicle chosen for this study. Consequently, most of the 12% efficiency improvements, on a Btu basis, would not be achieved with a state-of-the-art engine. Not because of a decrease in performance on natural gas, but rather a result of improved performance and fuel economy on gasoline.

For the purposes of the modeling work in Task 1.2, it was assumed that 1 kilogram of natural gas delivered about 12% greater range than 1 kilogram of gasoline, 10% as a consequence of the higher energy content of natural gas and 2% as the result of improved engine efficiency.

To conduct a more meaningful analysis of the potential efficiency improvement or vehicle range (beyond that performed here) would require the following:

- Modeling of natural gas-air and gasoline-air cycles for selected design specification of IC engines and numerical simulation of the performance within a defined range of operating conditions

- Selection, analytical modeling, and simulation of a reference driving cycle in terms of determined natural gas-air and gasoline-air cycle performance
- Comparison analysis of driving cycle performance for both natural gas and gas fuels carried out in terms of BSFC or distance unit of fuel mass.

II Estimation of the Fuel Economy of a Dedicated Natural Gas Engine

In general, natural gas exhibits excellent characteristics for use as an internal combustion spark-ignited engine fuel. The clearly identifiable advantages and disadvantages are as follows:

Advantages

1. High caloric value (lower heating value is 10% higher than gasoline)
2. High octane number (130 RON)
3. Good ignitability of natural gas-air mixture allows low equivalence ratios³
4. Simple oxidation reactions leading to complete combustion
5. Effective carburetion due to gaseous phase.

There are also certain negative natural gas characteristics:

Disadvantages

1. Relatively low laminar flame speed within quiescent combustion chamber
2. Lack of process of vaporization both during mixing and admission eliminates the cooling effect and accordingly decreases cylinder volumetric efficiency.

Advantages 1, 4, and 5 can be made use of in a careful conversion of a gasoline engine. The first disadvantage can also be partially corrected by advancing the ignition and also to varying degrees by the type of engine that is selected for conversion.

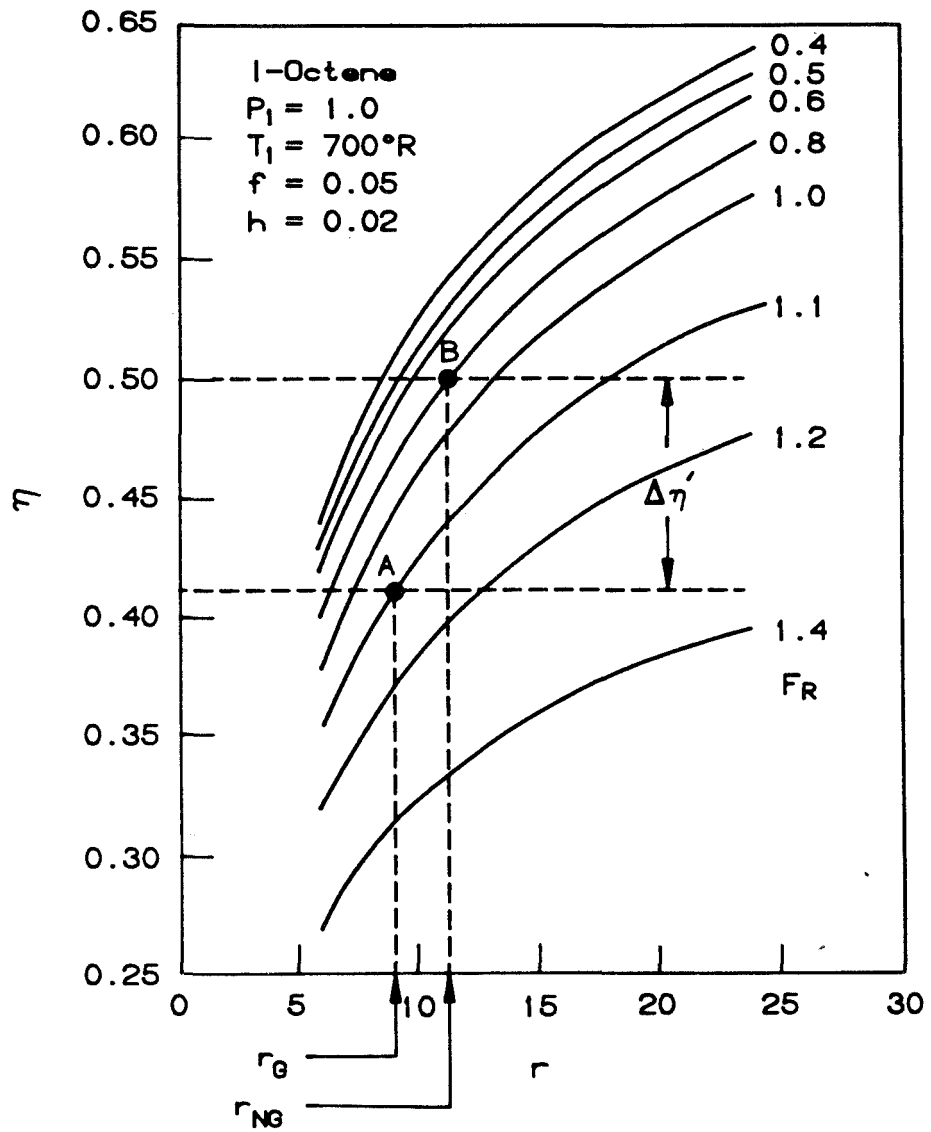
More complete utilization of advantageous characteristics of natural gas as an IC engine fuel as well as effective alleviation of the negative characteristics will require a dedicated natural gas-engine design. The most evident modification should involve:

- Increase of compression ratio (up to 14 to 1) in order to maximize thermal efficiency of cycle by extensive utilization of high octane number of natural gas

- Application of "fast burn" combustion system in order to alleviate disadvantage of slow flame propagation of natural gas-air mixture and enhance cycle thermal efficiency by bringing cycle conditions closer to those characterizing a constant-volume cycle
- Application of some sort of supercharging to alleviate the deterioration of volumetric efficiency caused by the lack of cooling upon carburetion.

Figure C-1 defines the functional relation between theoretical thermal efficiency of an internal combustion-spark ignition engine and design compression ratio developed for gasoline-air mixtures with different equivalency ratios F_R .⁴ The process of transition from a converted natural gas engine to a "dedicated" natural gas engine can be represented in this figure by the transition from Point A to Point B. Point A represents an engine with a compression ratio $r_G \approx 9$ typical for a modern gasoline engine operating on slightly over-stoichiometric mixture with $F_R = 1.1$ which seems to be appropriate for assuring the satisfactory combustion process in a gasoline engine converted to natural gas fuel. Although lean methane-air mixtures have good ignitability, their poor flame propagation characteristics seem to prevent effective burning in a conventional gasoline mixture combustion chamber. Satisfactory fast combustion of natural gas mixtures in such conditions will call for an ignition advance and for a rather enriched equivalency ratio. A dedicated design can be provided with a compression ratio $r_{NG} = 11.5$ and a combustion system intentionally promoting faster combustion, therefore capable of accepting leaner mixtures. Point B can be then quite realistically extrapolated as to be located on curve $F_R = 0.8$ and abscissa $r_{NG} \approx 11.5$. This extrapolation suggests a possible corresponding thermal efficiency gain $\Delta\eta' \approx 8\%$. $\Delta\eta'$ can still be increased by supercharging allowing for approximately a 5% additional increase in theoretical thermal efficiency of an IC engine. The total efficiency increase for a dedicated natural gas IC engine will then be approximately 13% over a natural gas converted version, or if the gasoline engine is taken as the baseline, the potential efficiency improvement of a natural gas dedicated design would be about 25%.

To a first approximation, the ranges of the model vehicle described in Task 1.2 and listed in Tables 21 and 22 for natural gas operation can be extended by 13% if a dedicated engine is substituted for a converted gasoline engine.



A83121640H

Figure C-1. FUNCTIONAL RELATIONSHIP BETWEEN THEORETICAL THERMAL EFFICIENCY AND COMPRESSION RATIO

References for Appendix C

1. Assessment of Methane-Related Fuels for Automotive Fleet Vehicles, DOE/CE/50179-1, February 1982, page 2-29.
2. Sheraton, D. F., "B. C. Methane Power Vehicle Program Test Results." Symposium papers, Nonpetroleum Vehicular Fuels III, 1982.
3. Thring, R. H., "Gasoline Engines and Their Future," Mechanical Engineering, October 1983.
4. Taylor, C. F., "The Internal Combustion Engine in Theory and Practice." The MIT Press, Second Edition, 1977.

APPENDIX D.

EVALUATION OF CLATHRATION COMPOUNDS AS A MEANS OF STORING NATURAL GAS

CLATHRATES¹⁻¹⁶

1. Background

Interest in inclusion compounds in recent years has been found in two major areas. In the first and most recent, the binding or complexing of guest species by unimolecular hosts, in solution, has received much attention, particularly in the fields of biology and catalysis. The second relates to the study of crystalline inclusion compounds or clathrates which may be subclassified as:

- The cage clathrates in which the guest molecules are imprisoned in discrete closed cavities or cages in the host crystal and include the hydroquinone and ice clathrates
- The channel type in which the guest species are accommodated in continuous channels in the crystal such as the urea and thiourea adducts
- The layer type in which the guest species are situated between layers (e.g., with graphite and certain clays).

In addition, molecular sieves and, in particular, the zeolites are sometimes classified as clathrate or inclusion hosts since they possess discrete cages and channels, and inclusion depends on the molecular dimensions of the guest molecules relative to that of the channels and cages of the host.^{17,18} From the point of view of methane storage, the clathrate type of inclusion is of greatest interest. However, there may be a large overlap in concept and principle between inclusion in the solutions and in clathrates. Furthermore, inclusion in solutions may provide a means of significantly enhancing methane storage.

The term clathrate was originally defined, on the basis of x-ray diffraction structural analysis of a number of such entities by Powell and associates, as a compound "in which two or more molecular components are associated without ordinary chemical union but through complete enclosure of one set of molecules in a suitable structure formed by another."¹⁵ Two aspects of the clathrates are noteworthy:

- The crystalline lattice structure of the host is usually not in its normal crystalline mode (α -form) but in a form (usually referred to as the β -form) which is usually less stable in the absence of guest molecules than the α -form.

- The composition over which the clathrate is stable with respect to decomposition into guest and normal host can vary over a large range.

Thus, clathrates are not stoichiometric compounds but ones in which the restrictions on which molecules can become guests and the minimum fraction of the total number of cavities which must be filled for stability are largely determined by geometric considerations.¹⁵

Although the literature concerning clathrate inclusion compounds extends back to the early 1800's, most of the activity in the field has occurred since the late 1940's and early 1950's after a basic understanding of the phenomenon was developed by H. M. Powell and associates. Since then, the work in the field has been prodigious. Thus, Bhatnager (1970)¹ lists 1339 references which is certainly not complete since this includes only 293 references on hydrates compared to 1458 references cited by Davidson.³ Nonetheless, Bhatnager's bibliography yields an interesting breakdown of the types of clathrating agents of greatest interest:

● Urea and thiourea adducts	610 refs.
● Hydrates	293
● Phenolics including hydroquinone, Dianin's compounds, and various phenols	116
● Cyclodextrins (starches)	63
● Werner complexes	134
● Miscellaneous including phosphonitrile, steroids, adamantane, cholesterol, dinitrophenol, hexamethylisocyanide chloride, and cyclohexatriene	41
● Reviews	82

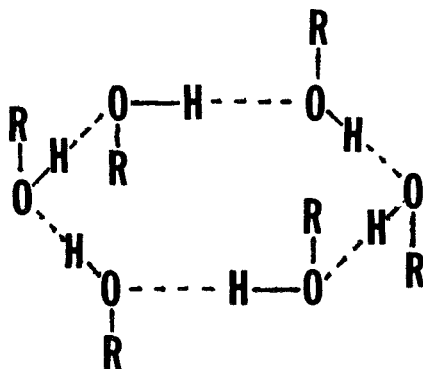
It is interesting to note that many of these clathrating agents exhibit a strong hydrogen bonding propensity (e.g., amides, water, phenols, and cyclodextrin) which is undoubtedly involved in the binding of the crystals of the host molecules. In the case of the Werner Complexes and other inorganic coordination systems, the binding energy for the host crystal certainly involves ionic as well as ion to ligand attractions.

Since 1967, the work in the field has begun to shift toward developing the know-how to synthesize new host structures, a priori, on the basis of

molecular structure rather than on a purely empirical basis. One area of considerable interest in the biological field is the synthesis of water soluble host molecules, which are organic molecules that contain cavities of dimensions capable of accommodating simple ions and molecules in which the binding is provided by hydrogen bonding, ion pairing, metal ion to ligand attractions, acid-base attractions, and van der Waals forces. Hosts may contain cavities which result from reorganization of the molecule during complexation with a guest molecule or rigid cavities which exist prior to complexation (cavitands).^{19,20}

This work is an outgrowth of the studies of the structure and properties of the cyclodextrins, which are naturally occurring cyclic oligomers made up of 6-8 glucoside units bound head-to-tail and which enclose cavities of 6, 8, or 10Å diameter, depending on the number of units in the oligomer. The ether oxygens and hydrogen atoms are oriented inwardly and hydroxyls are oriented outwardly. Thus, guest molecules of a range of sizes from methane to much larger organic species can be clathrated. Similar behavior was first achieved with the synthesis of cyclic polyethers containing six (-CH₂-CH₂-O-) units with inwardly oriented ether groups.¹⁹ Furthermore, this approach has now been extended to include macrocycle compounds made up of substituted aromatic units, for which the size and shape of the cavities as well as the nature of the inwardly oriented binding groups has been varied.²¹

Independently, MacNicol and associates^{14,21-23} have developed a synthesis strategy based on mimicking the "hexa-host" behavior of several phenolic clathrating agents such as Dianin's compound and hydroquinone, in which clathration involves the formation of a hexagonal ring of hydrogen-bonded oxygen atoms from six phenolic hydroxyl groups:



Each group of six substituted phenol molecules is associated with two cavities, one above the hexagonal hydrogen bonded planes and one below.

They were then able to demonstrate that the clathration ability of such hexagonal structures could be simulated using the permanent structure of certain hexa-substituted benzene ring compounds. Thus, two independent approaches, starting with empirical observations of two radically different types of clathrates have converged on a cyclic model for the synthesis of new clathrate hosts. However, the guest molecules bound by both types of clathrate hosts so far have been relatively larger than methane.^{21,22}

Thermodynamics of Clathrate Stability¹⁶

The thermodynamics of clathrate stabilities has been reviewed by Child (1964)¹⁵ and will not be repeated here. However, the gist of his analysis is of interest in guiding further synthesis attempts. He points out that in many respects clathrates are similar to equilibrium solutions in that:

- Solute molecules are placed in cavities within the solvent
- The energy of interaction between host and guest is normally small and the entropy term is similar in magnitude to the entropy of vaporization of a solute from a solution which obeys Raoult's law
- The guest may be said to obey Henry's law in the sense that guest-guest interactions are negligible compared to the guest-host interactions.

On this basis, Child suggests that the entropy term contribution to stability is relatively small and that the stability depends primarily on the overall heat of formation of the clathrate and, therefore, on the magnitude of interaction between host molecules, and between the guest and the surrounding molecules of the host lattice. Thus, the heats of formation (ΔH_p) for a number of clathrates formed from hydroquinol and water have been shown to be about 0.8-2.2 of the value of two times the heat of vaporization ΔH_{vap} of the guest molecules, i.e., $\Delta H_p = 0.8$ to $2.2 (2\Delta H_{vap})$.

An explanation for these high ratios was given in terms of:

- The removal of a guest molecule from a clathrate leaves an empty cavity (with little interaction between host molecules across the hole), whereas the removal of a molecule of guest from a liquid leaves no hole
- The interactions between guest molecules and the wall of the cage may be greater than between the two guest molecules in the liquid state

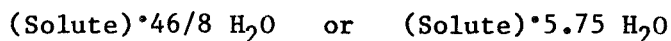
- The coordination number of the guest molecule may be larger in the cavity than in the liquid state. Thus, the vaporization of the pure guest may be visualized as a two-step process in which the vaporization step leaving empty holes in the remaining liquid has an enthalpy increase of $2\Delta H_{\text{vap}}$, and the subsequent collapse of the holes an enthalpy decrease of $-\Delta H_{\text{vap}}$, for a net change of ΔH_{vap} . In the case of clathrates, on the other hand, the vaporization enthalpy change of $2\Delta H_{\text{vap}}$ is counterbalanced not by the collapse of the holes remaining, but by the enthalpy change in converting the β structure to the α -form which is often much less than ΔH_{vap} . Furthermore, the heat of vaporizing the guest molecule from the clathrate structure may actually be greater than the heat of vaporization of the pure liquid because of the interaction between guest and host by an amount depending on the energy of interaction (which depends on the chemical nature of the guest and host) and the coordination number of interaction (which will depend on the size and shape of the cavity relative to that of CH_4).

Since methane is non-polar in nature, the host-guest interactions are likely to be limited to van der Waals forces. Thus, the most important host-guest interaction factor affecting the stability of its clathrates will probably be the diameter of the cavities formed by the host molecules. This is consistent with the fact that measured $\Delta H_p/2\Delta H_{\text{vap}}$ ratios for its clathrate with hydroquinone (1.8) and with water (0.8) are approximately inversely proportional to the cavity diameters of the two, 4.2 and 5.2 Å respectively. However, the interactions between methane and its host might be enhanced somewhat if the host cavities were lined with groups (such as hydroxyl or amino groups) having a high hydrogen bonding power as in the case of the apparently enhanced solubility of methane in alcohol solvents at a given solubility parameter. In the case of clathrates with hydrogen bonding power, one would not have to be concerned with the solubility parameter of the host.

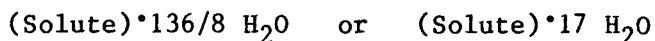
1.0 Natural Gas Hydrates^{3,25,26}

Perhaps the most familiar example of clathration to the gas industry are the hydrates of methane and other natural gas hydrocarbons. These hydrates became of interest to the U. S. gas industry around 1934 when it was noted that plugging of natural gas transmission lines was not due to freezing of water at 0°F, but to formation of hydrates of hydrocarbon constituents of natural gas at temperatures as high as 150°F.²⁴ It was subsequently found that gas hydrates exist in two distinct but different crystal structures depending on the size of the guest molecule:

- Structure I hydrates consist of small hydrating (guest) molecules, for example, Ar, Kr, Xe, CH_4 , C_2H_6 , H_2S , and CH_3Cl . The cubic unit cells have 46 water (host) molecules and 8 cavities (voids, cages) where guest (hydrating) molecules may be located. The ideal formula (all cavities filled) would be --



- Structure II hydrates consist of larger hydrating (guest) molecules; for example, C_3H_8 , CHCl_3 , and $\text{C}_2\text{H}_5\text{Cl}$. The cubic unit cells have 136 water (host) molecules and 8 voids (cavities, cages) for guest molecules. The ideal formula (all cavities filled) would be —



The above stoichiometry indicates that methane could be stored as the hydrate to the extent of 0.155 g of methane/g water.

Unfortunately, methane hydrate is not sufficiently stable for purposes of storage at ambient conditions. This is shown by Figure D-1 which indicates that methane hydrate is most stable above 4000 psig at 70°F (27.7 MPa at 21°C), or above 20,000 psig at 100°F²⁷ (138 MPa at 38°C). The equilibrium pressure at a given temperature is reduced considerably for the mixed hydrates of methane with either ethane (Figure D-2)²⁸ or propane (Figure D-3).²⁹ Thus, the overall vapor pressure of the hydrate at a given temperature can be reduced by blending methane with higher hydrocarbons. However, the effect with ethane and propane is not sufficient to make the hydrate useful for storage under truly ambient conditions. Furthermore, the hydrates of hydrocarbons above C_5 are not known.

Dissolved salts such as sodium chloride significantly decrease the temperature at which the hydrate is stable at a given pressure (Figure D-4),³⁰ presumably because they interfere with the crystallization (freezing point lowering).

Thus, it would appear that the mechanical strength of the crystalline water host in these hydrates is not sufficient to contain the vapor pressure of methane at ambient temperatures. Furthermore, it does not appear that the vapor pressure to be contained can be lowered sufficiently by blending the methane with higher hydrocarbons or other lower vapor pressure molecules. One wonders then if the strength of the host ice crystal structure can be increased in some other way. It was suggested that hydrate forming salts such as MgCl_2 might have this effect. However, the data on the effect of sodium chloride above suggests that the presence of MgCl_2 would also be deleterious. In particular, inorganic cations tend to complex with water (i.e., form chemical hydrates) through the oxygen atom, thus interfering with the hydrogen bonding between hydrogen and oxygen and, thus, with ice formation. On the other hand,

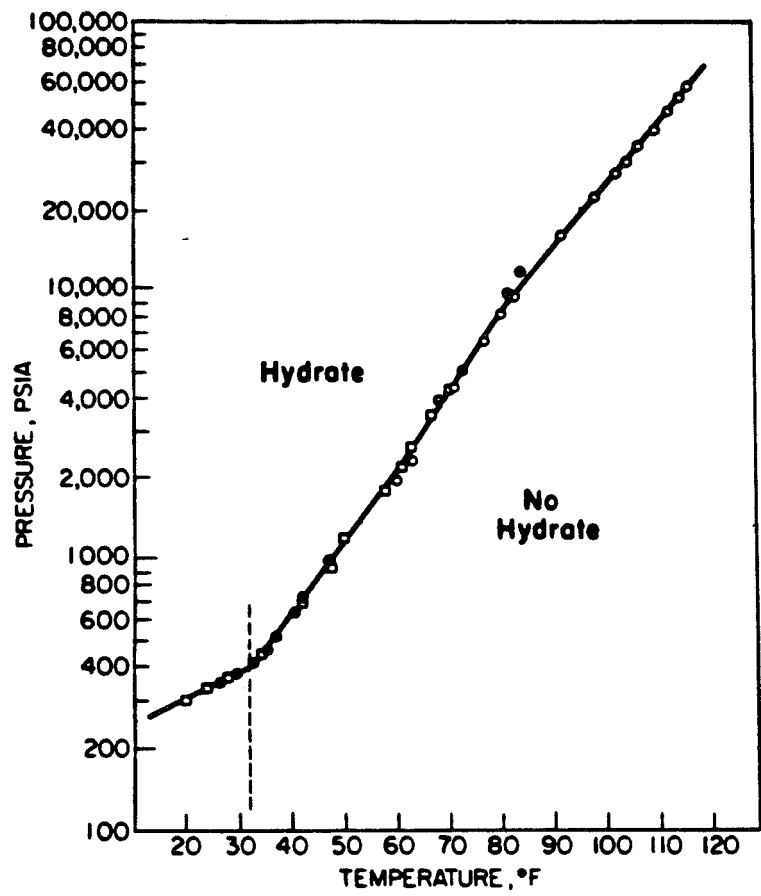


Figure D-1. PRESSURE-TEMPERATURE (P, T) CONDITIONS FOR HYDRATE FORMATION USING METHANE GAS AND PURE WATER

⊗

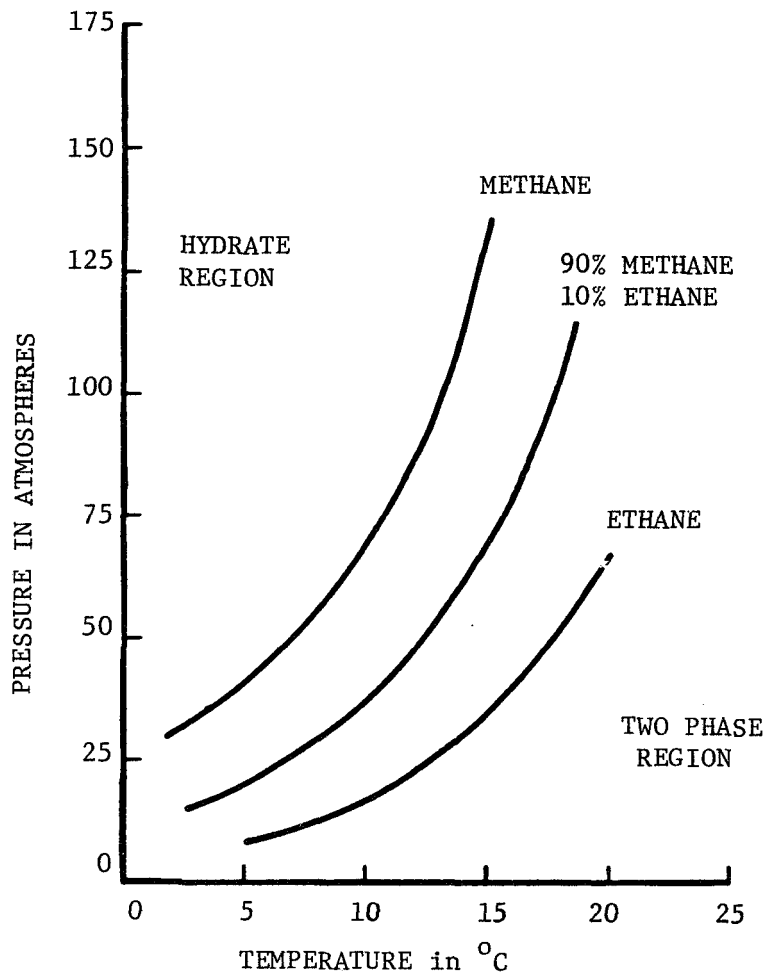


Figure D-2. HYDRATE EXISTENCE CONDITIONS FOR METHANE, ETHANE, AND A 90% METHANE-10% ETHANE MIXTURE (0.6 Sp. Gr. Gas) FROM REFERENCE 28

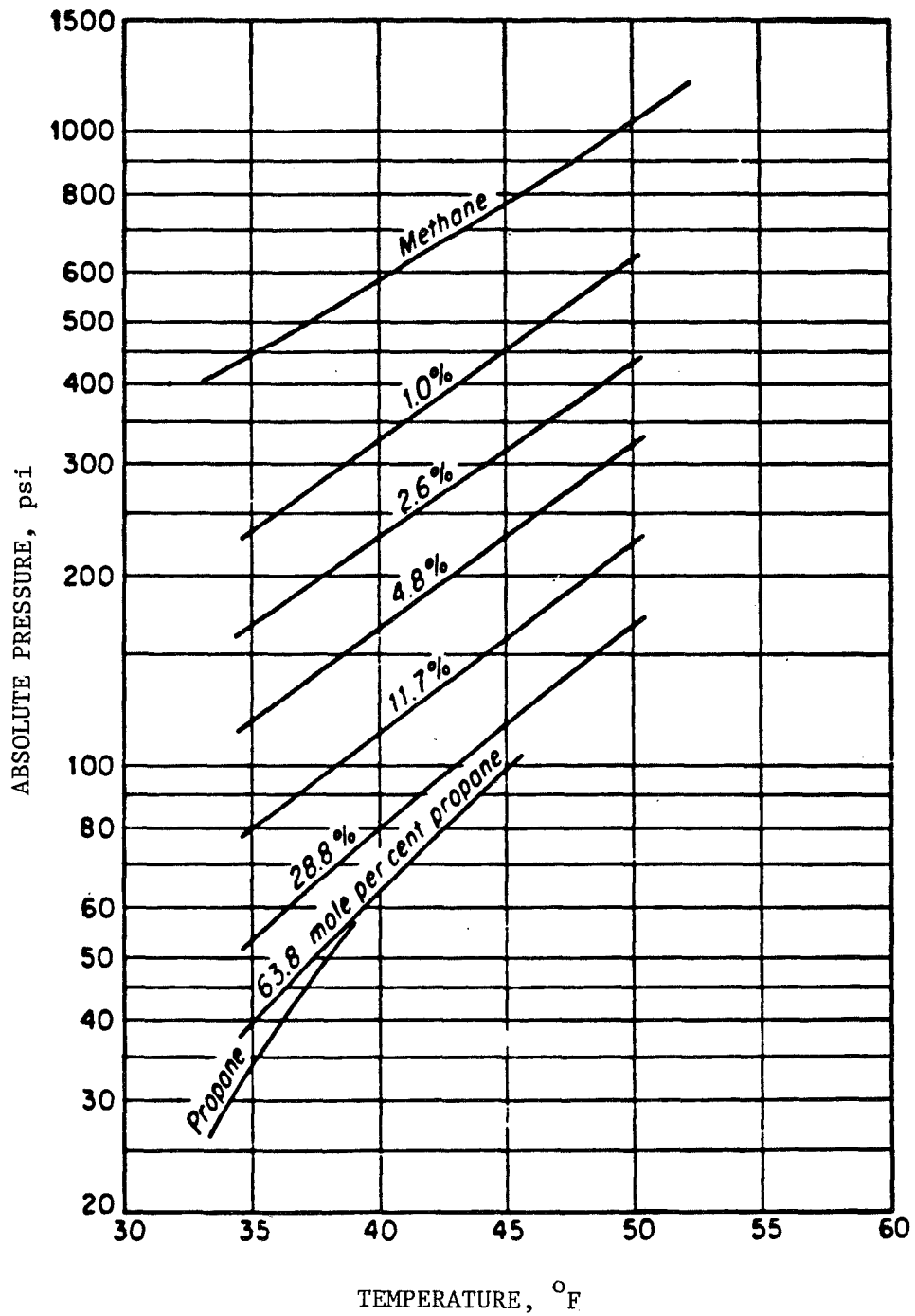


Figure D-3. HYDRATE-FORMING CONDITIONS FOR METHANE-PROPANE MIXTURES (From Reference 29)

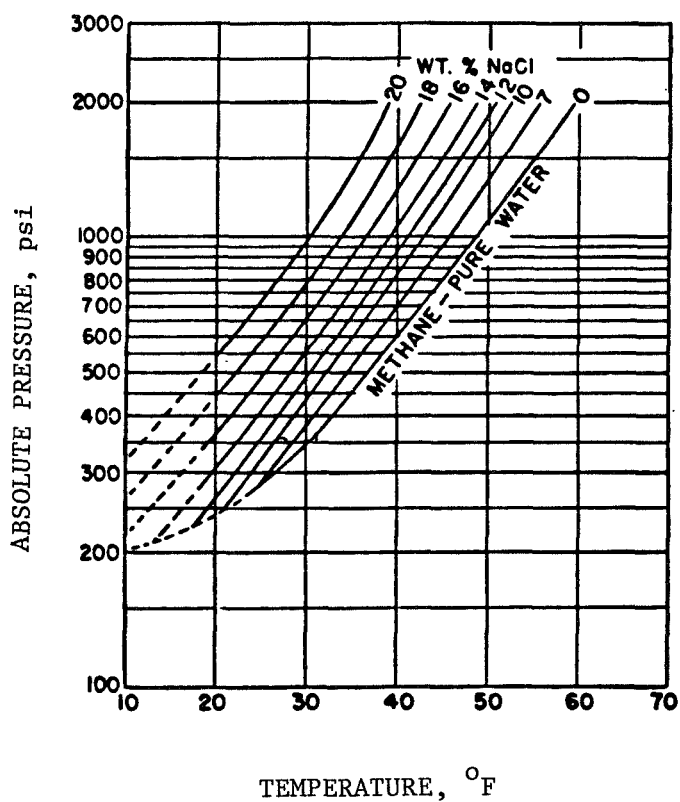


Figure D-4. METHANE HYDRATE PRESSURE-TEMPERATURE CONDITIONS FOR VARIOUS SODIUM CHLORIDE BRINE CONCENTRATIONS (From Reference 10)

it might be possible to find a suitable inorganic salt which, in the process of crystallizing as a hydrate, will clathrate small molecules such as methane. However, such a system would not be an extrapolation from the gas hydrate or any other known system but rather a new and unexplored area.

A traditional method of increasing the strength of materials, of course, is by reinforcement of the material with fiber (composite materials). A common example is glass fiber reinforced epoxy resins. Perhaps then, methane hydrate formed in the presence of a matrix of colloidal silica which gels into a highly cross-linked fibrous mass could show enhanced vapor pressure-temperature relationships. However, this is obviously a speculative suggestion at the moment.

Urea and Thiourea Inclusion Compounds^{1,4,8,10,11}

Considerable literature exists on the preparation and properties of urea and thiourea clathrates, primarily because of their use in the separation of isomers or other mixtures on the basis of difference in molecular size and shape. In particular, straight chain paraffin hydrocarbons (and fatty acids) have been separated commercially on the basis of the fact that the urea clathrate structure will accommodate n -paraffin chains but not branched chain hydrocarbons. Thus, a number of excellent reviews are available.

The urea and thiourea adducts are examples of the tunnel clathrates formed by crystallization through hydrogen bonding of the host molecules in the form of an extended helix or tunnel around the guest molecule. The tunnel diameter is of the order of 0.52 nm for urea and about 0.61 nm for thiourea.

The adducts are usually prepared basically by crystallization from a suitable solvent (e.g., water or methanol) in the presence of the guest molecule. n -hexane appears to be the shortest straight chain hydrocarbon that will form a urea adduct at ambient conditions. However, urea adducts of propane and butane have been prepared by Schlief by lowering the temperature to slightly below the boiling point of the hydrocarbon with methanol as solvent.³¹ It is possible that the urea adduct of methane may actually exist and be stable under ambient temperatures at elevated pressures.

Figure D-5 from Schlief³¹ suggests that if it does exist, the methane/urea adduct would have a composition approximating 1 CH₄/3 ureas corresponding

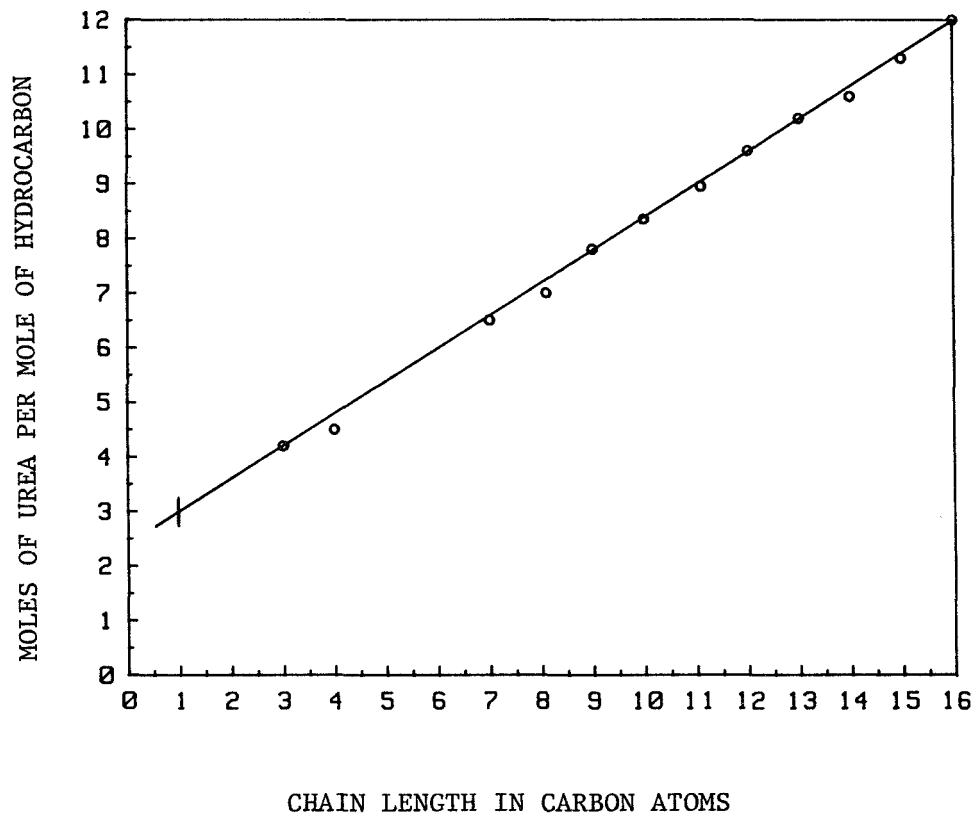


Figure D-5. DEPENDENCE OF THE GUEST/HOST RATIO UPON CHAIN LENGTH FOR HYDROCARBON/UREA CLATHRATES (From Reference 31)

to a weight ratio of 0.089 g/g which is of the same order of magnitude as that for adsorption on activated carbon at 3.6 MPa.

2.0 Phenolic Clathrates^{1,2,4,5,12,13}

Of considerable interest is the clathration behavior of phenols in general, and hydroquinone in particular. In the presence of small gaseous molecules such as methane (or O₂, N₂, C₂H₂, CH₃OH, HCl, SO₂, Ar, Kr, Xe), hydroquinone crystallizes in the metastable "β" modification in a ratio of 1 cavity to every 3 hydroquinone molecules. This crystal modification, however, is stable only if a certain fraction of the cavities are filled with guest molecules which are neither too small (He) nor too large (CCl₄). The cavity has a diameter of 3.95Å when occupied by small molecules comparable to 3.8Å for methane. However, larger molecules can be accommodated by distortion of the cavities. Although the crystal structure is held together by hydrogen bonding in a manner similar to ice, the stability of the hydroquinone clathrate is far greater: the CH₄·3C₆H₄(OH)₂ complex is quite stable at ambient temperature and pressure. X-ray diffraction studies indicate that the clathrate involves the formation of the typical hexagonally hydrogen bonded structure formed from six hydroxyl groups as discussed above.

The clathrate can be prepared by crystallization from a saturated solution of hydroquinone in ethanol in the presence of methane pressure³² or from the vapor phase comprising hydroquinone vaporized in a methane carrier gas.³⁴ In both cases, the fraction of the cavities filled with methane is highly dependent on the methane pressure (Figure D-6); thus, complete filling to yield the one to three stoichiometry requires a pressure of about 100 atm (10.4 MPa). The methane can be recovered for use by dissolution in water or ethanol or by heating (melting). No data was found on the thermal stability of the clathrate. However, the melting point of the modification of hydroquinone is 50°C (123°F). Thus, it is probable that it will decompose at about that temperature.

Unfortunately, the gravimetric capacity of the methane/hydroquinone clathrate is only 0.0485 g CH₄/g hydroquinone due to the high molecular weight of the host.

Phenol and several substituted phenols also form clathrates with methane and other gases, including rare gases, ethane, propane, and the butanes.^{1,34}

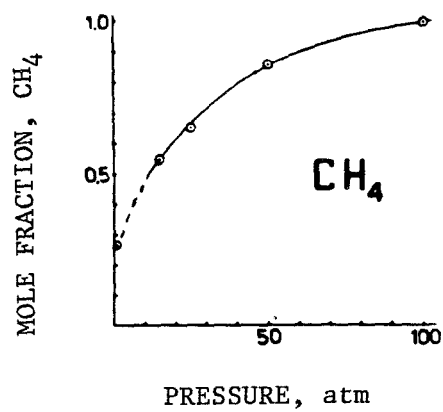


Figure D-6. FRACTION OF CAVITIES FILLED WITH METHANE AS A FUNCTION OF PRESSURE (from Reference 32)

These clathrates are also presumed to involve the typical hexagonal hydrogen bonded oxygen structure from six phenol groups together with the typical 1/3 stoichiometry. However, the data for methane clathrates with the phenols prepared at -196°C indicate a stoichiometry closer to 1 CH_4 /2.4-2.6 phenol molecules (instead of 1/3 as with hydroquinone). This may indicate that more than 1 methane molecule can be accommodated in the cage structure of the less lightly bound phenol group. This hypothesis is supported by the fact that hydrocarbons up to n-butane can also be clathrated by the phenols although at levels less than 1 molecule per cavity.³⁴

The data of Lahr and Williams on rare gas/phenol clathrates indicates that the CH_4 /phenol clathrate would be much less stable than the hydroquinone analog at ambient temperature.³⁵

Dianin's Compound^{1,2,4,5,12-14}

Dianin's compound ($\text{C}_{18}\text{H}_{20}\text{O}_2$) is the product of the condensation of mesityl oxide with phenol and is another example of the hexa-host class of clathrates described above, based on the hydrogen bonding of the phenolic hydroxyl groups. The cavities formed are hour-glass shaped, about 11Å in length, 4.2Å at the waist, and 6.4Å at the two widest points. Although best known for inclusion of solvent molecules, it also forms clathrates with fixed gases including methane (Barrer and Shanson).³⁶ Dianin's compound differs from other phenolic clathrates in that its β clathrate structure is stable whether the cavities are filled or not. Normally, three mole of phenolic or other hexa-host type are associated with each cavity. The apparent saturation capacity of Dianin's compound for methane is 6 CH_4 /6 Dianin compounds or 0.06 g/g which may indicate that three CH_4 molecules occupy each hour shaped cavity. However, this was measured at the boiling point, 182.5°C , and Barrer indicates that the apparent saturation capacity varies with temperature (at atmospheric pressure).³⁶ This suggests that such capacities might also exist at ambient temperature with elevated pressure.

Even more important, the data indicate that several CH_4 molecules can exist in a clathrate cavity, at least in more or less cylindrical cavities having diameters not too much larger than the kinetic diameter of methane.

Cyclodextrins^{1,2,9-13}

The cyclodextrins are cyclic oligosaccharides containing six (α), seven (β), or eight (γ) glucose units. The molecules in solution are presumably doughnut shaped with hole diameters of 6Å, 8Å, or 10-11Å, respectively, for the α , β , and γ forms. The voids in the center have been described as having a high electron density (Shaeffer and Dorsey),¹⁰ capable of complexing with various molecular species since no cage structure is evident. Furthermore, clathration has been shown to change the oxidation-reduction potential of certain molecules such as methylene blue.¹⁰

Alpha cyclodextrin (6Å) also forms clathrates with various fixed gases, including methane at ambient temperature-pressure to the extent of 0.014 g CH₄/g- α cyclodextrin. However, these clathrates are stable only in the dry state and, therefore, may involve cage structures. Nonetheless, this illustrates that cages as large as 6Å (about 2Å greater than the kinetic diameter of methane) can exhibit relatively high stability at ambient conditions, probably due to the inherent stability of the "beta" structure. The latter is identical to the "alpha" structure, at least in the dry state, since the cavity is held together by covalent bonds rather than hydrogen bonds. However, the vaporization of methane from the clathrate may also exhibit an enthalpy change greater than ΔH_{vap} in spite of the minimal coordination number due to the high electron density of the oxygen atoms lining the cavity walls.

The six, seven, and eight membered cyclodextrins are natural products produced by enzymatic action on amylose. However, one wonders whether a five membered analog could be produced synthetically. If so, the hole diameter would be of the order of 4Å (by extrapolation), just right for inclusion of methane ($d = 3.8-4.1\text{Å}$). Furthermore, it may be possible to synthesize cyclic polyethers (from ethylene oxide) tailored for inclusion of methane.

A further possible approach would involve the complete synthesis or modification of existing cyclic polyethers or cyclodextrins with low solubility parameter detergent-like tails to produce inclusion hosts soluble in solvents which also dissolve methane. In this manner, the solvent capacity for methane might be enhanced by the action of the dissolved inclusion hosts.

3.0 Encapsulation in Preformed Molecular Sieves^{17,18,37,38}

In the broadest sense, zeolites, molecular sieves, and activated carbons can be considered analogous to the host crystal of a clathrate except that the structure is preformed and stable without the included guest molecules. Such molecules have high internal surface areas contained within cages, or pores (tunnels) having precisely sized entries. Such materials are used not only for adsorption but also for separation of molecules having different kinetic diameters. Under ordinary conditions, the guest molecules must be smaller than the kinetic diameter of the host; otherwise, they will be excluded. It has recently been found that such molecular sieve structures can also be used for encapsulation or clathration of guest molecules larger than the characteristic pore opening size.³⁷ This is accomplished at high pressures and elevated temperatures such that the molecules are forced into the slightly expanded pore openings. Once inside, and after the temperature has been quenched to ambient levels, the molecules are trapped at high pressure inside the sieve. Such a system tends to be quite stable at ambient temperature and pressure until reheated, destroyed by acid, or exposed to a stronger absorbate (e.g., H₂O).

More specifically, it has been found that inert gases such as argon, krypton, and methane can be stored effectively in K-A-type zeolites at 25°C after encapsulation at 300° to 400°C and 200 to 400 MPa (2050 to 4100 atm). Data for encapsulation of CH₄ and ethylene as well as krypton and argon are shown in the following table.

Table 1. ENCAPSULATION OF GASES IN ZEOLITE A¹⁷

<u>Gas</u>	<u>σ (Å)</u>	<u>Temperature, (°C)</u>	<u>Pressure, (MPa)</u>	<u>cm³ STP/g</u>	<u>After t Days at 25°C</u>
CH ₄	3.8	350	268	105, t = 4	98, t = 37
C ₂ H ₄	3.9	250	84	81, t = 2	76, t = 35
Ar	3.4	350	268	109, t = 3	77, t = 79
Kr	3.6	350	436	90.5, t = 1	90.5, t = 30

Thus, at 350°C and 270 MPa, 105 cc STP/g are encapsulated. This corresponds to 0.075 g/g, which is of the same order of magnitude as for adsorption of CH₄ on zeolites at 3.6 MPa and 25°C. It should also be noted that after 37 days at 25°C and 1 atm, less than 7% of the CH₄ is lost. However, because of the drastic conditions required for the encapsulation of CH₄ into zeolite A, the process is obviously not feasible. Furthermore, the temperature required to decapsulate is undoubtedly too high (350°C).

Figure D-7 shows the pore sizes of a number of zeolites relative to the kinetic diameters of a number of gases including CH₄.¹⁸ It will be noted that zeolite KA has a pore size opening of about 3Å compared to 3.8Å for methane, while LiA at 3.3Å or NaA at 3.5Å are closer to that of methane. In addition, other molecular sieve materials, including activated carbons and the newly developed alumino phosphates, could be of interest.^{39,40} The average pore size of an activated charcoal can be varied over wide limits, depending not only on the conditions of activation, but particularly on the basic structure of the char substrate before activation. For example, Saran charcoals made by pyrolysis of polyvinylidene chloride have been shown to have a uniform slot-like pore structure between graphite-like layers of carbon. The slot-like pores are about 10Å in length and thin enough to restrict but not exclude the flow of branched chain hydrocarbons (neopentane) as compared to planar (benzene) or linear (n-pentane) hydrocarbons.³⁹ A molecular sieve carbon made by Takeda Chemical Industries, Osaka, Japan, exhibits an even smaller uniform pore structure of only 5Å.⁴² It is interesting to note that the heats of adsorption of various gases on these materials were twice those measured for graphitized carbon black.⁴³ The increased ΔH (adsorption) was attributed to the fact that adsorbed species interact with carbon layer planes on both sides, while molecules adsorbed on surfaces interact with only one carbon layer plane. Thus, even though the pore openings of these carbons are too large for encapsulates, the small pores offer the advantage of higher heats of adsorption which will result in the achievement of a given surface coverage at a lower pressure.

A new class of molecular sieves, the alumino phosphates, have recently been introduced by Union Carbide Corp.^{40,41} None of these materials, which

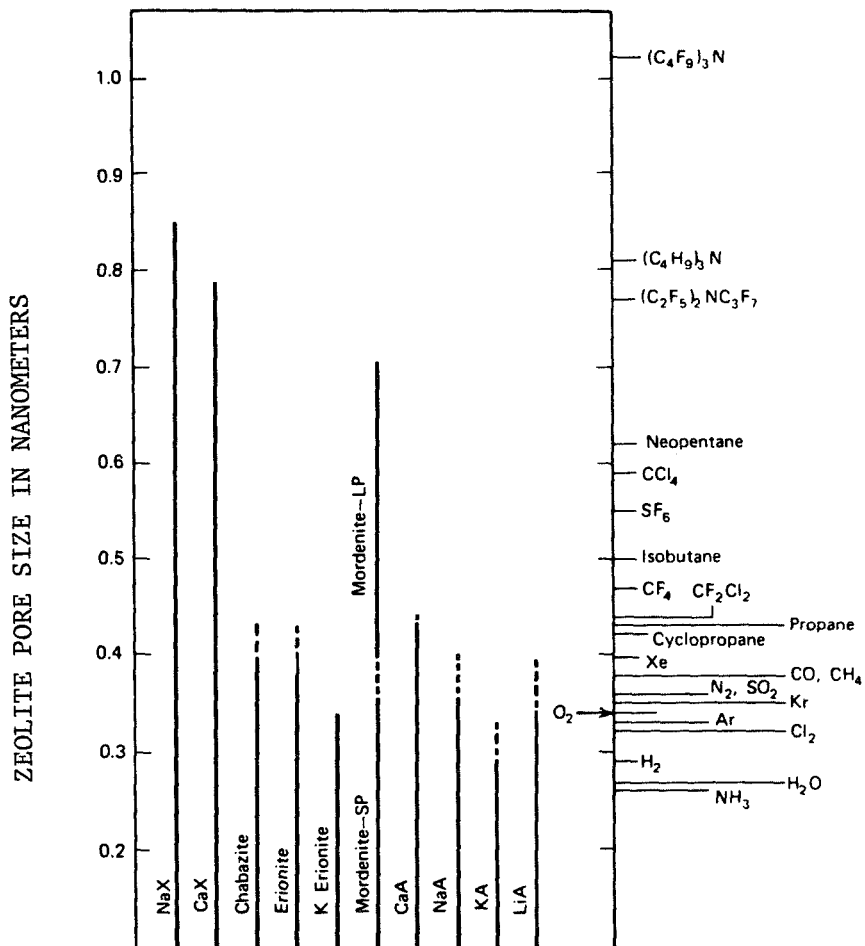


Figure D-7. MOLECULAR DIMENSIONS AND ZEOLITE PORE SIZE¹³

have so far been described, is particularly suited for encapsulating methane. Nonetheless, it seems a reasonable possibility that alumino phosphate or even zeolite molecular sieves could be tailored specifically for that possibility.

5.0 Cross-Linked Sorbents Formed in the Presence of Templates

The addition of templates or inclusion bodies during formation to control the size of the cavities and, therefore, the specificity of various adsorbents has been done with a number of materials including:

- Zeolites and alumino phosphates in which the templates are the cations involved^{18,42}
- Silica gels in which the gels are gelled around the template molecules, which are usually relatively larger, water-soluble molecules such as butyl orange dye¹³
- Modified dextrans which are macromolecular polysaccharides cross-linking to varying degrees in the presence of a suitable solvent and are used for gel permeation separation of molecules on the basis of molecular size.¹³

Thus, it may be possible to develop adsorbents or absorbents tailored specifically for methane by controlled cross-linking of organic as well as inorganic polymers in the presence of high pressures of methane (or other templates of a similar size, including propane and butane). Examples would include:

- Polymerization of isobutylene with suitable cross-linking agent (e.g., diisobutylene) in a propane or butane solvent
- Three-dimensional polymerization of a silicon monomer or oligomer with a suitable cross-linking agent
- Cross-linking of various polymers including a hydrogen bonding polymer such as cellulose (with its appended hydroxyl groups) or polyacrylamide (with its amido or substituted amido groups) or polymers having a solvent affinity for methane such as polyisobutylene swollen by a low molecular weight solvent which in the dry state should contain a multiplicity of cavities lined with either hydrogen bonding groups or methyl groups.
- Vapor phase formation of cross-linked silica gels in the presence of high concentrations or pressures of methane. This might be accomplished by saturating a methane stream with a suitable silicon compound (e.g., SiCl_4 or $\text{Si}(\text{O}-\text{CH}_3)_4$) followed by vapor phase hydrolysis or vapor phase thermal decomposition.

6.0 Other Clathrate Systems^{1,2,4,5,10-14}

There are many other molecules which have been shown to clathrate guest molecules including:

- Phosphonitrites
- Werner complexes
- Other metal ion-ligand combinations
- Steroids
- Cholesterol
- Hexamethyl isocyanide chloride
- Methyl naphthalene
- Cyclohexatriene.

These clathrate types will not be described here since no methane clathrates were attempted, even though higher molecular weight guests were included. However, such clathrate hosts should not be excluded from any further studies with methane since the latter was never even tried. For example, it is possible that some of these would crystallize differently in the presence of methane or may contain layer-like cavities which would accommodate methane as well as larger guest molecules. In any case, it may be possible to vary the molecular structures of the host to give the methane clathrate. Of particular interest are the metal-ion-ligand combinations since they are capable of wide variation in both the ion and the ligand used.

7.0 Summary

We have seen that methane clathrates exist which separately exhibit the various properties required for on-board storage, although not together in the same clathrate. Furthermore, a study of the literature suggests that nearly any chemical species near or below its freezing point has the potential of acting as a clathrate host under the right conditions and in the presence of a reasonable concentration of a suitable guest molecule. Thus, it is possible that a methane clathrate having all of the properties required for on-board storage can be found or developed although this may entail a compromise between stability, capacity, and methane release properties.

We also recognize that clathrates have properties akin to solutions on one hand and to molecular sieve-adsorbate interactions on the other. This is illustrated by a comparison of intracrystalline free volumes available for inclusion of β -clathrate hosts with the volumes available in zeolites as follows:⁷

Hydroquinone/argon	~0.05 cc/cc
Urea/paraffins	0.37
Thiourea/hydrocarbons	0.41
Gas hydrates	0.46
Zeolites	0.18-0.54

Thus, there is a large overlap in the potential inclusion volumes of zeolites and clathrates which is comparable to that in solutions. Inclusion of up to about 50% by volume are potentially possible by all three approaches, although the rules governing the accomplishment thereof are different.

For solutions, the primary influence appears to be the solubility parameter which appears to be inversely proportional to molecular weight so that 50% (by volume) solutions can only be achieved using solvents with molecular weights close to that of methane itself. This is not feasible for our purposes. With zeolites (and other adsorbents) for which the host structure is inherently stable by itself, the inclusion is limited at a reasonable pressure, e.g., 3.6 MPa, by the heat of adsorption of methane on the surface to less than a monomolecular coverage of the surface, which is usually less than potentially possible with inclusion compounds. The latter, however, can only be accomplished at high pressures or with large molecules at lower pressures.

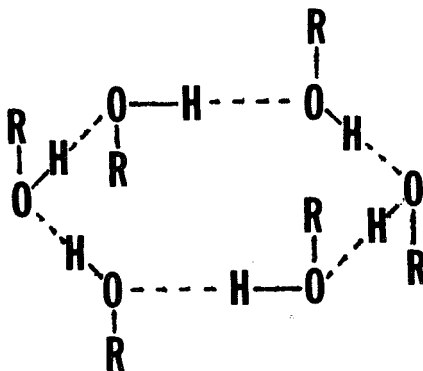
With clathrates, stability of the clathrate depends on the stability of the β -crystal lattice relative to that of the usual α -form and upon the magnitude of the heat of interaction between host and guest. Both contribute to the difficulty of removal of the guests. With most of the methane clathrates so far found, the potential saturation of the free volume available approaches 100%, probably because the clathrate is not discovered unless stability is achieved. As indicated above, stability under reasonable conditions is usually not achieved unless the cavity dimensions approach that of the guest molecule so that a relatively high coordination number for interaction is achieved.

Suggested Techniques for Future Clathration Host Development:

Although there is considerable work in progress toward developing the know-how for tailoring new clathrate hosts for specific guest molecules, most of the work is oriented toward biological and catalytic applications using enzymes and ionic species. No references have been found indicating ongoing work directed toward tailoring clathrate host molecules for small and relatively inert molecules such as methane or the inert gases. However, should such a program be undertaken, the following precepts are available to guide such development:

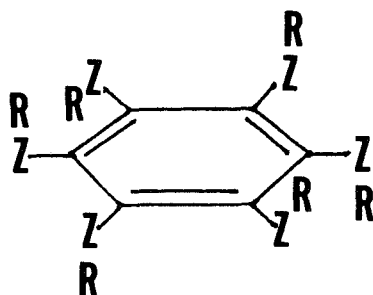
- Clathrate formation depends on the ability of the host molecules to form a crystal habit which has cavities large enough to accommodate the specified guest molecules. This is usually, although not necessarily, a crystal habit other than the normal crystal structure formed in the absence of the host. This ability would be difficult to predict, a priori, although it might be possible for a well versed crystallographer to develop such a predictability on the basis of molecular structure.

Indeed, this is essentially the approach used by MacNicol, et al.,¹⁴ who noted that many of the known clathrate structures involve the formation of a hexagonal ring of hydrogen-bonded oxygen atoms from six phenolic hydroxyl groups as shown below.



Structure A

The clathrate hosts which show this behavior include Dianin's compound,² related compounds,^{3,4} hydroquinone,⁵ phenols,⁶ and possibly water. MacNicol, et al., then demonstrated that the clathration ability of such hexagonal structures could be simulated using the permanent hexagonal structure of certain hexa substituted benzenes:



Structure B

where R-Z-radicals included a variety of substituted oxygen and sulfur radicals. However, the guest molecules bound by these clathrate hosts are larger than methane, indicating relatively large cavities.

By the same token, new clathrate hosts might also be derived by varying the nature of R- in Structure A to include substituted phenol and also various aliphatic, alicyclic, and olefinic species, substituted or unsubstituted. Furthermore, the formation of suitable hydrogen-bonded hexagonal structures can also be formed with elements other than oxygen from Rows 5A and 6A of the periodic table, in particular through nitrogen atoms in amides. In addition, the formation of a hexagonally arrayed hydrogen-bonded structure is not an exclusive prerequisite, since urea forms tunnel clathrates with straight chain paraffins by forming a hydrogen-bonded two-dimensional helix spiral (tunnel) around the paraffin molecule. Thus, the primary prerequisite is the hydrogen-bonding (or other complex forming) ability of the host while the secondary prerequisite is a molecular geometry (at least partially unpredictable) which will crystallize in the presence of a guest to a structure with cavities sized to accommodate the guest.

Methods for Increasing the Stability of Clathrates and Improving Methane Release Properties:

Stability is of major importance since it controls not only whether the methane can be contained at reasonable pressures under ambient conditions but

also the conditions under which the methane can be released. The hydrate of methane for example is not stable enough since it requires a pressure of 28 MPa to exist under ambient temperature conditions. On the other hand, the hydroquinone/methane clathrate is too stable. Thus, although it can be stored at ambient temperature and pressure, it requires an elevated temperature ($\sim 50^{\circ}\text{C}$) or the introduction of a solvent to release the methane. Obviously, a compromise is in order so that the clathrate will be stable at ambient conditions at a reasonable pressure of 1.4 to 3.6 MPa, in order that methane release can be achieved and controlled by pressure reduction.

The parameters controlling stability would include:

- Hydrogen bonding power of the groups through which the crystallization occurs, as determined by the nature of the groups themselves, as well as the size and electrophilic character of the other groups in the molecule. Of particular interest in this regard would be the amides and substituted amides.
- Geometry and symmetry of the host molecule as it affects the structure of the crystal habit formed. The importance of symmetry is suggested by the fact that the hydroquinone (p-dihydroxybenzene) gives a highly stable clathrate with HBr, whereas the meta analogue does not exist at atmospheric pressure.

Suggestions for Increasing Storage Capacity of Methane:

The capacity of a clathrate for storing methane depends on two factors:

- How many host molecules are required to provide one guest "cage" (i.e., the unit cell)
- Molecular weight of the host molecule.

The structure of the unit cell and, therefore, the number of host molecules per guest molecule is dependent in a very complex way on various crystallographic factors and is beyond prediction at this time, except perhaps for the "hexamer" clathrates (described above) which tend to give a 3/1 host to guest ratio. However, the unit cell is likely to contain a reasonably small number of host molecules, e.g.,

- 3 in the hydroquinone-methane clathrate and other "hexamer" hosts
- 5.75 in the methane hydrate.

Thus, molecular weight may be the factor of greatest importance in determining capacity.

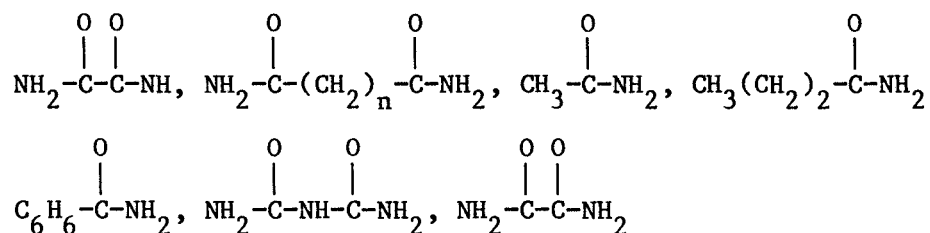
On the other hand, it may be possible that some higher molecular weight molecules with complex symmetries may form clathrate structures in which the host/guest ratio is significantly less than the 3/1 found for the hexamer types, or that form structures with cavities sufficiently large to accommodate two or more methane molecules, as in the case of the urea tunnel adducts. In the latter case, diffusion would be the primary barrier to decomposition and the system would function in a manner analogous to that of absorption in a zeolite. Most of the clathration entities forming larger cavities (and there are a lot of them, including Dianin's compound, the Werner complexes, deoxycholic acid, and urea and thiourea, etc.) have been evaluated only with larger guest molecules (usually the solvent used) at atmospheric pressure and not with permanent gases such as methane under elevated pressures. For example, urea adduction of the homologous n-paraffin series has been extended downward to include propane and butane, which are stable at atmospheric pressure only at subzero temperatures. However, it is possible that adduction could be extended to include methane and ethane as well at ambient temperatures and elevated pressures.

8. Future Research Recommendations

It is apparent from the above discussion that any future work toward the development of clathrate systems for storage of natural gas will be highly empirical in approach. Such a program would involve:

- 1) Evaluation of the formation and stability of clathrates of the known host systems toward methane at pressures up to 7.0 MPa. In particular, this would include the urea and thiourea systems and those whose cavities are presumed to be too large for methane as suggested above (particularly the ligand cross-linked metal ion, e.g., Werner complexes).
- 2) Evaluation of the effect of variations in structure on stability and capacity. Of particular interest would be:
 - N-substituted ureas and thioureas to enhance hydrogen bonding strength and, therefore, stability of the adducts
 - Diphenols including the effect of ring substitution on stability of hydroquinone clathrates and the use of meta and ortho diphenols
 - Variations based on cyclodextrin, including synthesis and evaluation of the five membered oligomer and conversion of the inwardly-oriented hydroxyl groups to ethers of varying size, amides, etc. to decrease the hole size, and/or the interaction chemistry with methane.

- 3) Determine the effect of more drastic changes in the molecular structure of amides on their clathration behavior, e.g.,



- 4) Synthesis and evaluation of cyclic polyamides (analogous to the crown ethers but with greater hydrogen bonding propensity)
- 5) Evaluation of systems based on aliphatic alcohol groups such as glycols and substituted glycols, glycols and substituted ethers and polyethers
- 6) Evaluation of systems based on aliphatic acids such as oxalic acid, acetic acid, chloroacetic acid, malonic acid, chlorinated malonic acid, maleic acid, and succinic acid derivatives.

REFERENCES FOR APPENDIX D

1. Bhatnagar, V. M., Clathrate Compounds, 1970, Chemical Publishing Co., NY
2. Makin, E. C., "Clathration," Encyclopedia of Chemical Technology, Vol. 6, p. 179-189, Kirk and Othmer, Eds., New York: Wiley (1978).
3. Davidson, D. W., Water: A Comprehensive Treatise, Vol. 2, Plenum Press, New York (1973).
4. Hagan, Sister Martinette, Clathrate Inclusion Compounds, 1962, Reinhold Publishing Co., NY
5. Powell, H. M., "Clathrates", Chapter 7 in Non-Stoichiometric Compounds, Mandelcorn, L., Ed., Academic Press, NY (1964).
6. Fetterly, L. C., "Organic Adducts," Chapter 8, Ibid.
7. Barrer, R. M., "Inorganic Inclusion Complexes," Chapter 6, Ibid.
8. Senti, F. R. and Erlander, S. R., "Carbohydrates," Chapter 9, Ibid.
9. Staveley, L. A. K., "Physics and Chemistry of Inclusion Complexes," Chapter 10, Ibid.
10. Schaeffer, W. D. and Dorsey, W. S., "Clathrates and Clathrate Separations," Chapter 3, Advances in Petroleum Char and Refining VI, 119-167 (1962).
11. Cramer, F. D., "Inclusion Compounds," Rev. of Pure and Applied Chem., Vol. 5, 143-164, (1955).
12. Mandelcorn, L., "Clathrates," Chem. Rev. 59, 827-839 (1959).
13. Frank, S. G., "Inclusion Compounds," J. Pharmaceutical Sciences, 64, #10, 1585-1604, (1975).
14. MacNicol, D. D., McKendrick, J. J., and Wilson, D. R., "Clathrates and Molecular Inclusion Phenomena," Chemical Soc. Reviews, 65-87 (1978).
15. Child, W. C., "Molecular Interactions in Clathrates: A Comparison with Other Condensed Phases," Quart. Rev., Vol. 18, p 321-346.
16. Van der Waals, J. H. and Platteeuw, J. C., "Clathrate Solutions" in Advances in Chemical Physics, Vol. II, Edited by Prigogine, I. Interscience Publishers, Inc., NY, 1959, p. 1-57.
17. Breck, D. W., "Crystalline Molecular Sieves," J. Chem. Ed. 41, 678-689, (1964).

18. Breck, D. W., Zeolite Molecular Sieves, John Wiley & Sons: New York, NY, 1974.
19. Cram, D. J., "Cavitands: Organic Hosts with Enforced Cavities," Science **219**, 1177-1183, (1983).
20. Cram, D. J. and Cram, J. M., "Host-Guest Chemistry," Science, **183**, 803-809, (1974).
21. MacNicol, D. D., and Wilson, D. R., "New Strategy for the Design of Inclusion Compounds: Discovery of the "Hexa-hosts"," J. Chem. Soc. Comm. p. 494-495, (1976).
22. Hardy, A. D. U., MacNicol, D. D., and Wilson, D. R., "A New Approach for the Design of Inclusion Compounds," J. Chem. Soc. Perkin II, 1011-1019, (1970).
23. MacNicol, D. D., Hardy, A. D. U., and Wilson, D. R., "Crystal and Molecular Structure of a "Hexa-host" Inclusion Compound," Nature, **266**, 611, (1976).
24. Scott, M. I., Randolph, P. L., and Pangborn, J. B., "Assessment of Methane Hydrates." Final report for period Dec. 1978 through June 1980, GRI-79/0070, Contract #5011-310-0097, Oct. 1980.
25. Hammerschmidt, E. G., Knapp, K. R. and Perkins, C. L., "Gas Hydrates and Gas Dehydration," in Gas Engineers Handbook. New York: Industrial Press, 1969.
26. Parent, J. D., "The Storage of Natural Gas as Hydrate," IGT Res. Bull. No. 1, Chicago, 1948.
27. Hand, J. H., Katz, D. L., and Verma, V. K., "Review of Gas Hydrates With Implication for Ocean Sediments," in I. R. Kaplan, Ed., Natural Gas in Marine Sediments, 179-94. New York: Plenum Press, 1974.
28. Baker, P. E., "Experiments on Hydrocarbon Gas Hydrates in Unconsolidated Sand," in I. R. Kaplan, Ed., Natural Gas in Marine Sediments, 227-34. New York: Plenum Press, 1974.
29. Katz, D. L. et. al., "Water-Hydrocarbon Systems," in Handbook of Natural Gas Engineering. New York: McGraw-Hill, 1959.
30. Kobayashi, R. et. al., "Gas Hydrate Formation with Brine and Ethanol Solutions," in Proceedings Thirtieth Annual Convention, Natural Gasoline Association of America, 27-31, Tulsa, Okla., April 25-27, 1951.
31. Schlieff, V. H., "Harnstaffein Schlußverb in dungen von η -Butan und ν -Propan," J. Prakt. Chem., **4**, 335-339 (1955).
32. Peyronel, G. and Barbieri, G., "On Some New Clathrates of Hydroquinon," J. Inorg. and Nuclear Chem., **8**, 582-585 (1958).

33. Coutant, R. W., "Solventless Preparation of Hydroquinon Clathrates," J. Org. Chem., 39, 1593-1594 (1974).
34. Barrer, R. M. and Shanson, V. H., "Clathration by Para-Substituted Phenols," J. Chem. Soc., Faraday, T., 2348-2354, (1976).
35. Lakr, P. H. and Williams, H. L., "Properties of Some Rare Gas Clathrate Compounds," J. Phys. Chem., 63, 1432-1433, (1959).
36. Barrer, R. M. and Shanson, V. H., "Dianin's Compound as a Zeolitic Sorbent," J. Chem. Soc. Comm., 333-334, (1976).
37. Sesny, W. J. and Shaffer, L. H., U.S. Patent No. 3,316,691 (1967).
38. Fraenkel, D., "Encapsulate Hydrogen," Chemtech., 11, 60-65 (Jan. 1981).
39. Dacey, J. R. and Thomas, D. G., "Adsorption on Saran Charcoal," Trans. Faraday Soc., 50, 740-748 (1954).
40. Wilson, S. T., et. al., "Alumino Phosphate Molecular Sieves: A New Class of Microporous Crystalline Inorganic Solids," JACS, 104, 1146-47, (1982).
41. Haggin, J., "Alumino Phosphates Broaden Shape Selective Catalyst Types," C&EN, June 20, 1983, 36-37.
42. Kawazoe, K., et. al., "Correlation of Adsorption Equilibrium Data of Various Gases and Vapors on Molecular-Sieving Carbon," J. Chem. Eng. of Japan, Vol. 7, p. 158-162 (Eng.), (1974).
43. Kazuyuki, C., Suzuki, M., and Kawazoe, K., "Adsorption Rate on Molecular Sieving Carbon by Chromatography," A.I.Ch.E. Journal, Vol. 24, March, 237-246, (1978).

APPENDIX E.

EVALUATION OF DISSOLUTION AS A MEANS OF STORING NATURAL GAS SOLUTIONS

1. Background

The concept of an ideal solution is used to describe the behavior of actual solutions as a first approximation, similar to the manner in which the concept of the ideal gas is used to describe real gases. In both cases, the degree of accuracy of the approximations are reasonable for many chemical entities, at least within certain limits, i.e., for dilute solutions or for gases at low pressures.¹ "In both cases, the idealized limiting behavior can be either: 1) defined thermodynamically by means of empirical expressions; or 2) derived from idealized models of molecular systems."¹ The thermodynamic definition of an ideal solution is: "one in which the activity equals the mole fraction over the entire composition range and over a non-zero range of temperature and pressure." Thus, for solutions of gases which approximate the ideal gas laws reasonably closely, the ideal solution is defined by Raoult's law:

$$\begin{aligned} P_1^i &= P_1^0 X_1 \\ \text{and} \\ P_2^i &= P_2^0 X_2 \end{aligned} \tag{1}$$

where:

P_1^i or P_2^i = Ideal partial vapor pressures of Components 1 and 2

X_1 or X_2 = Mole fraction of Components 1 or 2 in liquid mixture

P_1^0 or P_2^0 = Equilibrium vapor of Components 1 and 2 over pure materials.

Raoult's law, in this case, was deduced on the assumption of zero heat of mixing and an entropy of mixing that is independent of temperature and of peculiarities of molecular sizes and shapes. Thus, an ideal solution is defined in terms of zero heat of mixing. A corollary of this definition is Henry's law which states that the equilibrium value of the mole fraction of a gas dissolved in a liquid is directly proportional to the activity (or partial pressure if the gas approximates ideality) of that gas above the liquid surface.

$$X_1 = K_H P_1 \tag{2}$$

Where:

K_H = Henry's law constant.

Henry's law is not restricted to ideal solutions, at least if corrections for deviations of the gas from ideality are taken into account. Thus, solubilities of gases in various solutes are often defined in terms of the Henry's law constant determined at 1 atmosphere pressure (or partial pressure).

According to Raoult's law, methane can be stored at ambient temperatures at substantially reduced pressures as an ideal solution in a liquid of low volatility. However, the vapor pressure of liquid methane at 25°C (extrapolated) is 29.3 MPa (4248 psia).¹ Thus, methane stored at 25°C as a 50 mole percent solution in a non-volatile solvent will still exert a pressure in excess of 14 MPa (2000 psi). To reduce the ambient storage pressure to 3.6 MPa at 25°C requires reducing the mole fraction of methane in the solution to somewhat less than 0.135; reduction to 1.8 MPa, to less than 0.07 mole fraction. It is apparent, therefore, that the utility of storage as an ideal solution is not a particularly promising approach, unless a nonideal solvent can be found such that the solution with methane exhibits a large negative deviation from Raoult's law.

2. Regular Solution Theory^{1,2}

Many non-ideal solutions have sufficient thermal energy to overcome the tendency to segregate, thus displaying nearly ideal entropy of mixing. Such solutions have been designated by Hildebrand and Scott as "regular" solutions.¹ Differences in solubility (i.e., differences in the change of free energy of mixing, ΔF_M) compared to ideality will depend on differences in the heat of mixing, ΔH_M . On the basis of regular solution theory, Hildebrand developed an equation for the solubility of gases in the form:

$$\log X_2 = \log X_2^i - \frac{V_2}{2.303 RT} (S_1 - S_2)^2 \quad (3)$$

Gjaldbaek and Hildebrand³ subsequently modified the equation for Flory-Huggins mixing as follows:

$$\log X_2 = \log X_2^i - \frac{V_2}{2.303 RT} (S_1 - S_2)^2 - \left[\log \frac{V_2}{V_1} + 0.434 \left(1 - \frac{V_2}{V_1}\right) \right] \quad (4)$$

Where:

X_2 = Equilibrium mole fraction of Component 2 in a liquid mixture

X_2^i = Ideal solubility of Component 2 in mixture

V_1, V_2 = Molar volumes of components

R = Gas constant = 1.9865

T = Temperature of solution, °K

S_1, S_2 = Solubility parameters of Components 1 and 2.

The solubility parameter, also called the cohesive energy density, S , in turn is defined as follows:

$$S_1 = \left(\frac{\Delta H_1^V - RT}{V_1} \right)^{1/2} \quad (5)$$

Where:

ΔH_1^V = Heat of vaporization of Component 1 at solution temperature

R, T, V_1 = As above.

The ideal solubility, X_2^i , can be estimated by the following equation:

$$\log X_2^i = \frac{\Delta H}{2.303 R} \left(\frac{1}{T} - \frac{1}{T_B} \right) \quad (6)$$

Where:

T = Solution temperature, °K

T_B = Boiling point, °K.

Thus, the primary parameters controlling the solubility of a non-polar gas such as methane in non-polar solutions is presumably the temperature of the solution relative to the boiling point of the gas, the molal volumes of the components and, in particular, the solubility parameter, S , as defined above.

It will be noted that if methane (or any other non-polar gas) is dissolved in a solvent having the same molal volume and the same solubility parameter as methane, the last two terms in the equation would be zero and the solubility would be that calculated for an ideal solution.

The Hildebrand treatment of regular solutions has been modified empirically to yield better correlations with non-associated polar solvents by Yen and McKetta.⁴ However, the differences in actual solubility covered by these correlations are marginal compared to the effects sought in this review. Other reviews of the literature on gas solubility in liquids include Battino,²² Lawson,²³ and Pierotti.²⁴

Considerable data on the solubility parameters of various molecular species are available in the literature, most of which are based on heats of vaporization measured at 25°C.^{1,2,5,6,9} The data presented by Hildebrand and Scott^{1,2} specifies the temperature at which ΔH^V was measured. However, the temperature at which the ΔH^V were derived is not necessarily clear in other sources although 25°C is usually implied. In particular, sufficient data for methane and ethane ($\Delta H^V + V$) were not found to give good estimates of S at 25°C. Furthermore, in some literature sources, solubility parameters were estimated from solubility data in solvents for which S values are available.^{1,2,7,8} However, in this case, variations attributed to S may actually be the result of variations in molar volume (i.e., in the Flory Huggins correction).

Alternate methods of estimating the solubility parameter are also available as outlined by Hildebrand and Scott^{1,2} and by others.⁵

According to the data cited by Hildebrand and Scott,² methane behaves in most solutions like other non-polar molecules, subject primarily to the van der Waals forces. For example, the solubility of methane in various solvents correlates nicely with that of other non-polar gases, including H₂, N₂, CO, O₂, CO₂, and the rare gases, on the basis of their "force constants," the parameters of the intermolecular energy function as expressed by Lennard-Jones. Furthermore, the solubility of methane correlates rather well with the solubility parameter of the solvent, which is a measure of the cohesive energy density of the solvent. Exceptions to this, which tend to indicate solvation or some degree of polar or acid-base interaction (as in the case of CO₂-benzene mixtures), have not been found for methane solutions.

The efficacy of Equation 4 for estimating the solubilities of a number of non-polar gases, including CH_4 , in various solvents has been tested by Gjaldbaek and associates with reasonably positive results.^{3,7,8} However, these results were dependent on estimations of the solubility parameter of methane (and other gases near or above their critical points) from Equation 4 using solubility data in other solvents of known solubility parameters. Their estimate of S for methane on this basis is 6.2, far greater than our own estimate of something less than 4.

It is also interesting to note that some of the higher members of the paraffin series, such as n-heptane (C_7H_{16}) and in particular isooctane (C_8H_{18}), behave in solutions with perfluorocarbons as if their solubility parameters are significantly greater than those calculated from presumably reliable ΔH^V density data at solution temperature.²

The effect is greatest with i- C_8H_{18} , which has a labile tertiary hydrogen atom that may behave somewhat as a Lewis acid. However, the effect apparently disappears with paraffins below 7 carbon atoms whose hydrogen atoms are less labile (at least toward thermal decomposition). Thus, such an effect would not be expected with methane.

Negative deviations from ideal solution behavior would be expected primarily with strong interactions (e.g., dipole, acid-base, or hydrogen bonding) between solute and solvent, which appear to be unlikely to occur with methane, at least with common solvents.

On the other hand, physical adsorption of methane on surfaces such as activated carbon or silica gel do in fact represent strong (van der Waals forces) interactions between methane and a chemical substrate (solid, in this case) which are comparable to negative deviations from "ideal interaction." Thus, negative interactions with methane are possible and might be simulated in the liquid phase by surface forces either in mixed interacting solvent combinations or by adding solid surfaces to form a colloidal suspension.

Data Collection

The solubility data found in this study, covering a broad spectrum of solubility parameters and molal volumes as well as polarities, are shown in Table 2, and in Figure 1 plotted as a function of solubility parameter. In general, the data correlates reasonably well with the solubility parameter

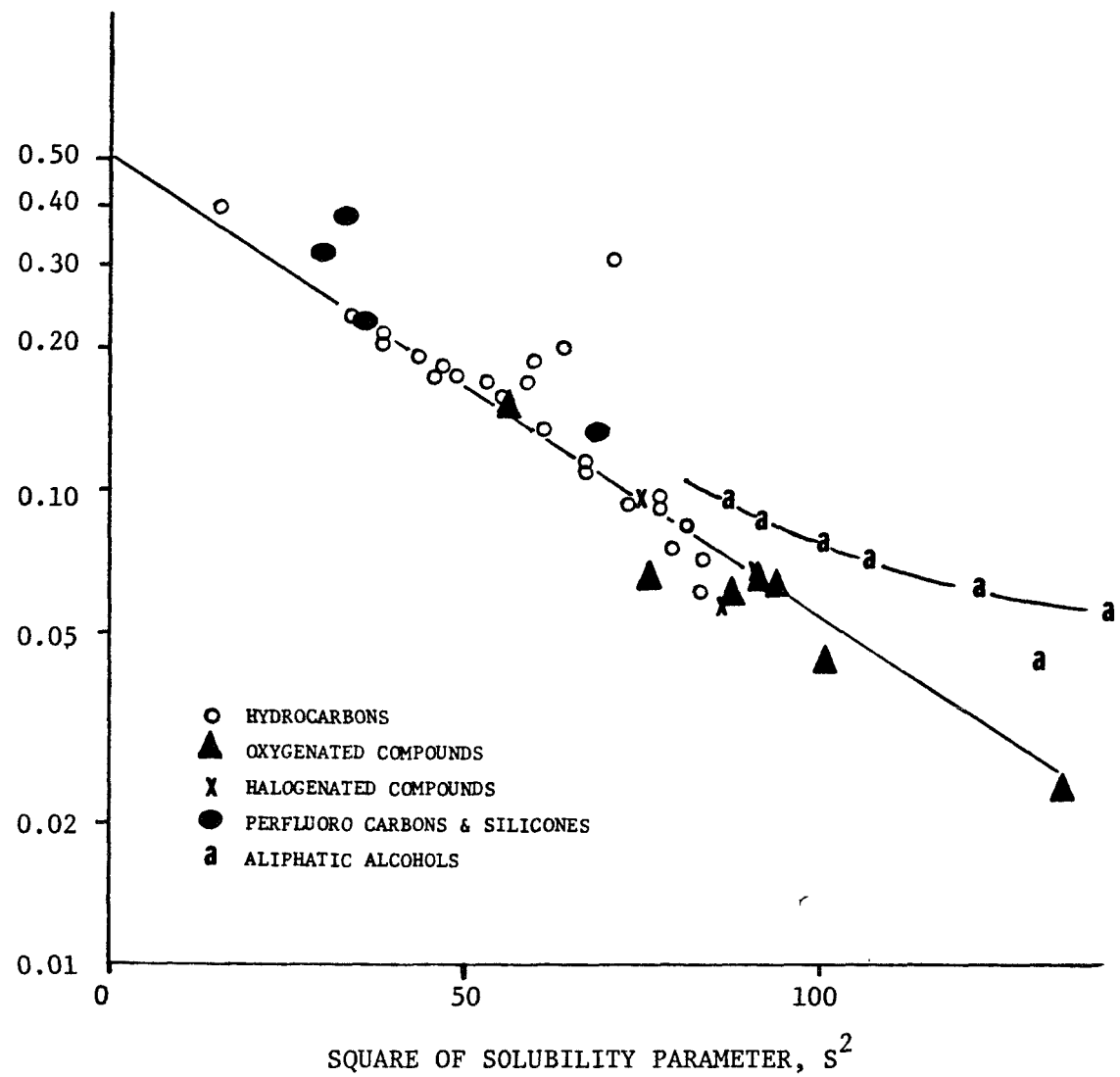


Figure E-1. METHANE SOLUBILITY - SOLUBILITY PARAMETER CORRELATION

from 5.5 to 10 with solubility decreasing with increasing solubility parameter.

Most of the solubility data available in the literature were measured in terms of mole fraction of methane in equilibrium solution at the standard conditions of 25°C and 1 atmosphere total pressure. For our purposes, these data have been converted to molal solubilities at more practicable conditions of 34 atmospheres (500 psia) and 25°C (77°F) assuming that Henry's Law is obeyed, which is reasonably accurate for methane up to at least 34 atm. Solubilities in the lower paraffinic hydrocarbons (C₂-C₄), however, were derived from vapor-liquid equilibrium data for those systems in which both components have appreciable, or high concentrations in both phases in two ways: 1) equilibrium concentrations in liquid at a total pressure of 34 atm as measured, and 2) by correcting the measured mole fractions of methane in the liquid phase at 25°C to a methane partial pressure of 34 atm via Henry's Law.

Solubility @ 34 atm CH₄, 25°C =

$$\frac{\text{Mole Fraction in Liquid Phase @ 25°C}}{\text{Mole Fraction CH}_4 \text{ in Vapor Phase} \times \text{Total Press}} \times 34 \quad (7)$$

Such values are fictitious in the sense that they can be achieved only at pressures much greater than 34 atm or not at all in the case of ethane. However, they do represent the approximate solubilities which would be achieved if the solvent had the same solution properties as C₂-C₄ hydrocarbons but were non-volatile.

It will be noted from Figure 1 that the solubilities of methane in a wide variety of solvents other than alcohols correlate more or less linearly with the solubility parameter of the solvent on a log molal solubility versus S² basis, semiquantitatively in agreement with Equations 3 or 4. However, Figure 1 is intended primarily to be illustrative and not as a definitive correlation. Thus, the scatter in the data may result from failure to account properly for differences in molal volume of solute and solvent as well as inaccuracies in:

- Solubility measurements
- Estimation of solubility parameters

- Deviations from ideal gas behavior.

There are several features of the correlation that need comment.

1. Applicability of Solubility Parameter Values

Although the correlation conforms, in general, to Equation 3 which has a theoretical basis, it should not be considered rigorous and quantitative. In particular, the assignment of quantitative values to the solubility parameter, S , is somewhat in question since values of heats of vaporization and molar volumes at solution temperature (25°) are sometimes difficult to find. Furthermore, as Hildebrand has pointed out, in some cases paraffin hydrocarbons in perfluorocarbons tend to behave as if the solubility parameter of one (or both) of the components is shifted.² Thus, there is a tendency in the literature to use alternate methods of estimating S , in particular, by defining the solubility parameter using empirical solubility determinations with solvents or solutes whose solubility parameters are known.

The solubility parameter of methane at 25°C cannot be estimated by the method used in this study (based on $\Delta H_V + V_M$), since 25°C is considerably above its critical temperatures ($T_C = -82^\circ\text{C}$). Thus, the heat of vaporization at 25°C is presumably zero and the net energy of vaporization ($\Delta H^V - RT$) may actually be negative (i.e., $(0 - RT) = -592$ cal/mole). However, in our case we have skirted the problem by correlating in terms of S_2^2 rather than $(S_1 - S_2)^2$ as suggested by Equations 3 or 4. In any case, the solubility parameter of methane corresponding to the values used for various hydrocarbon solvents is presumed to be less than those estimated for propane ($S = 5.85$) from actual $\Delta H_V + V_M$ data, and for ethane ($S = 4.05$) estimated by extrapolation of ΔH_V from lower temperatures and by extrapolation of S values at lower temperatures from measured $\Delta H_V + V_M$ data. Thus, the solubility parameter of methane is presumably less than 4.0, comparable only to the perfluorocarbons, silicones, or lower hydrocarbons which have been found to be the best solvents.

2. Effect of Molecular Weight

It will be noted that with the paraffin hydrocarbon series, the correlation appears to hold up to about C_7 above which the mole fraction solubility increases with increasing molecular weight. These deviations are qualitatively if not quantitatively accountable in terms of the differences in molal

volumes which affect the third term in Equation 4. The somewhat high solubilities in perfluoroheptane and octamethyl cyclotetrasiloxane can also possibly be explained in these terms. However, the physical explanation of this phenomenon may be that in the larger molecular weight solvents, the dissolved methane is interacting not with the molecule as a whole but with smaller segments of the molecule. This physical picture is consistent with the fact that $(n-C_4F_9)_3N$ which might be expected to behave as a spherical entity appears to conform to the solubility parameters correlation very well, whereas $n-C_7F_{16}$ and octamethyl cyclotetrasiloxane do not. This concept could be important in designing higher molecular weight solvents having good capacity on a gravimetric as well as a mole fraction basis. It is unfortunate that with the *n*-paraffin series of solvents, the increase in solubility on a mole fraction basis with increasing molecular weight above *n*-heptane is not sufficient to overcome the loss in gravimetric capacity due to the molecular weight increase (compare solubilities in Table 2 on a mole fraction and lb/lb basis).

On the other hand, if high solvency of propane or particularly methane, ethane, and propane could be simulated in terms of a multiplicity of methyl-, ethyl-, or propyl-group branches on a surface (e.g., silica gel) or on an oligomer, the increase in molecular weight might be overcome by the increase in solvency in the side chains so that the solvent maintains the methane capacity on a gravimetric basis close to that of methane, ethane, or propane. Ethane at 3.6 MPa vapor pressure, for example, would dissolve methane at a ratio of 0.35 g CH_4 /g ethane. If this solvency can be maintained with the ethyl group branches on a low polymer, a gravimetric capacity exceeding that of adsorption could be achieved.

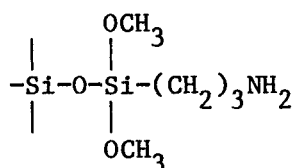
3. Aliphatic Hydroxyl-Group Effect

The solubilities of methane in aliphatic alcohols, although correlatable with solubility parameters appear to be greater at the same solubility parameter value than found for the other solvents having no hydroxyl groups. This suggests that hydrogen bonding, if strong enough, does contribute to solvent power for methane independent of the solubility parameter. However, the contribution of the hydroxyl groups to solubility tends to be overwhelmed by their effect on solubility parameter. Nonetheless, the very existence of the effect suggests that it should be possible to utilize it to design systems with enhanced solubility for methane as discussed below.

a. Chemical Modification of Adsorbents

One approach would be to enhance the adsorption capacity of solid adsorbents by providing a multiplicity of hydroxyl (or other hydrogen bonding group, including amides) on the surface. Such adsorbent surfaces might be expected to exhibit a higher heat of adsorption, so that greater surface coverage would be achieved at lower pressures than for adsorbents with non-polar surfaces. This would suggest the coverage of high surface area adsorbents with the specific groups (organic or inorganic) having the highest affinity for methane presumably by hydrogen bonding.

This concept is consistent with the results of Chuik, et al.,¹⁰ which showed that reaction of the silanol groups of a silica gel with an amino organo silane compound reduced both the surface concentration of silanol groups and the adsorption capacity for methane and other hydrocarbons. However, these results are not straightforward, since the treatment replaced the silanol groups with rather bulky



groups, which could have prevented adsorption by bulk alone.

b. Multicomponent Liquid Solvent System

Design multicomponent liquid solvent systems in which the hydroxyl or other hydrogen bonding function is built-in in such a way as to enhance solvency. One approach might be a dual colloidal system in which a discrete second liquid or solid phase material provides a multiplicity of hydroxyl groups, interfaced with and dispersed in a continuous phase having a low solubility parameter. The easiest example would involve a dispersion of colloidal silica (millimicron diameter) in a low solubility parameter solvent such as a hydrocarbon, perfluorocarbon or silicone. Such a material could, of course, be made either solid or liquid. In this case, the dispersing function would be provided by a partial coverage (by reaction) of the surface with low solubility parameter tails compatible with the matrix phase (silicones).

c. Dual Function Solvents

Design single, dual function molecules or dual functional mixtures of solvent molecules containing both a low solubility parameter function and a hydrogen bonding or other affinity function in the form of a hydroxyl, amido or other groups. In particular, if the hydroxyl group effect on the solubility parameter of the solution could be minimized by either:

- Hindrance of the hydroxyl effect on S by surrounding it with low solubility tails in a single solvent molecule.
- Neutralization of the effect of the hydroxyl group on solubility parameter of the solution by hydrogen bond formation in a manner similar to the effect of ether formation on solubility parameter and solvent power of alcohols (e.g., S for diethyl ether = 7.5 compared to 12.7 for ethyl alcohol from which it is made). Similarly perhaps, the solubility parameter of $R-O^{\cdots}H-CH_3$ may be considerably less than ROH itself. If so, solvent mixtures containing a low solubility parameter solvent molecule as a matrix plus a strongly hydrogen bonding species (such as alcohol) in concentrations comparable to that of the expected solute concentrations could exhibit the advantages of both hydrogen bonding and low solubility parameter.

d. Hydrogen-Bonding Groups Other than Hydroxyl

Find other organic or inorganic groups having even greater hydrogen bonding power than aliphatic hydroxyl groups. In particular, Wolfenden has reviewed and analyzed the "hydrophilicity" of various organic groups in terms of the water-to-vapor distribution coefficients for various aqueous solutions of uncharged organic compounds containing these groups.¹² The results suggest that the hydrogen bonding propensity of various groups increases in the following order: Alkanes < -SH < -Cl < ethers and thioethers < esters < aldehydes and ketones < nitriles < amines < alcohols < H₂O < acids, phosphotriesters < Amides and diols < η-substituted amides < peptides < guanidines. This suggests that η-substituted amides and guanidines in which the η-substituent is a long chain hydrocarbon or perfluorocarbon dissolved in an appropriate solvent of low solubility parameter should be worthy of evaluation.

Solubility of Methane in Polymers¹⁴

Considerable literature exists on the solubility of various gases including methane in a number of polymers. Most of this work was aimed at determining the diffusion characteristics of polymeric films, one of the basic parameters

of which is solubility. The best polymeric solvent found so far is silicone rubber, which exhibits a significantly greater capacity for methane (0.018 g/g) than polyethylenes, polyisobutylene and other systems.¹⁴ Unfortunately, the gravimetric capacity of even silicone rubber is very low compared to the low molecular weight solvents.

The factors controlling solubility of fixed gases in these systems was not completely delineated by the literature review. For example, the solubility of methane in polyethylene in some studies appears to be limited to (or correlatable with) the amorphous phase.^{18,19} Yet other studies have found relatively little difference between the highly crystallizable linear polyethylene and amorphous systems such as polyisobutylene.¹⁶ The theory seems to be trending toward a "hole" theory comparable to adsorption in such common adsorbents as activated carbon in that the solubility is a function of the "hole" volume.^{16,20}

Nonetheless, solubility would be expected to be greatest in relatively low solubility parameter polymers such as polyisobutylene and the silicones. Furthermore, amorphous polymers would be expected to exhibit greater "hole volume" than crystalline polymers. In any case, one wonders if the free "hole" volume in polyisobutylene or silicone polymers could be controlled by controlled cross-linking while in a swollen state with an easily volatilized solvent. Of particular interest would be silicon-containing polymers including:

- Polyvinyl trimethyl silane which has been shown to dissolve methane to the extent of four times that of polyethylene terephthalate.¹³
- Poly 1-(Trimethyl Silyl)-1-propyne which has recently been shown to dissolve oxygen to an extent ten times that of other known polymers.²¹

It is interesting to speculate as well that specialized adsorbents, as opposed to absorbents, could be developed from polymeric systems cross-linked in the swollen state, containing hydrogen bonding groups such as hydroxyl or amide groups, e.g., polyvinyl alcohol or polyethylene terephthalate. Such polymeric systems are sometimes called reticulated polymers and offer the possibility of adsorbents with surface chemistries tailored for the particular adsorbate desired. We do not have surface area data on such systems but dry reticulated ion exchange resins have been evaluated as catalysts.

Such systems could be of considerable interest, at least conceptually, since they may lead to negative deviations from ideal interaction at the solid surfaces. However, strong adsorption would be expected to occur only for monomolecular surface coverage. Thus, surface area would be important.

SUMMARY AND CONCLUSIONS

The available literature data on the solubility of methane in a wide variety of solvents has been collected and analyzed and the general conclusions are as follows:

- In general, the data pretty well conforms to the classical views of Hildebrand on regular solutions, i.e., solutions "in which orienting and chemical effects are absent and in which the distributions and orientations are random..." In other words, methane behaves in most solutions as non-polar molecules (including the rare gases) subject primarily to Van der Waals dispersion forces.
- The primary parameters controlling solubility in regular solution theory are the molal volume and the Hildebrand solubility parameter relative to that of methane, the solubility parameter (or cohesive energy density) being defined as:

$$S = \left(\frac{\Delta H_T^V - RT}{V_1} \right)^{1/2}$$

where:

ΔH_T^V = Heat of vaporization at solution temperature

V_1 = Molal volume of Component 1.

- Since the solubility parameter of methane is at the lower end of the scale ($S = <4$), the best solvents for methane are the perfluorocarbons, the silicones, and the lower aliphatic hydrocarbons such as propane.
- The best solvent for methane so far identified is propane, in which methane is soluble to the extent of 0.15 mole fraction or 0.063 g CH_4/g solvent. However, this is a lower capacity on a mass ratio basis than can be expected from adsorption on activated carbon.
- On a mole fraction basis, the solubility of methane in octamethyl cyclo-tetrasiloxane (0.32) and in perfluoro n-heptane (0.28) is greater than in propane but on a gravimetric basis the solubilities are much lower (0.025 and 0.016 respectively) due to their high molecular weight. Thus, methane solubilities in lower molecular weight perfluorocarbons and silicones should be determined.
- In the aliphatic hydrocarbon series, the solubility of methane decreases with increasing molecular weight (and increasing S) up to about C_6 (n-hexane). Above C_6 , however, the solubility of methane on a mole fraction basis in this class of solvents increases rapidly with increasing molecular weight to 0.32 for C_{32} (squalane). Unfortunately, the solvent weight increases more rapidly than solubility so that the solubility on a gravimetric basis continues to decrease with molecular weight.

- The solubility of methane in isobutane (0.061 g/g) and neopentane (0.057 g/g) suggests that the solubility on a gravimetric basis may be maintained while molecular weight increases for highly branched paraffin hydrocarbon. Unfortunately, data on the solubility of methane in higher molecular weight highly branched paraffins is lacking.
- In particular, preliminary calculations suggest that it may be possible to design higher molecular weight solvents having gravimetric capacities in the range of, or greater than, for adsorption. The solubility data presented above for the lower paraffinic hydrocarbons (e.g., propane) actually represent the concentration of methane in the liquid phase of a mixture in equilibrium with a vapor phase containing a considerable proportion of solvent vapor. For example, if the equilibrium concentration of methane in propane at 25°C and 3.5 MPa total pressure is corrected to 3.5 MPa partial pressure of methane, the solubility would increase from 0.063 g/g to 0.11 g/g propane. With ethane, the equilibrium concentration of methane in the liquid phase at 25°C and 4.9 MPa is about 0.05. Thus, if corrected to 3.5 MPa partial pressure of methane, the solubility in methane becomes 0.35 g/g of ethane. Thus, if we could tie down the methyl, ethyl or propyl groups and still achieve their solvent power for methane, it may be possible to achieve a viable non-volatile solvent for our purposes. In particular, if we could simulate the high solvency of methane, ethane, or propane in terms of a multiplicity of methyl, ethyl, or propyl groups as branches on a surface (e.g., silica gel) or an oligomer, the gravimetric solution capacity for methane might be maintained at a reasonable level. For example, if the solvency of ethane can be maintained with ethyl groups on a low molecular weight polymer, a gravimetric capacity exceeding that for adsorption might be achieved:

	Calculated g/g
CH ₃ -CH ₃	0.35
<pre> CH₃ CH₃ CH₃ CH₂ CH₂ CH₂ ... C - C - C ... n </pre>	0.24
<pre> CH₃ CH₃ CH₂ CH₂ .C- C - C - C ... n </pre>	0.18

- The solubilities of methane in aliphatic alcohols, although correlatable with solubility parameters, appear to be greater at the same solubility parameter value than for other solvents having no hydroxyl groups. This suggests that hydrogen bonding power can contribute to solvent power for

methane independent of the solubility parameter. However, this contribution to solvency by the hydroxyl group is overwhelmed by its effect on solubility parameter. Nonetheless, the effect suggests that it may be possible to:

- 1) Enhance the adsorptive capacity of solid adsorbents by providing a multiplicity of hydroxyl groups on the surface.
- 2) Design multicomponent liquid solvent systems in which the hydroxyl or other hydrogen bonding function is built into the system to enhance solvency.
- 3) Design dual function systems, either single detergent-like molecules or a dispersion of hydroxyl group containing molecules in a matrix of low solubility parameter, in which the hydroxyl group effect on the solubility parameter of the solvent as a whole is suppressed or minimized by.
- 4) Evaluate the effect of other groups having stronger hydrogen bonding power than aliphatic hydroxyl groups including amides, n-substituted amides and n-substituted guanidines.
- 5) Of particular interest would be tailor-made polymers (or oligomers) of various silicon containing monomers and particularly the trialkyl silanes (as opposed to the dialkyl silicone type).

REFERENCES FOR APPENDIX E

1. Hildebrand, J. H. and Scott, R. L., The Solubility of Nonelectrolytes, New York: Reinhold (1950).
2. Hildebrand, J. H. and Scott, R. L., Regular Solutions, Englewood Cliffs, NJ: Prentice Hall (1962).
3. J. C. Gjaldbaek and J. H. Hildebrand, J. Am. Chem. Soc., 71, 3147 (1949).
4. Yen, L. C. and McKetta, J. J., "A Thermodynamic Correlation of Non-Polar Gas Solubilities in Polar Non-Associated Liquids," A.I.Ch.E. Journal, 8, 501-507 (1972).
5. Burrell, H., "Solubility Parameters for Fil Formers," Official Digest, 27, 726-758 (1955).
6. Lieberman, E. P., "Quantification of the Hydrogen Bonding Parameter," Official Digest, 34, pp 30-50 (1972).
7. Thomsen, E. S. and Gjaldbaek, J. C., "Solubility of Propane in Non-Polar Solvents," Acta Chemica Scand. 17, 134-138 (1963).
8. Thomsen, E. S. and Gjaldbaek, J. C., "The Solubility of Hydrogen, Nitrogen, Oxygen, and Ethane in Normal Hydrocarbons." Acta Chemica Scand., 17, 127-133 (1963).
9. Sebastian, H. M., Lin, H. M., and Chao, K. E., "Correlation of Solubility of Hydrogen in Hydrocarbon Solvents," A.I.Ch.E J., 27, 138-148 (1981).
10. Chuiko, A. A., et. al., "Aminoorgeno Silicon Compounds as Chemically Active Sorbents and Fillers of Polymer Materials. I. Surface Reaction of (γ -amino propyl) Triethoxysilane with Silica and Adsorption Properties of Amino Organo Silicon Compounds," Chemical Abstracts, 64, 6825d (1966).
11. Koltsov, S. I., et. al., "Molecular-Layers Deposition of Carbon on Siliceous Adsorbents of Different Porous Structure," Chemical Abstracts, 91, 27745h (1979).
12. Wolfenden, Richard, "Waterlogged Molecules," Science, 222, 1087-1093 (1983).
13. Volkov, V. V., et. al., "Solubility of Gases in Poly (Vinyltrimethylsilane)," Chemical Abstracts, 86, 122132r (1977).
14. Robb, W. L., "Thin Silicone Membranes - Their Permeation Properties and Some Applications," Annals, NY Acad. Sciences, Vol. 46, 119-137 (1968).

15. W. L. Robb, Thin Silicone Membranes - Their Permeation Properties and Some Applications, General Electric, Technical information series, 65-C-031 (Okt. 65), Research and Development Center, Schenectady, NY.
16. Lundberg, J. L. and Mooney, E. J., "Diffusion and Solubility of Methane in Polyisobutylene," J. Poly. Sci., Part A-2, Vol 7, 974-962 (1969).
17. Van Amerongen, G. J., "The Permeability of Different Rubbers to Gases and its Relation to Diffusivity and Solubility," J. Applied Physics, 17, 972-985 (1946).
18. Michaels, A. S. and Parker, R. B., "Sorption and Flow of Gases in Polyethylene," J. Poly. Sci., XLI, 53-71 (1959).
19. Michaels, A. S. and Bixter, H. J., "Solubility of Gases in Polyethylene," J. Poly. Sci., Vol. L, 393-412 (1961).
20. Michaels, A. S., Vieth, W. R., and Barrie, J. A., "Solution of Gases in Polyethylene Terephthalate," J. Applied Physics, 34, 1-20 (1963).
21. Takada, K., et al., J. Am. Chem. Soc., 105, 7473 (1983).
22. Battino, R. and Clever, H. L., "The Solubility of Gases in Liquids," Chem. Rev., 66, 395 (1966).
23. Lawson, D. D., "Methods of Calculating Engineering Parameters for Gas Separations," Applied Energy 6, 240-251 (1980).
24. Pierotti, R. A., "The Solubility of Gases in Liquids," J. Phys. Chem. 67, 1810-1845 (1963).

Table 2. EXPERIMENTAL SOLUBILITIES OF METHANE
IN VARIOUS SOLVENTS

Solvent	Ref.	S	Methane Solubility at 25°C 34 atm CH ₄ Pressure, @ Mol		Equilibrium Liquid Composition at 25°C and 34 atm Total Pressure	
			Faction, CH ₄	g CH ₄ /g Solvent	Weight Percent	g/g
ALIPHATIC HYDROCARBONS						
Ethane	38	4.05	0.40	0.21	0.05	0.027
Propane	1,2,3	5.85	0.235	0.11	0.148	0.063
n-Butane	4,5	6.6	0.192	0.66	0.17	0.054
i-Butane	6	6.2	0.205	0.071	0.18	0.061
n-Pentane	7	7.0	0.175	0.175	0.046	0.046
i-Pentane		6.8	0.177	0.	0.165	--
neo-Pentane	14	6.2	0.218	0.062	0.206	0.057
n-Hexane	8-11,13,35	7.3	0.17	0.038		
z-Methylperitane	12	--	0.17	0.038		
n-Heptane	35	7.45	0.16	0.030		
n-Octane	17	7.65	0.17	0.029		
224-Trimethyl Pentane	15	6.85	0.184	0.032		
n-Decane	17	7.7	0.20	0.028		
Polyethylene	41	--	--	0.005		
ALICYCLIC HYDROCARBONS						
Cyclohexane	9	8.2	0.11	0.024		
CIS 1,2 Dimethyl Cyclohexane	24		0.135			
Trans-Cyclohexane 1,3 Dimethyl	24		0.145			
Cyclohexane CIS 1,4 Cyclohexane	24		0.145			
Methyl Cyclohexane	24		0.147			
Bicyclohexyl	25	7.8	0.135			
Cyclooctane	16	8.2	0.115			
	28	8.5	0.094			
AROMATIC HYDROCARBONS						
Benzene	9,23	9.15	0.071	0.012		
Toluene	19,25,35	8.9	0.076	0.013		
o-Xylene	26	9.0	0.085	0.014		
m-Xylene	26	8.8	0.092			
p-Xylene	26	8.8	0.098	0.016		
Diphenyl Methane	16	9.1	0.061			
1-Methyl Naphthalene	31,32		0.053			

Table 2. EXPERIMENTAL SOLUBILITIES OF METHANE
IN VARIOUS SOLVENTS, CON'T.

Solvent	Ref.	S	Methane Solubility at 25°C 34 atm CH ₄ Pressure, @ Mol		Equilibrium Liquid Composition at 25°C and 34 atm Total Pressure	
			Faction, CH ₄	g CH ₄ /g Solvent	Weight Percent	g/g
PERFLUOROCARBONS AND SILICONES						
(C ₄ F ₉) N	21	5.9	0.23			
C ₇ F ₁₆ Hexafluoro Benzene	22	5.7	0.28	0.016		
Octamethylcyclo Tetrasilane	23	8.25	0.13			
Silicone Rubber	31	5.5	0.32	0.025		
	42			0.018		
CHLORINATED HYDROCARBONS						
CH ₂ Cl-CH ₂ Cl	35		0.029			
CCl ₄		8.6	0.097	0.011		
Chlorobenzene	9, 35	9.5	0.068			
CHCl ₃	35	9.25	0.058	0.008		
CCl ₂ F-CClF ₂	15		0.17			
ALIPHATIC ALCOHOLS						
H ₂ O		23.4	0.0009			
Methyl Alcohol		14.5	0.029			
Ethyl Alcohol		12.7	0.044			
Propyl Alcohol		11.9	0.055			
i-Propyl Alcohol		11.5	0.049			
n-Butyl Alcohol		11.0	0.065			
n-Amyl Alcohol		10.3	0.073			
n-Hexyl Alcohol		10.0	0.080			
n-Heptyl Alcohol		9.5	0.088			
n-Octyl Alcohol		9.3	0.095			
n-Decyl Alcohol			0.108			
Cyclo Hexyl Alcohol			0.043			

Table 2. EXPERIMENTAL SOLUBILITIES OF METHANE
IN VARIOUS SOLVENTS, CON'T.

Solvent	Ref.	S	Methane Solubility at 25°C	
			34 atm CH ₄ Pressure, @ Mol Faction, CH ₄	g CH ₄ /g Solvent
MISCELLANEOUS OXYGEN COMPOUNDS				
Diethyl Ether	9	7.45	0.154	0.039
Dioxane	9	10.0	0.044	
Methyl Acetate	9	9.5	0.066	
Acetone	9	9.65	0.063	
Ethylene Oxide	27		0.055	
Methyl Ethyl Ketone		9.3	0.06	
Propylene Carbonate	39	13.3	0.023	
Glycerol tri- Acetate	39		0.065	
Sulfur Dioxide			0.035	
COS	29		0.076	
CS ₂	21,22	10.0	0.044	
Dimethyl Sulfoxide	30		0.013	
Tributyl Phosphate	39		0.155	
MISCELLANEOUS NITROGEN COMPOUNDS				
Ammonia	33		0.012	
Aniline	35	11.6	0.023	
Cyclohexyl Amine	29	8.7	0.065	
Methyl Pyrrolidane	39		0.033	
Nitrobenzene	35	10.0	0.030	

REFERENCES FOR TABLE 2 ONLY

1. Reamer, H. H., Sage, B. H., and Lacey, W. N., "Phase Equilibria in Hydrocarbon Systems Volumetric and Phase Behavior of the Methane-Propane System, Ind. Eng. Chem., 42, 534-539 (1950).
2. Sage, B. H., Lacey, W. N., and Schaafsma, J. G., "Phase Equilibria in Hydrocarbon System II Methane-Propane System, Ind. Eng. Chem. 26, 214-217 (1934).
3. Akers, W. W., Burns, J. F., and Fairchild, W. R., "Low Temperature Phase Equilibria Methane-Propane System," Ind. Eng. Chem. 46, 2531-2536 (1954).
4. Sage, B. H., Hicks, B. L. and Lacey, W. N., "Phase Equilibria in Hydrocarbon Systems. The Methane-n-Butane System in the Two Phase Region," Ind. Eng. Chem. 32, 1087-92 (1940).
5. Roberts, L. R. et. al., "Methane-n-Butane System in the Two Phase Region," J. Chem. & Eng. Data, 7, 484-85 (1962).
6. Olds, R. H., Sage, B. H., and Lacey, W. N., "Methane-Isobutane System," Ind. Eng. Chem., 34, 1008-1013 (1942).
7. Sage, B. H., et. al., "Phase Equilibria in Hydrocarbon Systems, Volumetric and Phase Behavior of Methane-n-Pentane System," Ind. Eng. Chem., 34, 1108-1113 (1942).
8. Shim, J. and Kohn, J. P., "Multiphase and Volumetric Equilibria of Methane-n-Hexane Binary System at Temperatures Between -110° and 150°C," J. Chem. & Eng. Data, 7, 3-8 (1962).
9. Lanning, A. and Gjaldbaek, J. C., "The Solubility of Methane in Hydrocarbons, Alcohols, Water and Other Solvents," Acta. Chem. Scand., 14, 1124-1128 (1960).
10. Reamer, H. H., Sage, B. H., and Lacey, W. N., "Phase Equilibria in Hydrocarbon Systems, Volumetric and Phase Behavior of the Methane-Cyclohexane System," Ind. & Eng. Chem., Chem. & Eng. Data Series, 3, 240-245 (1958).
11. Lin, Y. et. al., "Vapor-Liquid Equilibrium of the Methane-n-Hexane System at Low Temperatures," J. Chem. & Eng. Data, 22, 402-408 (1977).
12. Kohn, J. P. and Haggin, J. H. S., "Low Pressure Vapor-Liquid Isotherms in the Methane-3-Methylpentane Binary System," J. Chem. & Eng. Data, 12, 313-315 (1967).
13. Poston, R. S. and McKetta, J. J., "Vapor-Liquid Equilibrium in the Methane-n-Hexane System," J. Chem. & Eng. Data, 11, 362-363 (1966).

14. Rogers, B. L. and Prausnitz, J. M., "High Pressure Vapor-Liquid Equilibrium for Argone and Neopentane and Methane and Neopentane," J. Chem. Thermodynamics, 3, 211-216 (1971).
15. Hiraoka, H. and Hildebrand, J. H., "The Solubility and Entropy of Solution of Certain Gases in $(C_4F_9)_N$, $CCl_2F \cdot CClF_2$ and $2,2,4(CH_3)_3 C_5H_9$," J. Phys. Chem., 68, 213-214 (1964).
16. Cukor, P. M. and Prausnitz, J. M., "Solubilities of Gases in Liquids at Elevated Temperatures. Henry's Constants for Hydrogen, Methane, and Ethane in Hexadecane, Bicyclohexyl and Diphenylmethane," J. Phys. Chem., 76, 598-602 (1972).
17. Wilcock, R. J., et. al., "Solubilities of Gases in Liquids. II. The Solubilities of He, Ne, Ar, Kr, O_2 , N_2 , CO, CO_2 , CH_4 , and SF_6 in n-Octane, 1-Octanol, n-decane, and 1-decanol," J. Chem. Thermodynamics, 10, 817-822 (1978).
18. Cukor, P. M. and Prausnitz, J. M., "Apparatus for Accurate Rapid Determinations of the Solubilities of Gases in Liquids at Elevated Temperatures," Ind. Eng. Chem. Fundam., 10, 638-640 (1971).
19. Lin, Y., Hwang, S., and Kobayashi, R., "Vapor-Liquid Equilibrium of the Methane-Toluene System at Low Temperatures," J. Chem. & Eng. Data, 23, 231-234 (1978).
20. Senturk, N. H., Kalra, H., and Robinson, D. B., "Vapor-Liquid Equilibrium in the Methane-Carbonyl Sulfide Binary System," J. Chem. & Eng. Data, 24, 311-313 (1979).
21. Powell, R. J., "Solubility of 16 Gases in $(C_4F_9)_N$ and CS_2 ," J. Chem. & Eng. Data, 17, 302-304 (1972).
22. Kobatuke, Y. and Hildebrand, J. L., "Solubility and Entropy of Solution of He, N_2 , A, O_2 , CH_4 , C_2H_6 , CO_2 , and SF_6 in Various Solvents; Regularity of Gas Solubilities," ACS, 65 331-335 (1961).
23. Evans, F. D. and Baltuno, R., "The Solubility of Gases in Liquids. 3. The Solubilities of Gases in Hexafluoro Benzene and in Benzene. 4. Calculations on Gas Solubilities in Hexafluoro Benzene and Benzene," J. Chem. Thermo., 3, 753-760 (1971).
24. Geller, E. B., Battino, R., and Wilhelm, E., "The Solubility of Gases in Liquids. 9. Solubility of Ne, Ne, Ar, Kr, N_2 , O_2 , CO, CO_2 , CH_4 , CF_4 , and SF_6 in Some Dimethylcyclohexanes at 298° to $313^\circ K$," J. Chem. Thermo., 8, 197-202 (1976).
25. Field, L. F., Wilhelm, E., and Battino, R., "The Solubility of Gases in Liquids. 6. Solubility of N_2 , O_2 , CO, CO_2 , CH_4 , and CF_4 in Methyl Cyclohexane and Toluene at 283° and $313^\circ K$," J. Chem. Thermodynamics, 6, 237-243 (1974).

26. Byrne, J. E. and Battino, R., "The Solubility of Gases in Liquids. 8. Solubility of He, Ne, Ar, Kr, CO₂, CH₄, CF₄, and SF₆ in O-, m-, and p-xylene at 283° to 313°K," J. Chem. Thermo. 7, 515-522 (1975).
27. Olson, J. D., "Solubility of Nitrogen, Argone, Methane, and Elbane in Ethylene Oxide," J. Chem. Eng. Data, 22, 326-329 (1977).
28. Wilcock, R. N., Battino, R., and Wilhelm, E., "The Solubility of Gases in Liquids. 10. The Solubility of He, Ne, Ar, Kr, N₂, O₂, CO, CO₂, CH₄, CF₄, and SF₆ in Cyclooctane at 289° to 313°K," J. Chem. Thermodynamics, 9, 111-115 (1977).
29. Keevil, T. A., Taylor, D. R., and Streitweiser, A., "Solubility of Hydrocarbons in Cyclohexylamin," J. Chem. & Eng. Data, 23, 237-239 (1978).
30. Dymond, J. H., "Solubility of a Series of Gases in Cyclohexane and Dimethylsulfoxide," J. Phys. Chem., 71, 1829-31 (1967).
31. Chappelow, C. C., III, and Prausnitz, J. M., "Solubilities of Gas in High Boiling Hydrocarbon Solvents," A.I.Ch.E. J., 20, 1097-1104 (1974).
32. Sebastian, H. M., Lin, H., and Chao, K., "Correlation of the Solubility of Methane in Hydrocarbon Solvents," Ind. Eng. Chem. Fundam., 20, 346-349 (1981).
33. Kaminishi, G., "Gas-Liquid Equilibrium under High Pressure. V. The Solubility of Methane and Argone in Liquid Ammonia at Elevated Pressure." Chem. Abstracts, 63, 4999 (1965).
34. Boyer, F. L. and Bircher, L. J., "The Solubility of Nitrogen, Argone, Methane, Ethylene, and Ethane in Normal Primary Alcohols," J. Phys. Chem., 64, 1330-31 (1960).
35. Gerrard, William, "Significance of the Solubility of Hydrocarbon Gases in Liquids in Relation to the Intermolecular Structure of Liquids and the Essential Pattern of Data for all Gases," J. Applied Chem. Biotechnol., 23, 1-17 (1973).
36. Yen, L. C. and McKetta, J. J., "A Thermodynamic Correlation of Nonpolar Gas Solubilities in Polar Non-Associated Liquids," A.I.Ch.E. Journal, 8, 501-507 (1967).
37. Frolich, P. K., et. al., "Solubilities of Gases in Liquids at High Pressure," J&E C, 23, 548-550 (1931).
38. Bloomen, O. T., Gami, D. C., and Parent, J. D., "Physical Chemical Properties of Methane-Ethane Mixtures," IGT Research Bulletin 22, July 1953.
39. Shakhova, S. F. and Zubchenko, Y. P., "Solubility of Methane and Argone in Organic Solvents," Chemical Abstracts, 79, 140139L (1973).

40. Koonce, K. T. and Kobayashi, R., "A Method for Determining the Solubility of Gases in Relatively Non-Volatile Liquids. Solubility of Methane in n-decane," J. Chem. & Eng. Data, 9, 490-494 (1964).
41. Michaels, A. S. and Bixter, H. J., "Solubility of Gases in Polyethylene," J. Polymer Sci., 50, 393-412 (1961).
42. Robb, W. L., "Thin Silicone Membranes - Their Permeation Properties and Some Applications," Annals N.Y. Acad. Sciences, Vol. 146, 119-137 (1968).

1. Report No. NASA CR-174655		2. Government Accession No.		3. Recipient's Catalog No.	
4. Title and Subtitle Advanced Onboard Storage Concepts for Natural Gas-Fueled Automotive Vehicles				5. Report Date June 1984	
				6. Performing Organization Code 61067	
7. Author(s) R. J. Remick, R. H. Elkins, E. H. Camara, and T. Bulicz				8. Performing Organization Report No.	
				10. Work Unit No.	
9. Performing Organization Name and Address Institute of Gas Technology 3424 South State Street Chicago, Illinois 60616				11. Contract or Grant No. DEN 3-327	
				13. Type of Report and Period Covered Contractor Report	
12. Sponsoring Agency Name and Address U. S. Department of Energy Office of Vehicle and Engine R&D Washington, D.C. 20545				14. Sponsoring Agency Code Report No. DOE/NASA/0327-1	
15. Supplementary Notes Final Report. Prepared under Interagency Agreement DE-AI01-81CS50006. Project Manager, Fred Simon, Aerothermodynamics and Fuels Division, NASA Lewis Research Center, Cleveland, Ohio 44135.					
16. Abstract The objective of this study was the evaluation, both through experimentation and a literature review, of several advanced concepts for storing natural gas at reduced pressure. The advanced concepts included adsorption on high surface area carbon, adsorption in high porosity zeolite, storage in clathration compounds, and storage by dissolution in liquid solvents. Results indicated that high surface area carbons with high packing density were the best low pressure storage mediums. A simple mathematical model was used to compare adsorption storage on a state-of-the-art carbon with compression storage. The model indicated that a vehicle using adsorption storage of natural gas at 3.6 MPa will have 36 percent of the range, on the EPA city cycle, of a vehicle operating on a compression storage system having the same physical size and a peak storage pressure of 21 MPa. However, preliminary experiments and current literature suggest that the storage capacity of state-of-the-art carbons could be improved by as much as 50 percent, and that adsorption systems having a capacity equal to compression storage at 14 MPa are possible without exceeding a maximum pressure of 3.6 MPa.					
17. Key Words (Suggested by Author(s)) Natural gas vehicles Low pressure storage Alternative fuels			18. Distribution Statement Unclassified - Unlimited STAR Category 44 DOE Category UC-96		
19. Security Classif. (of this report) Unclassified		20. Security Classif. (of this page) Unclassified		21. No. of pages 134	22. Price* A07